AN IMPROVED HELIUM-3 NEUTRON SPECTROMETER

WILLIAM ALOIS BAIR

UCRL-16595

UNIVERSITY OF CALIFORNIA
Lawrence Radiation Laboratory
Berkeley, California

AEC Contract No. W-7405-eng-48

AN IMPROVED HELIUM-3 NEUTRON SPECTROMETER

William Alois Bair

(M. S. Thesis)

January 21, 1966

AN IMPROVED HELIUM-3 NEUTRON SPECTROMETER

Contents

AN IMPROVED HELIUM-3 NEUTRON SPECTROMETER

William A. Bair

Lawrence Radiation Laboratory
University of California
Berkeley, California

ABSTRACT

This report is a preliminary analysis of a ^{3}He neutron spectrometer being developed at the Lawrence Radiation Laboratory, Berkeley. The spectrometer will be capable of presenting neutron spectra to an upper limit of 14.0 MeV. The spectrometer employs a ^{3}He-Kr gas mixture in a proportional counter, and the reactions $^{3}He(n, p)T$ and $^{3}He(n, d)D$ are utilized to obtain the incident neutron energies. Recoils from ^{3}He, Kr, and the stabilizing gas (CO_2) are electronically removed from the spectra by taking advantage of the shorter rise times of the recoil pulses. An analytic analysis of the rise time discrimination pulse rejection, the wall effects, and the spectrometer efficiency is presented.

The computer program for the removal of the above corrections is lengthy, and although an outline of the methods of machine computation is presented, this concept is not carried to fruition. Instead a computer program and an "inversion matrix" are developed (based on the analytic analysis presented) by means of a "random probability analysis." The "inversion matrix" should permit the correction of a raw neutron spectrum output from a multichannel analyzer to a final neutron spectrum by

correcting in a single operation for: (a) rise time discrimination, (b) wall effects, and (c) spectrometer efficiency.

Appendices include a table of comparative physical and operational characteristics of all ^{3}He proportional counters and ionization chambers constructed and reported in the technical literature to date (Fall 1965). The complete electronic circuitry necessary to construct the rise time discriminator units, and the computer program "CATMAN" developed for the random probability analysis are also presented as separate appendices.

I. INTRODUCTION

A. Background and Purpose

This report concerning an improved ^{3}He neutron spectrometer is a preliminary report concerning the theory, design, and construction of a ^{3}He neutron spectrometer by the Health Physics Department of the Lawrence Radiation Laboratory. The actual operation and performance of the spectrometer will be the subject of a later report by the Health Physics Department and will be authored by Mr. Wai-Kit Quon.

The detection of neutrons and especially the measurement of their energy have from the first attempts presented a more difficult problem than the other common nuclear particles. This difficulty is because the usual methods depend on effects resulting from charges on the particles. Most methods of neutron detection depend upon the scattering of particles after a collision with the neutron, and the measurement of the energy deposited by the scattered charged particles. The drawback to any method that is designed to measure neutron spectra which is based on scattering lies in the conversion of the definite energy of the incident neutron to a continuum of energies of the recoiling particle. To avoid this continuum of energies, a neutron induced nuclear transformation was sought in which the energy release would correspond unambiguously to the neutron energy. Investigations of several potential reactions, and the elimination of those that had sharp resonances, low lying energy states in the residual nucleus, and large positive--or any magnitude

negative Q values, led to the selection of the following reaction:

$$^{1}n_{0} + {}^{3}He_{2} \longrightarrow {}^{3}H_{1} + {}^{1}H_{1} + 0.764 \text{ MeV}.$$

In addition, the $^{3}He(n, p)T$ cross section is fairly large and varies smoothly with energy, and the ability to discriminate against γ rays enhances this selection for the task of neutron spectroscopy. Now, if the charged particles produced by the neutron interaction were to be completely stopped in the active volume of a proportional counter, the ionization caused by the loss of particle energy would be equal to the energies of the charged particles. This energy would then appear as free electrons and positive ions within the active volume. If an electrical field gradient is present, the electrons would migrate to the anode, and the charge deposited by the electrons would be proportional to the energy, E_n of the incoming neutron.

Several experimenters have examined the neutron interactions with the ^{3}He nucleus, and have constructed neutron detectors, and to a limited extent, neutron spectrometers[1-13] utilizing proportional counters and ionization chambers. The work of the majority of the previous experimenters has, in general, concerned itself with the neutron energy spectra of only a few MeV, although Sayres reports success with neutron energies up to 8.1 MeV[10] and the measurement of a cross section at 17.5 MeV [5,14] using monoenergetic neutrons.

In the majority of the previous work accomplished, two problems seem to inhibit the usefulness of a ^{3}He neutron spectrometer.

First, an ambiguity arises from the fact that ^{3}He has a relatively large cross section for elastic scattering. The elastic $^{3}He(n, n)^{3}He$ cross section is equal to the nonelastic cross section at .072 MeV, but increases rapidly with increasing energy. At 4.2 MeV the elastic cross section is 4.6 times as large as the inelastic cross section. The ratio decreases slightly with further increasing energy, but the elastic cross section is at least double the inelastic cross section from 0.25 MeV to 14 MeV. The probability of an undesired recoil pulse is thus at least twice the probability of a desired inelastic collision. Unfortunately, the recoil events, in addition to being more probable, also produce a continuum of energy pulses from 3/4 E_n to zero depending upon the angle that the incoming neutrons strike a ^{3}He nucleus. This prevents utilizing any simple subtraction process in the determination of the initial neutron spectra.

Second, the possibility of a nuclear event occurring in an orientation such that the charged particles produced by the event intersect the walls of the containing vessel before expending their full energy was recognized. This phenomena gives rise to a count that is of less energy than a count that goes full track in the gas medium. ^{3}He nonelastic collisions with high energy neutrons produce tracks that are of considerable length in relation to the dimensions of the proportional counter, and the wall correction effects increase significantly with increasing neutron energies.

Solutions to the above two problems were attempted in various manners. Brown[8,9,15] constructed a "wall-less" counter composed of a peripheral ring of 16 small counters surrounding a central counting wire and an anticoincidence circuit to remove the wall effects. He then developed a computer program to unfold the ^{3}He recoil events. Brown's work was extended by Wang[16] who developed a computer program to unfold the "wall effects" in addition to the "recoil events." Sayres and Coppola[10] developed a "risetime discriminator" circuitry that removes the recoil events (and a fraction of the desired events) by taking advantage of the shorter track length of a ^{3}He recoil in comparison with the larger track lengths of the inelastic particles produced by neutron interaction with a ^{3}He nucleus. Batchelor[3,4] uses an approximate method of computation to remove the wall effects which appears to be useful at low energies, and short range of track in relationship to the counter dimensions.

The purpose of this paper is to attempt to combine the removal of the ^{3}He(n, n)^{3}He recoil effect developed by Sayres[10] with the unfolding of the wall effect developed by Brown[9] and Wang.[16] It is further the purpose of this paper to report attempts to extend the energy range of the ^{3}He proportional counter to 14.0 MeV (which appears to be about a practical upper limit for these devices) and to develop a means whereby the spectrometer can be utilized with some degree of 4π efficiency. The spectrometer will be used by the Health Physics Department, Lawrence

Radiation Laboratory, Berkeley for radiation surveys--hence the requirement for 4π sensitivity.

B. Description of the Spectrometer

The experimental apparatus for this ^3He spectrometer consists of a proportional counter, electronic components, and a computer program.

1. Proportional counter

The proportional counter is a cylindrical tube with an active length of 15 inches, a 4-inch outside diameter, and a wall thickness of 0.035 inch. The diameter of the anode wire is 0.003 inch. The proportional counter is designed with independently adjustable field tubes. Gas filling is 10 atmospheres of krypton, 2 atmospheres of high purity ^3He (less than 10^{-10}% tritium),[17] and 1/2% CO_2 as a stabilizing gas. The tube was specially constructed by the Texas Nuclear Corporation for this spectrometer. A line diagram showing the tube and pertinent dimensions are shown in Fig. 1.

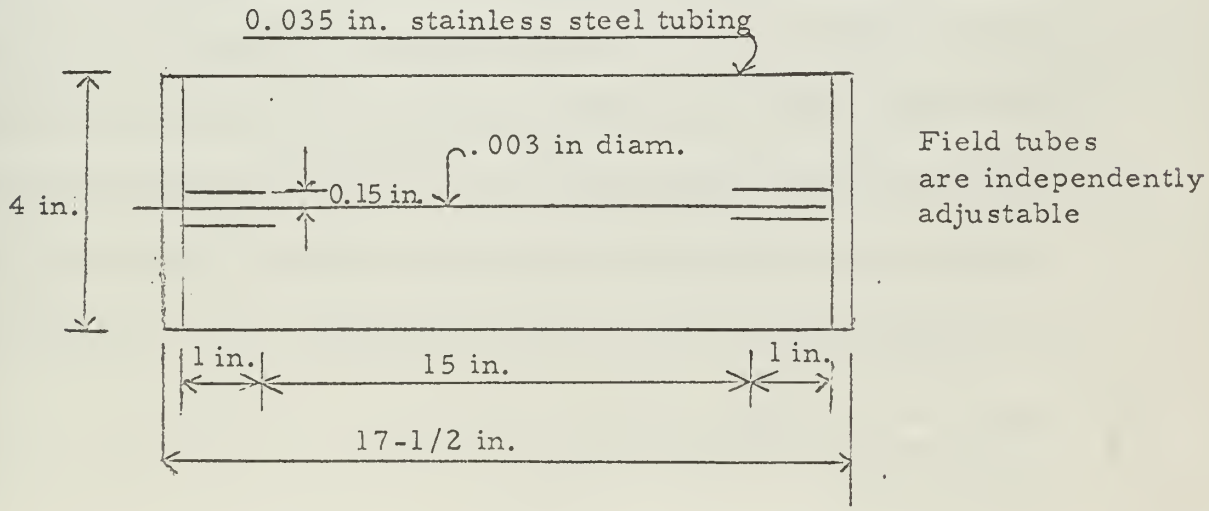

Fig. 1. ^3He proportional counter tube

A discussion of the design parameters and the design variables is included in Appendix A.

2. Electronic components

The electronic components are designed to be able to distinguish between a pulse generated from a ^{3}He recoil* and a ^{3}He inelastic event. To understand the operation of the electronics (a detailed description of which appears in Appendix A), it is first necessary to understand what the electronics are to accomplish. Basically, the length of track of a ^{3}He recoil (or any heavy particle recoil), is dependent upon the mass of the incident particle, the mass and charge of the recoil particle, the energy of the incident particle, the scattering angle, and the composition of the absorbing medium. (An analysis of the collision dynamics involved are included in Appendix B.) In general it can be stated that for equal recoil energies, a heavier particle, or a particle of the same mass but a higher atomic number, will traverse a shorter distance in the same stopping medium than a particle of less mass. In a proportional counter, a track's radial component from the center wire determine the length of time that it takes to collect the charge, i.e. the pulse rise time. Since the track length of the recoils is always less than the track lengths of the disintegration particles (which are the desired events), it is possible to select a rise time that will effectively exclude all recoil

*The arrangement also serves to eliminate recoils from the krypton gas and the CO_2.

events, yet retain a certain portion of the desired events which will have a longer rise time because of their longer track lengths. Unfortunately, the rise time criterion also eliminates many "good pulses" whose tracks are oriented with respect to the center wire in such a way that their rise times are within the discrimination criterion. The electronic circuitry developed in Appendix A is designed to accomplish this pulse rise time discrimination.

3. Computer program

The computer program is developed to accomplish the "unfolding" of the wall effects and to restore those desired pulses which were electronically eliminated by rise time discrimination. The wall effects computer program follows the method outlined by Wang,[16] but is not identical. Differences are primarily in the computation of the probability function $P(E \rightarrow E_i)$ which is the probability per unit energy that the reaction products of energy E will deposit energy E_i inside the sensitive volume due to the wall effect. In addition, a new probability function is analytically developed to replace mathematically the valid pulses which were eliminated due to rise time discrimination. An inversion matrix is proposed which will combine the two probability functions, and enable a complete reconstruction of the neutron spectra, above a minimum energy that is determined by our rise time discrimator setting. The neutron spectrum below this minimum energy cutoff level is unfortunately lost in the process of recoil elimination.

Unfortunately, the computer program analytically developed in this paper requires so much computer time that it was not considered warranted to carry it to completion. Instead, a random probability analysis was carried out, and the inversion matrix was developed on the basis of these random probability calculations. An outline of the random probability method is included in Section II-E and Appendix E.

II. DEVELOPMENT OF THE ^{3}He SPECTROMETER

A. Helium-3 and Neutron Interactions

A neutron can interact with a ^{3}He nucleus in five possible ways. These reactions which are energy dependent are as follows:

1. ^{3}He(n, p)T for neutrons of all energies
2. ^{3}He(n, n)^{3}He for neutrons of all energies
3. ^{3}He(n, d)D for neutrons of energies $\geq$ 4.36 MeV
4. ^{3}He(n, pn)D for neutrons of energies $\geq$ 7.32 MeV
5. ^{3}He(n, p2n)^{1}H for neutrons of energies $\geq$ 10.3 MeV

The cross sections for these reactions are reasonably well known in the energy range 0.001 eV to 14.0 MeV[18] with the exception of the ^{3}He(n, pn)D for which no data are available. It is assumed that this exceptional case has a small cross section, even though it is energetically possible. A comparative chart of the other reaction cross sections is included as Fig. 2. In addition to the ^{3}He(n, pn)D reaction, the ^{3}He(n, p2n)^{1}H reaction will not be considered in the determination of either wall effects or rise-time discrimination. The reasons for this omission are:

a. At the maximum energy expected to be encountered in this proportional counter (i.e. 14.0 MeV), the (n, 2n) cross section is only 15% of the total non-elastic cross section .

b. The neutron induced disintegration of the ^{3}He nucleus involves four separate product particles--only two of which are charged. Four particle

dynamics are complicated, and the energy imparted to the various particles may span a wide range of variables. Note, however, that the threshold for this reaction is 10.3 MeV and the kinetic energy of the charged particles produced by even a 14.0 MeV incoming neutron cannot exceed 3.7 MeV. Since some of the energy of the incoming neutron will undoubtedly be carried away as kinetic energy of the two product neutrons, it is highly probable that the sum of the charged-particle kinetic energies will be less than 3.7 MeV. Pulses from a 14.0 MeV neutron (n, 2n) reaction would thus appear on a multichannel analyzer at less than 3.7 MeV. Referring to Fig. 2, it is to be noted that the cross section of the $^{3}He(n, p)T$ reaction is fairly constant between about 0.4 and 2.5 MeV, and the cross section at these energies is at least 14 times as great as the (n, 2n) reaction at 14.0 MeV. Distortions of the neutron spectra would thus appear above 10.3 MeV at essentially 0% at threshold, up to a maximum of 15% at 14.0 MeV. This distortion would also manifest itself as a lower energy pulse, ($\leq$3.7 MeV) but the allocation of reaction particle kinetic energies would result in an energy distribution that would not be unique, but rather span from 0 to 3.7 MeV. For a continuous neutron spectra this "lower energy distortion" is not considered serious due to the more probable (n, p) reaction at these lower energies which would essentially mask these degenerate pulses from higher energies.

If we were to consider only single interactions within the active volume of our container (i.e. no multiple scattering events), and to

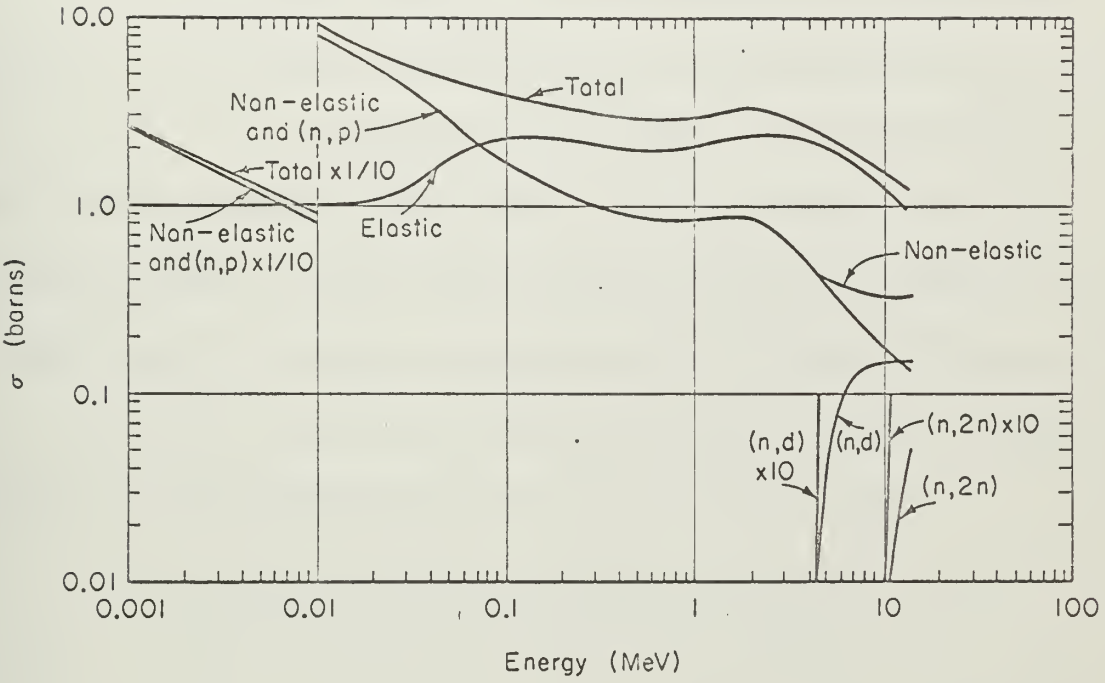

Fig. 2. Energy Dependent ^{3}He Neutron Cross Sections

likewise consider no neutron disintegration interactions with the material in the container walls, we would find that (after recoils are eliminated by rise-time discrimination and wall effects mathematically resolved) three reactions which would still tend to disturb our spectrum (irrespectiv of all corrections). These reactions therefore limit the maximum efficiency of our spectrometer. The three interactions are:

1. The disturbance of the energy spectrum above 10.3 MeV and below 3.7 MeV from the $^{3}He(n, p2n)^{1}H$ reaction.

2. The disturbances of the energy spectrum above 7.32 MeV and below 6.68 MeV from the $^{3}He(n, pn)D$ reaction (if this reaction does in fact occu

3. The disturbance of the energy spectrum at all energies due to the neutron induced krypton disintegrations.*

The cumulative error introduced by neglecting these reactions is unknown.

The remainder of this paper is to be divided into four parts. The plan of "unfolding" the raw spectra to develop a complete neutron spectrum is as follows:

Development of a probability function to replace the pulses eliminated by "rise-time discrimination." (II-B)

Development of a probability function to remove the wall and end

---

*This problem is discussed in detail in Appendix A, although no attempt is made to correct the spectrum.

effects. (II-C)

Combination of the two correction factors to reconstruct the neutron spectra. (II-D)

Reasons for and development of a random probability inversion matrix in lieu of the above II-D. (II-E)

Finally, it should be mentioned here that the work leading to the mathematical expressions for wall and end effects is primarily a restatement of the work of Dr. W. R. Brown[9] and Mr. H. T. Wang[16], although some modifications have been made to the analysis of the later author. A number of their drawings, graphs, and formulas are repeated in this text for continuity and to facilitate explanations. They will be designated by a "dagger" (†) if attributed to Dr. Brown, and by a "double dagger" (††) if developed by Mr. Wang.

B. Development of a Probability Function to Replace Pulses Eliminated by "Rise-time Discrimination"

As a result of the arbitrary orientations of the disintegration particles of the $^{3}He(n, p)T$ and the $^{3}He(n, d)D$ reactions, some tracks will be positioned such that the time difference between the arrival of the first electron and the last electron to the central counting wire will be quite short. This situation will occur when the radial component of the track lengths is small, or when the event takes place near the central portion of the counter where the electrical field gradient is high. In both of these orientations the count produced by a "valid event" will be rejected by the

electronic circuitry as though it were a recoil pulse. It was considered that if an analytical expression could be developed for determining the time difference between the arrival of the first and the last electron to the central counting wire, the "rise time" of the pulses could be determined mathematically. A probability function could then be developed based on the registered counts that would be representative of those good events that were rejected with the recoils. To develop this probability function, it is necessary however, to make four assumptions:

(1.) The time required for the charged particles to deposit their energy in the gas medium is instantaneous.*

(2.) A nuclear event can occur with equal probability within any unit volume in the sensitive region of the proportional counter.

(3.) The mobility of the electrons in the gas mixture is directly proportional to the field gradient over the limited range of the electrical field gradients in which we are interested.

(4.) The electron mobility in the gas mixture (2 atmospheres ^{3}He, 10 atmospheres Kr, and 0.5% CO_2) can be computed by assuming that the

---

*As an approximation, it can be shown that by relating a specific particle energy $E_i = \frac{1}{2} m v_i^2$; solving for v_i; and then relating an average velocity to track length ($\ell_i(E)$) and solving for time $t_i = \frac{(\ell_i(E))}{\frac{(v_i - 0)}{2}}$ that the time required for a particle to deposit its energy is about 3 nanoseconds for a proton (longest track length, highest velocity) of 10.0 MeV energy, and 0.6 nanoseconds for a 10.0 MeV ^{3}He recoil particle (shortest track length, smallest velocity). Rise times of interest to our counter circuitry are in excess of 3 microseconds.

electrons behave as ions, and that the mixture mobility can be computed as can the "mixture mobilities" of ions.

Assumptions (3) and (4) will be discussed in greater detail in the following sections.

1. Electron migration time from any point r in coaxial cylindrical geometry. In a cylindrical proportional counter, the electrical field gradient can be determined at any point r from the center of the counter by the relationship:

$$E(r) = \frac{V_o}{r \ell n \frac{r_c}{r_a}} \qquad (1)$$

where E(r) is the field gradient at any radial distance r from the anode.

V_o = applied voltage

r_c = radius of the cathode

r_a = radius of the anode

(This formula is developed in Appendix D.)

For our counter dimensions we can plot the field gradient at any radius from the center wire by using the appropriate applied voltage and counter dimensions. Instead of directly plotting the field gradient as a function of radius however, let us divide both sides of Eq. 1 by the total pressure of the counter filling gas in cm of mercury and plot this value instead. The reasons for this will become evident shortly. This plot can be seen in Fig. 3 for representative counter voltages.

An electron produced by ionization at a radial position r will drift slowly towards the anode under the influence of the electrical field gradient.

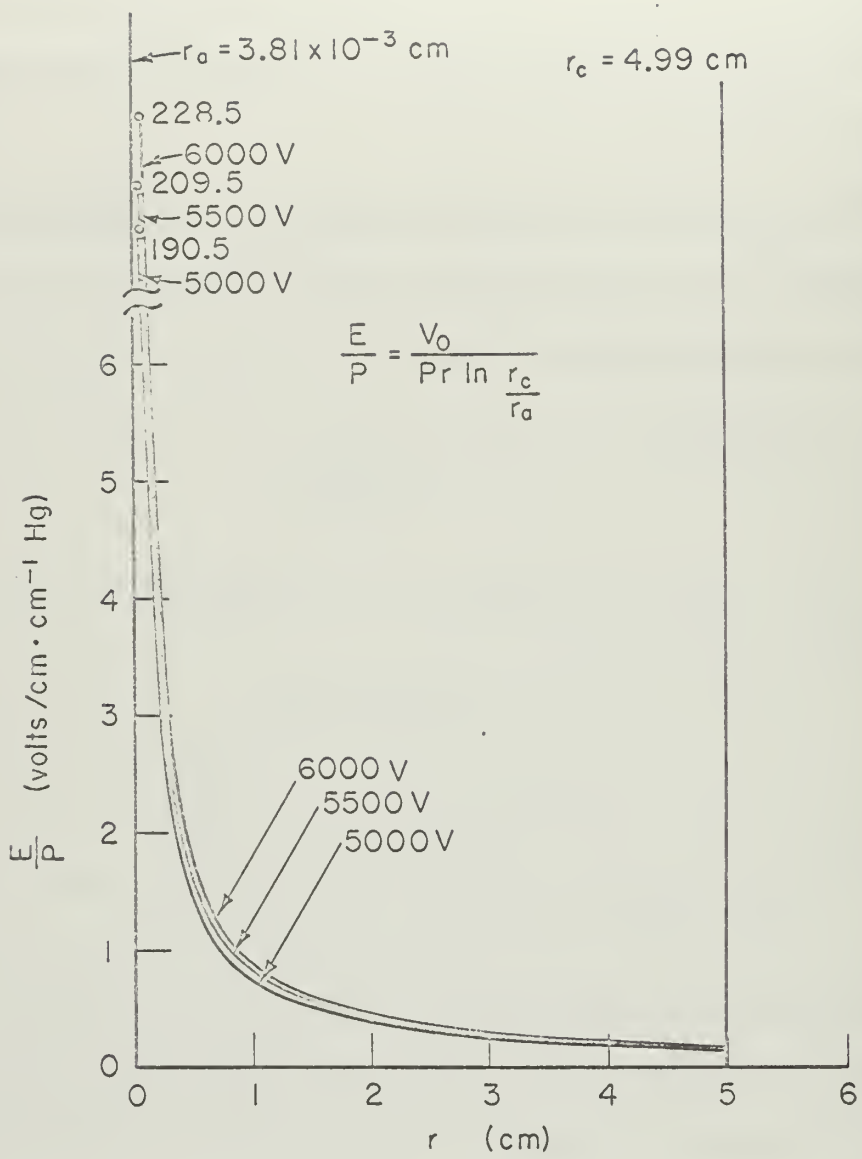

Fig. 3. Variation of Field Gradient/Filling Pressure (E/P) for Representative Applied Voltage

As can be seen in Fig. 3, the electrical field gradient at regions beyond about 1 cm from the cathode varies very slowly. After the electron passes this point in its inward radial drift, the field gradient sharply increases. If we assume a direct proportionality between the drift speed and the E/P ratio, we can obtain an expression in cylindrical geometry for the time it requires for an electron to reach the cathode, i.e.

$$t = \int_{r_a}^{r} \frac{dr}{m(E/P)} \tag{2}$$

where m, the electron mobility is the slope of the speed vs E/P curve.[19] Measurements[19,20] of drift speed for ^{3}He and Kr with 0.5% CO_2 indicate that within the limited range of E/P which is the most important in determining the drift time of electrons for cylindrical proportional counters, that this assumption of linearity does not appear to be unreasonable. Substituting the expression for field strength in the case of cylindrical coaxial geometry, we obtain the electron drift time from any radial position r.

$$t = \int_{r_a}^{r} \frac{dr}{m\left(\frac{V_o}{rP\ln\frac{r_c}{r_a}}\right)} = \frac{1}{m}\frac{P}{V_o}\ln\frac{r_c}{r_a}\int_{r_a}^{r} r\,dr$$

$$t = \frac{1}{m}\frac{P}{V_o}\ln\frac{r_c}{r_a}\left[\frac{r^2}{2}\right]_{r_a}^{r} \tag{3}$$

$$t \approx \frac{1}{2}\frac{1}{m}\frac{P}{V_o}\ln\frac{r_c}{r_a}\cdot r^2$$

Since $\frac{r_a^2}{2}$ is very small, the time necessary to travel from the surface of the anode to the geometrical center is negligible.

The development of Eq. 2 and 3 follows the logic developed by Harling.[19]

We still must determine however, some means of combining the mobilities of the electrons in a "gas mixture" since data is available only for mixtures of individual noble gases and moderating gases. A theoretical development of this "gas mixture" mobility problem was presented by Staub,[21] however the necessary gas constants are not available to compute the final result. We must therefore make use of assumption (d) and assume that as a first approximation, the electron mobilities behave as do ionic mobilities.

While it is realized that no simple theory can account for the electron diffusion, attachment, recombination, and agitation velocity, as the electron moves through a changing field gradient, it is considered that this approximation will cause at most an error of a constant factor. The electron mobilities are thus assumed to follow the same physical laws as do ions--although it is realized that the situation is considerably more complex for the fast moving electrons.

Staub's method of combining ion mobilities[21] is as follows:

$$\frac{1}{\mu_{12}} = \frac{P_1}{P} \cdot \frac{1}{\mu_1} + \frac{P_2}{P} \cdot \frac{1}{\mu_2}$$

where μ_{12} = the ion mobility in the gas mixture

$\mu_{1,2}$ = the ion mobility in the component gases

$P_{1,2}$ = partial pressures of the component gases

$P = P_1 + P_2$ = total gas pressure.

Substituting m (the electron mobility) for μ we have:

$$\frac{1}{m_{mix}} = \frac{P_{He}}{P_{tot}} \cdot \frac{1}{m_{He}} + \frac{P_{Kr}}{P_{tot}} \cdot \frac{1}{m_{Kr}} \qquad (4)$$

Using the sources explained in the footnote,* we find that for our tube

$$m_{He} = 0.3 \text{ cm}/\mu\text{-sec} \cdot \left(\frac{V}{cm} \cdot cm^{-1} \text{ Hg}\right)$$

$$m_{Kr} = 1.0 \text{ cm}/\mu \text{ sec} \cdot \left(\frac{V}{cm} \cdot cm^{-1} \text{ Hg}\right)$$

$$P_{He} = 2.01 \text{ atmosphere}$$

$$P_{Kr} = 10.05 \text{ atmospheres}$$

Substitution of the above values into Eq. 4 yields $m_{mix} = 0.72$ $\text{cm}/\mu\text{-sec} \cdot \left(\frac{V}{cm} \cdot cm^{-1} \text{Hg}\right)$. Utilizing this value in Eq. 3 and the appropriate counter dimensions we can plot migration time for an electron from any radial point in the counter. This has been accomplished in Fig. 4.for representative counter operating voltages.

2. Rise time. Rise time of the pulse has been defined as the time difference between the arrival of the first electron at the central counting wire and the arrival of the last electron. By use of assumptions (c) and (d)

*The mobility factor for Kr was taken from the data of English and Hanna.[20] The mobility factor for the helium is taken from the data of Friedes and Chrien,[11] which is plotted in reference 19 (Harling). The reason for this use of Friedes and Chrien's data rather than Harling's is that Harling, (1) made his measurements using ^4He with only small amounts of ^3He, and (2) he used substantial percentages of CO_2. Although drift velocity of electrons in ^3He appears to be rather insensitive to moderating gases, the CO_2 content of Friedes and Chrien was considerably less than that utilized by Harling.

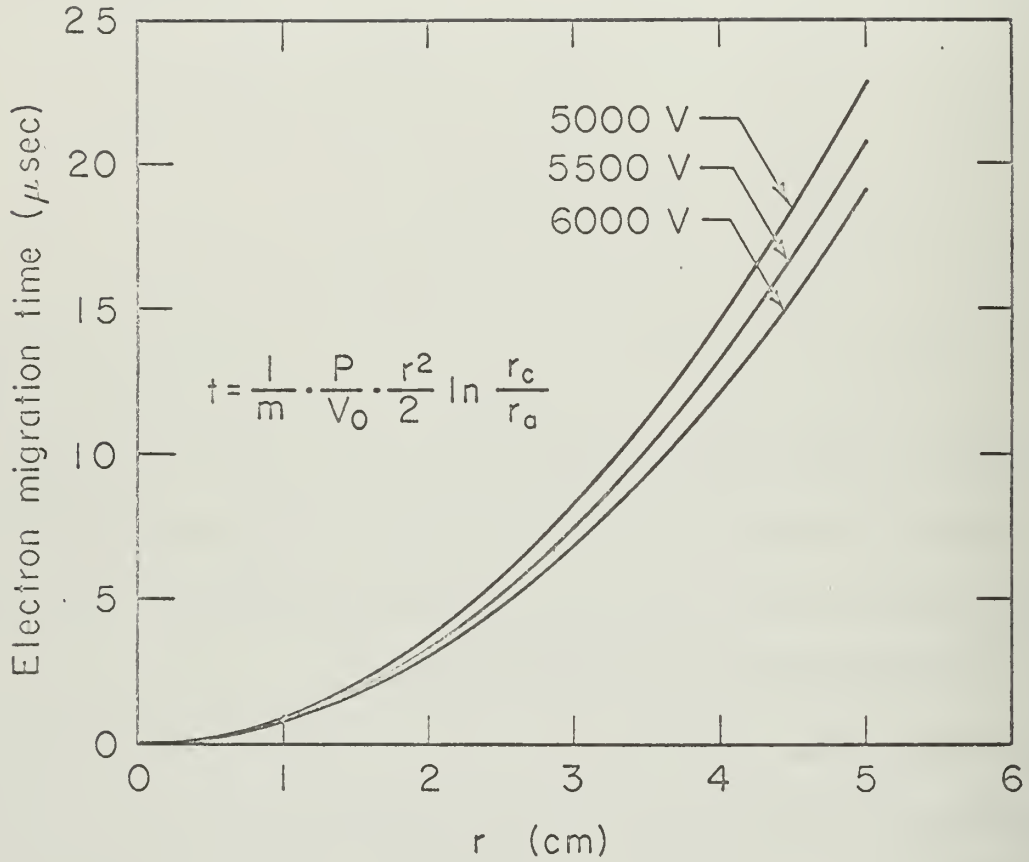

MU.37196

Fig. 4. Variation of Electron Migration Time from Various Radial Positions for Representative Voltages

we have been able to determine migration time, and have formulated an expression for the time for an electron to transit any radial distance. Thus the rise time (t_r) can be expressed as

$$t_r = t_2 - t_1 = \frac{1}{2}\,\frac{1}{m}\,\frac{P}{V_o}\,\ell n\,\frac{r_c}{r_a}\,\left(r_f^2 - r_n^2\right). \qquad (5)$$

Note that this is identical to the time that it takes an electron at position r_f (furthest distance) to migrate to r_n (nearest distance) if we charge the limits of Eq. 3 from r to r_f and r_a to r_n. We have previously noted that the field gradient charges very slowly beyond about 1 cm from the anode wire (see Fig. 3). Therefore, if we select our rise time discriminator in such a manner that pulses which spend their full energy within the active volume enclosed by a 1 cm radius are rejected. We can see that the assumption regarding the linear dependence of mobility and E/P is not too serious a concept since the pulses which depart from this assumed linear dependence(at high E/P values) are automatically eliminated. As it turns out, the "dead volume" of our counter will extend to about 2.75 cm, as will be shown later. Pulses which originate in the "dead volume" and extend outwards will be treated in detail later, as will pulses which do the reverse. (Section II-B.7)

3. Electron production. From the above, we now have a means of calculating rise times for electrons that are located at various radial distances in the counter active volume. We do not, however, have any indication of where these electrons will be located--in fact there will be

millions of electrons generated along the path length of a charged particle that is stopped in the gas medium. Let us now turn our attention to the formation of these electrons in a gas medium. We have previously discussed the various reactions that can occur with a ^3He neutron interaction, and have determined that only three of the five potential reactions are of interest in our counter. Neglecting the energy distribution within the three events for the moment,* let us now determine the ranges of the various particles in the gas medium.

Friedlander and Kennedy[22] present an empirical relationship for the determination of the ranges of charged particles in a gas mixture. This relationship, adapted for our specific usage, can be used to determine the ranges of protons, tritons, deuterons, and ^3He recoils as follows:

Range formulas for the individual gases (mg/cm^2)

Protons

$$R_p \text{ in Kr } (E) = R_p \text{ in air } (E) \left[1.89 - 0.25 \log_{10} (E)\right] - 0.36$$

$$R_p \text{ in He } (E) = R_p \text{ in air } (E) \left[0.82 + 0.043 \log_{10} (E)\right] \quad (6$$

^3He Recoils

$$R_{^3He} \text{ in Kr } (E) = \frac{3}{4} \left\{R_p \text{ in air } \left(\frac{E}{3}\right) \left[1.89 - 0.25 \log_{10} \left(\frac{E}{3}\right)\right] - 0.36\right\} \quad ($$

$$R_{^3He} \text{ in He } (E) = \frac{3}{4} R_p \text{ in air } \left(\frac{E}{3}\right) \left[0.82 + 0.043 \log_{10} \left(\frac{E}{3}\right)\right]$$

*The energy distribution is discussed in Appendix C and in Section II-B.6.

Tritons

$$R_T \text{ in Kr } (E) = 3\left\{R_P \text{ in air } \left(\frac{E}{3}\right)\left[1.89 - 0.25 \log_{10}\left(\frac{E}{3}\right)\right] - 0.36\right\} \quad (6c)$$

$$R_T \text{ in He } (E) = 3\, R_P \text{ in air } \left(\frac{E}{3}\right)\left[0.82 + 0.043 \log_{10}\left(\frac{E}{3}\right)\right]$$

Deuterons

$$R_d \text{ in Kr } (E) = 2\left\{R_P \text{ in air } \left(\frac{E}{2}\right)\left[1.89 - 0.25 \log_{10}\left(\frac{E}{2}\right)\right] - 0.36\right\} \quad (6d)$$

$$R_d \text{ in He } (E) = 2\, R_P \text{ in air } \left(\frac{E}{2}\right)\left[0.82 + 0.043 \log_{10}\left(\frac{E}{2}\right)\right]$$

The particle ranges can be converted into centimeters by use of the relationship:

$$\ell \text{ (cm)} = \frac{R_{tot} \text{ (mg/cm}^2\text{)}}{\left(\frac{P_{He}}{14.7}\right)\rho_{He} + \left(\frac{P_{Kr}}{14.7}\right)\rho_{Kr}} \quad (7)$$

where ℓ is the particle range in centimeters in the gas mixture,

P = partial pressure of the individual gases (psi)

ρ = gas density at STP

R_{tot} = total particle range in the gas mixture (see below)

$$\frac{1}{R_{tot}(E)} = \frac{W_{He}}{R_{He}(E)} + \frac{W_{Kr}}{R_{Kr}(E)} \quad (8)$$

W = weight fraction, $W_{He} + W_{Kr} = 1$

$$W_{He} = \frac{P_{He}\ \rho_{He}}{P_{He}\ \rho_{He} + P_{Kr}\ \rho_{Kr}}$$

$$W_{Kr} = \frac{P_{Kr}\ \rho_{Kr}}{P_{He}\ \rho_{He} + P_{Kr}\ \rho_{Kr}} = 1 - W_{He}$$

where

P = partial pressure of gas (psi)

ρ = gas density at STP

ρ_{He} = 0.16629 g/liter ($\dagger$)

ρ_{Kr} = 3.455 g/liter ($\dagger$)

The above relationships enable us to conveniently compute the ranges of the charged particle in the gas mixtures, and are amenable to machine computation. The ranges computed as above are plotted in Fig. 5 for comparison. Note the substantial difference in the length of the track for various particles of the same energy--particularly above about 1.0 MeV. It is this difference in track length that will enable us to remove the recoil spectrum from our spectrometer.

4. Rise time discriminator values. The rise time discriminator setting for the pulses can now be determined since we now have a means of determining the pulse rise times and the length of track of various particles in the gas medium. If we recognize that it is only the radial component of the track length that is important in our determination of rise time descrimination, we can select the most unfavorable recoil situation that may be encountered. Setting the discriminator at the rise time appropriate to this most unfavorable case, we will remove from consideration all pulses that can be attributed to recoils (^{3}He, C, O, and Kr). This worst case can be considered to be composed of two factors: (1) The maximum energy that can be imparted to a recoil nucleus, and (2) the longest rise time that this maximum energy recoil can cause, due

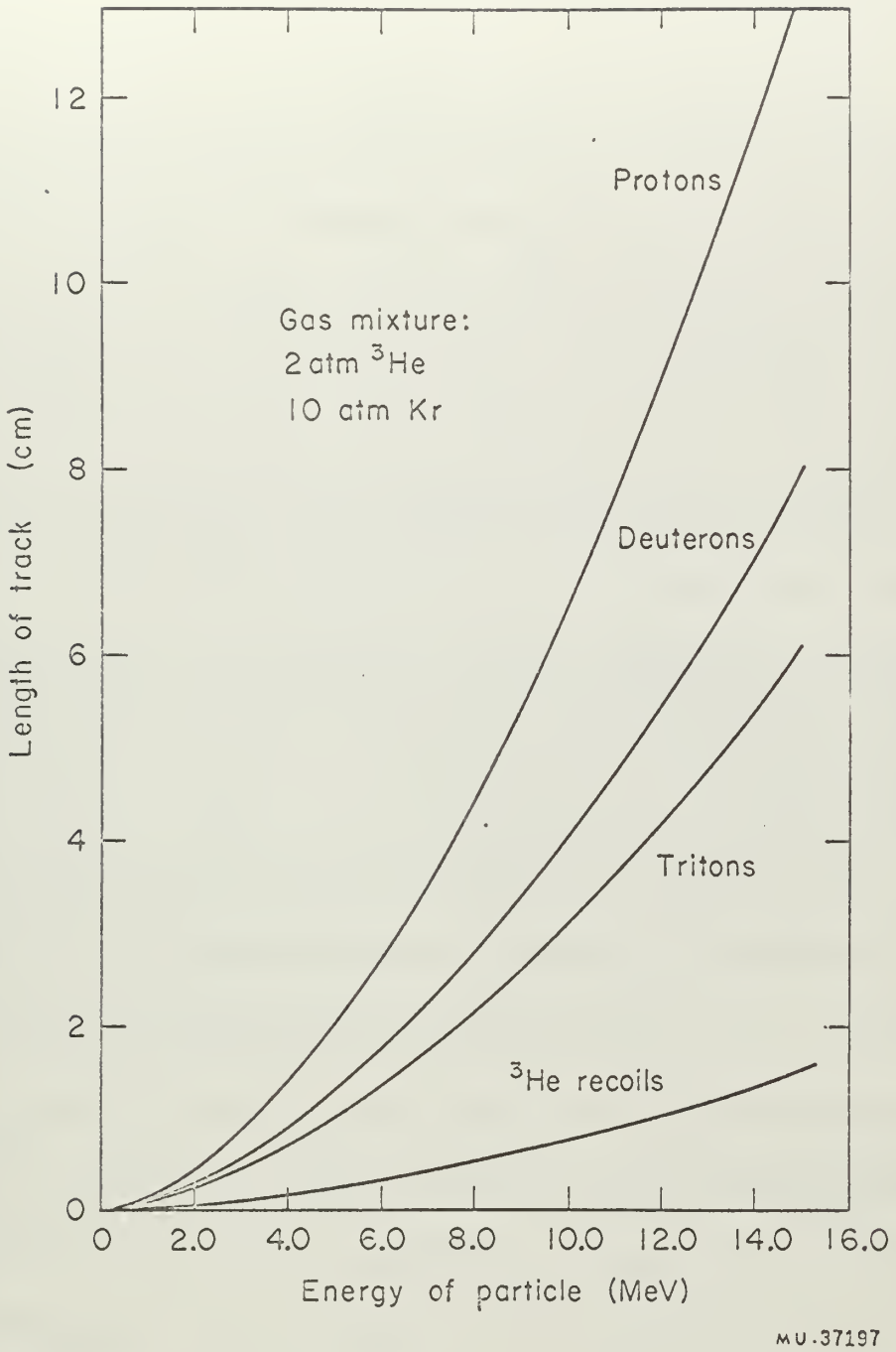

Fig. 5. Ranges of Various Charged Particles in Gas Mixture of 10 Atmos. Kr, 2 Atmos. ^{3}He, and 0.5% CO_2

to its geometrical position in the counter.

Appendix B (Case 1) summarizes the maximum energy that can be imparted to the various recoil nuclei. It can be readily seen that the ^3He nucleus can absorb up to a maximum of 3/4 the energy of the incident neutron. The other possibilities for energy absorption are of considerably smaller magnitude. The ^3He recoil is thus selected as the recoil of concern. The ranges of the other recoil particles in the gas mixture is likewise less for equal energies when compared with ^3He. The worst geometrical case that can occur is if the track length of the recoil ^3He nucleus is oriented in a directly radial position with one end of the track at an infinitesimal distance from the wall of the cathode. This positioning is illustrated in Fig. 6.

Rise time discriminator setting can then be determined by:

(1) calculating the maximum recoil energy that can be imparted

$$E_{^3He}\ (max) = 0.75\ E_N\ (max)$$

(2) determining the path length in the gas medium, $\ell(E_{^3He}\ (max))$ from the equations presented in Part II-B3,2.

(3) determine maximum rise time by substituting into Eq. 5 the value b, the radius of the cathode, for r_f, and $[b - \ell(E_{^3He}\ (max))]$ for r_n.

This rise time discriminator setting (t_r') will then exclude all recoils from the resultant spectra.

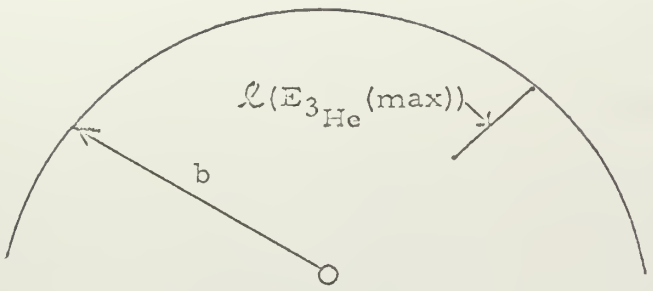

Fig. 6. ^{3}He recoil track position to give maximum pulse rise time.

5. Determination of radial positions of the nearest (r_n) and furthest (r_f) electrons from the anode for ^{3}He(n, p)T and ^{3}He(n, d)D reactions.

Consider the fact that to define the positioning of any event in space, it is necessary to define six degrees of freedom. Three of these degrees of freedom are necessary to define the positioning of the center of gravity, and three are required to explain the orientation of the event with respect to the center of gravity. For the purposes of discussion, let us assume that we can define the "center of gravity" as the position where the neutron strikes a ^{3}He atom. Since the reaction occurs within the boundaries of the counting tube, we can define the positioning of the event (center of gravity) in cylindrical coordinates of radius, length, and angular dependence. The operation of the counter, however, is independent of the positioning of the event in terms of length (except for end effects, which will be discussed later) and completely independent of any angular relationship,

with respect to the anode wire. This means that the positioning of the center of gravity can be defined in terms of a single parameter r.

To define the orientation of the resultant ionization tracks produced by ^3He disintegration let us first turn our attention to the $^3He(n, p)T$ reaction. For a neutron of given energy E_n, and given resultant proton energy E_p, we can determine the energy E_T of the triton particle and the laboratory angle α_L between the proton vector and the triton vector by use of the relationships developed in Appendix B.

$$E_T = E_N + Q_{n,p} - E_P \tag{9}$$

and

$$\cos \alpha_L = - \frac{(2 E_T + Q_{n,p})}{2\sqrt{3 E_T E_P}} \tag{10}$$

Note that α is always obtuse in the laboratory system of coordinates.

Let us now define a coordinate system. The coordinate system for our calculations is selected as follows:

(1) The event occurs at a perpendicular radial distance r_0 from the center line of the anode. The end point of r_0 defines the zero point (0, 0, 0) of the coordinate axis.

(2) The z axis is selected to include the vector r and extensions thereof.

(3) The x axis extends parallel to the anode wire and passes through the point (0, 0, 0).

(4) The y axis passes through the point (0, 0, 0) defined as above, and is mutually perpendicular to the x and z axis.

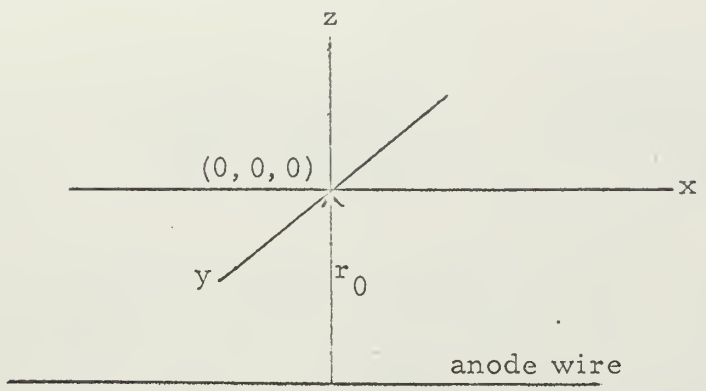

Fig. 7. .Selection of coordinate system.

With this selection of coordinate axis, the event is angularly independent of the center anode wire. Calculations of the path orientations of the ionizing tracks will be made in terms of polar coordinates using these axes as reference lines. We must now determine the distances of the nearest and farthest electrons from the anode wire. For the purpose of illustration let us visualize the E_P and E_T track lengths as solid lines. The orientation of these two vectors can have three degrees of freedom. Let us select the three rotational axes as shown in Fig. 8.

Neglecting for the moment the E_T vector, let us turn our attention to the E_P vector.

We are able to define a position r_2 which we call the tip of the E_P

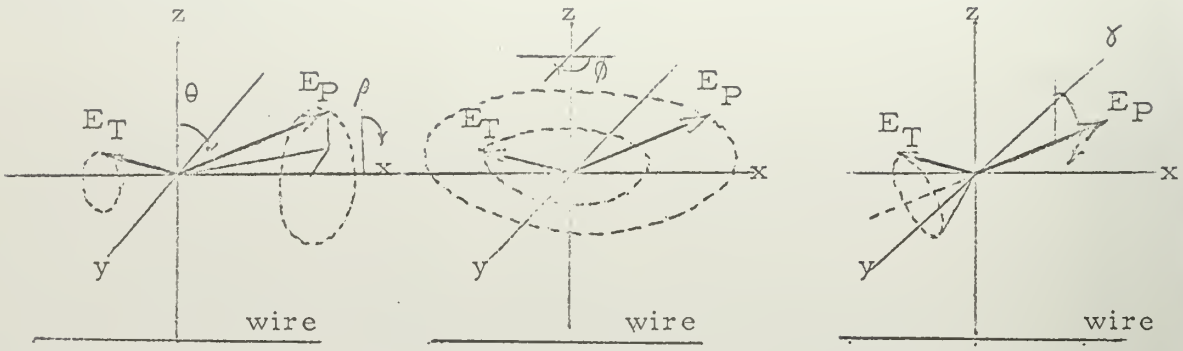

Fig. 8. Rotational axes.

vector. (We will refer to the E_P vector, although in reality we are speaking of a definite length of path of a proton of set energy in the counter gas medium.) We can completely describe this point r_2 with respect to our coordinate axis by the polar angle θ_2, the asmuthal angle ϕ_2 and the length of the vector E_P. We can thus determine $r_2(E_P, \theta_2, \phi_2)$

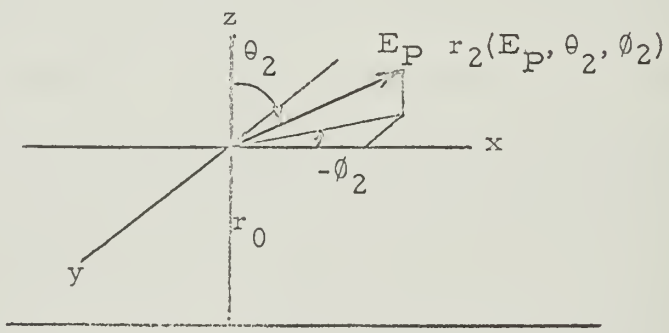

Fig. 9. $r_2(E_P, \theta_2, \phi_2)$.

We need an expression of r_2 in terms of r_0 since in determining migration times we are concerned with the radial distance from the central

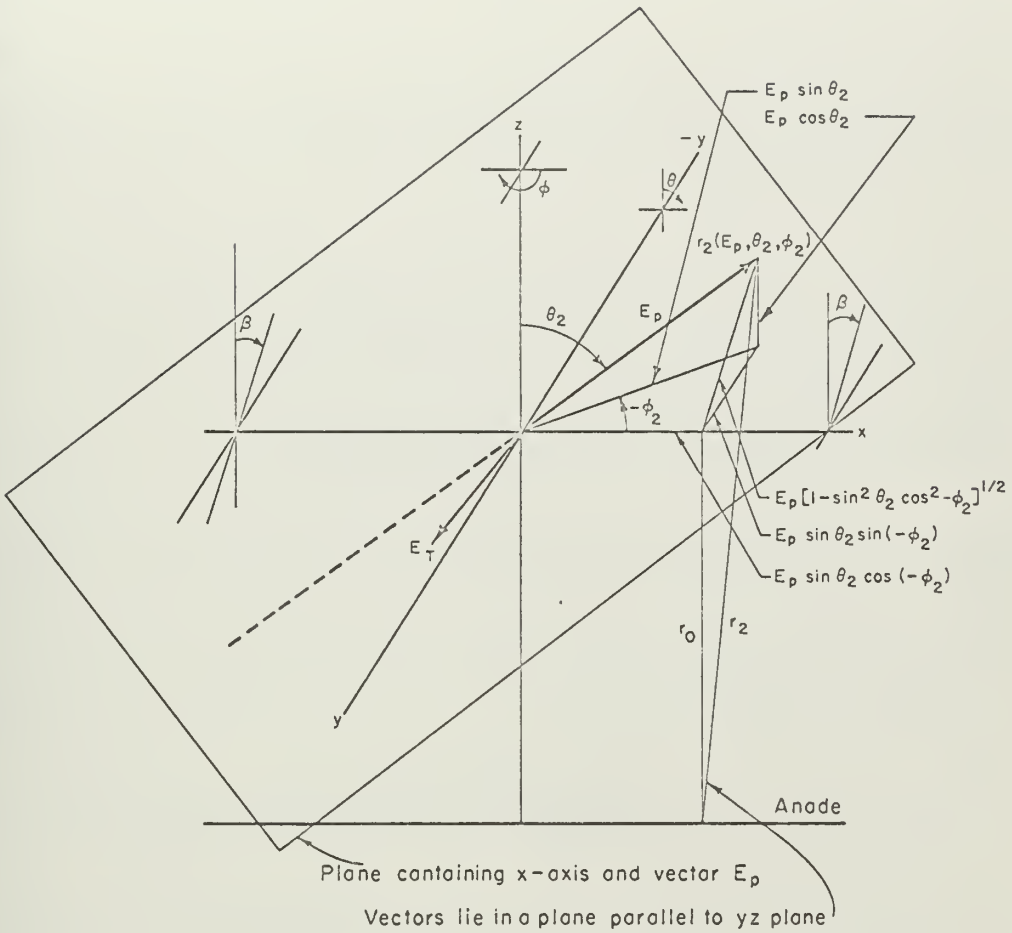

Fig. 10. Determination of $r_2(r_0, E_p, \theta_2, \phi_2)$

counting wire to the point $r_2\ (E_P, \theta_2, \phi_2)$, i.e. we need an expression of $r_2(r_0, E_P, \theta_2, \phi_2)$. To determine this expression let us pass a plane which contains the x axis and the vector E_P (a plane can be defined by two intersecting lines). This plane will intersect the z axis at (0, 0, 0) and will make an angle β with the z axis in the minus y direction. Referring to Fig. 10 we can derive an expression for $r_2(r_0, E_P, \theta_2, \phi_2)$. By the law of cosines:

$$r_2^2 = r_0^2 + E_P^2[1 - \sin^2\theta_2 \cos^2(-\phi_2)] - 2 r_0 E_P[1 - \sin^2\theta_2 \cos^2(-\phi_2)]^{1/2} \cdot \cos(180$$

but, $\cos(180 -) = -\cos\beta$

and from Fig. 10, $-\cos\beta = -\dfrac{E_P \cos\theta_2}{E_P[1 - \sin^2\theta_2 \cos^2(-\phi_2)]^{1/2}}$,

substituting this value for $\cos\beta$ into the above equation, we find that

$$r_2^2 = r_0^2 + E_P^2[1 - \sin^2\theta_2 \cos^2(-\phi_2)] + 2 r_0 E_P \cos\theta_2$$

or

$$r_2(r_0, E_P, \theta_2, \phi_2) = \sqrt{r_0^2 + E_P^2[1 - \sin^2\theta_2 \cos^2(-\phi_2)] + 2 r_0 E_P \cos\theta_2} \qquad (1$$

Let us now consider the possibility that since we have not placed a restriction on where our event can occur, that a skew line may develop and that the closest point to the anode wire may in fact lie somewhere along the length of vector E_P, rather than at the end point. Since E_P is a definite length in the gas medium for a given energy of the proton, let us call this length $\ell(E_P)$. An axiom of solid geometry is that the closest point of approach for skew lines is at a point where a line

connecting the skew lines is perpendicular to each. This means that a minimum distance can be determined. We have an expression for the length r_2. Therefore, if we take a partial derivative of r_2 with respect to E_p (note that this is actually $\ell(E_p)$)and set it equal to zero, we can determine a distance ℓ_p along the $\ell(E_p)$ vector whereby the skew lines are closest. We will call the closest distance between the vector E_p and the anode wire r_4.

$$\frac{\partial r_2}{\partial \ell(E_p)} = \frac{1}{2}\left(r_0^2 + \ell(E_p)^2\left[1 - \sin^2\theta_2 \cos^2(-\theta_2)\right] + 2\ell(E_p) r_0 \cos\theta_2\right)^{-1/2} \cdot \left[2\ell(E_p)\left(1 - \sin^2\theta_2 \cos^2(-\phi_2)\right) + 2 r_0 \cos\theta_2\right]$$

Set the above expression equal to zero and solve for ℓ_p; note that the first bracketed term can never equal zero. For real values of ℓ_p we obtain

$$\ell_p = -\frac{r_0 \cos\theta_2}{\left[1 - \sin^2\theta_2 \cos^2(-\phi_2)\right]} \qquad (12)$$

where $0 < \ell_p < \ell(E_p)$.

The negative sign indicates that ℓ_p cannot be positive unless θ_2 is greater than 90°. This is in accordance with the physical situation envisioned and the selection of the coordinate axes. At $\theta_2 = \pi$, ℓ_p must equal r_0 and the E_p vector is perpendicular to the anode wire. ℓ_p cannot exceed the physical length of E_p which has been assigned.

Substitution of this value of ℓ_p into Eq. 11 for E_p determines that:

$$r_4 = \sqrt{r_0^2 + \frac{r_0^2 \cos^2\theta_2 \cdot \left[1 - \sin^2\theta_2 \cos^2(-\phi_2)\right]}{\left[1 - \sin^2\theta_2 \cos^2(-\phi_2)\right]^2} - \frac{2 r_0^2 \cos^2\theta_2}{\left[1 - \sin^2\theta_2 \cos^2(-\phi_2)\right]}}$$

or

$$r_4 = r_0 \sqrt{1 - \frac{\cos^2\theta_2}{\left[1 - \sin^2\theta_2 \cos^2(-\phi_2)\right]}}$$

where $\frac{\pi}{2} \leq \theta_2 < \pi$

and $0 < \ell_p < \ell(E_p)$

Let us now turn our attention to the other portion of the ^{3}He (n, p)T event. Let us consider the E_T vector.

In a manner similar to the determination of the end of the proton vector E_p, we can position the end of the triton vector E_T. We shall call this position $r_1(E_T, \theta_1, \phi_1)$

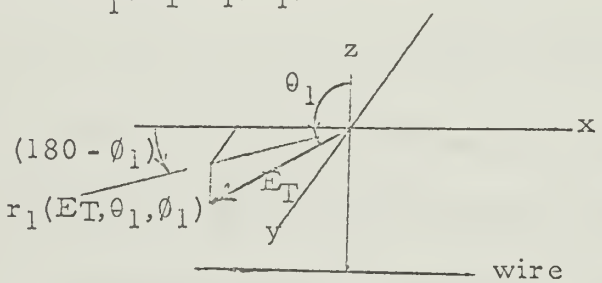

Fig. 11. $r_1(E_T, \theta_1, \phi_1)$

In the case of the triton however, we cannot arbitrarily describe the position of the end of the E_T vector with respect to the anode wire, since

there exists a unique relationship for the positioning of the triton vector for a given neutron and proton energy. (E_N and E_P respectively.) This relationship is characterized by the angle α_L, which is the obtuse angle between the proton and triton. We must therefore consider this constraint upon the direction that the triton can travel. We can visualize this restriction by the following:

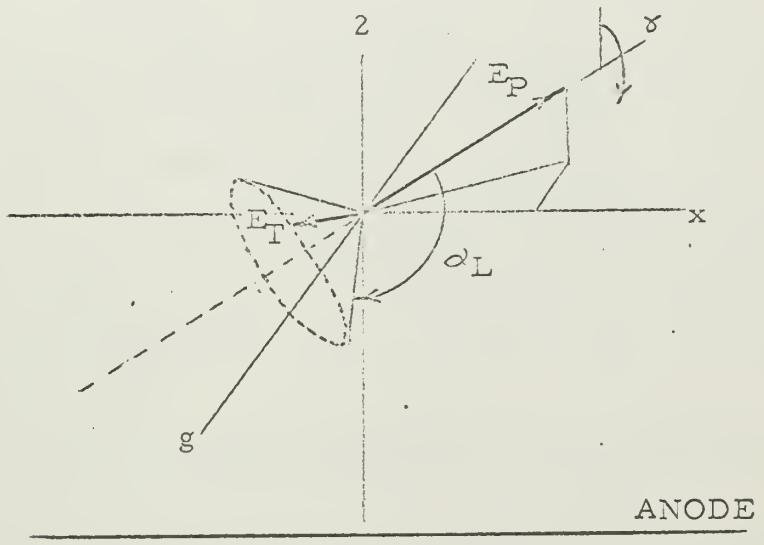

Fig. 12. Rotation of E_T vector about E_P axis.

If we were to rotate the E_P vector in Fig. 12 about its own axis while imagining that the E_T vector is rigidly attached to the E_P vector at an angle α_L from the axis of the E_P vector, we can see that the tip of the E_T vector would trace a circle in a plane that is perpendicular to the E_P vector. The determination of the radial distance to the center wire $r_1(r_0, E_T, \theta_1, \phi_1)$ must take this degree of freedom into account.

Let us now examine Fig. 13. The interior angle of the cone described

by the rotation of E_T is $(180 - \alpha_L)$. Let us now pass a plane through the z axis and containing the E_P vector. Since this plane contains the z axi it will by definition be perpendicular to the plane containing the x and y axis. We will use this plane to relate θ_1 to θ_2, and ϕ_1 to ϕ_2. Let us consider the rotation of the E_P vector from a "zero position" where the E_T vector is at a maximum position away from the center wire (i.e. top position) and is contained in the (z, E_P) plane. The E_P vector is then rotated in a counter clockwise manner (viewed from the tip of the E_P vector). The angle of rotation we call γ. By projecting the E_T vector back to the plane containing E_P and z we can determine the incremental angle between θ_1 and $(180 - \theta_2)$ this incremental angle is

$$\sin^{-1}\left[\frac{E \sin\alpha_L \cos\gamma}{E_T (1 - \sin^2\alpha_L \sin^2\gamma)^{1/2}}\right] \text{or} \quad \sin^{-1}\left[\frac{\sin\alpha_L \cos\gamma}{(1 - \sin^2\alpha_L \sin^2\gamma)^{1/2}}\right]$$

therefore θ_1 is related to θ_2 by

$$\theta_1 = (180 - \theta_2) \pm \sin^{-1}\left[\frac{\sin\alpha_L \cos\gamma}{(1 - \sin^2\alpha_L \sin^2\gamma)^{1/2}}\right]$$

or

$$\theta_1 = 180 - \theta_2 \pm \sin^{-1}\left[\frac{\sin\alpha_L \cos\gamma}{(1 - \sin^2\alpha_L \sin^2\gamma)^{1/2}}\right] \quad (1$$

where α_L as determined by E_N and E_P is a constant, γ varies from 0 to 2π. The sign of the incremental angle is positive for $-\frac{\pi}{2} < \gamma < \frac{\pi}{2}$ and negative for $\frac{\pi}{2} < \gamma < \frac{3}{2}\pi$. θ_2 is arbitrarily selected.

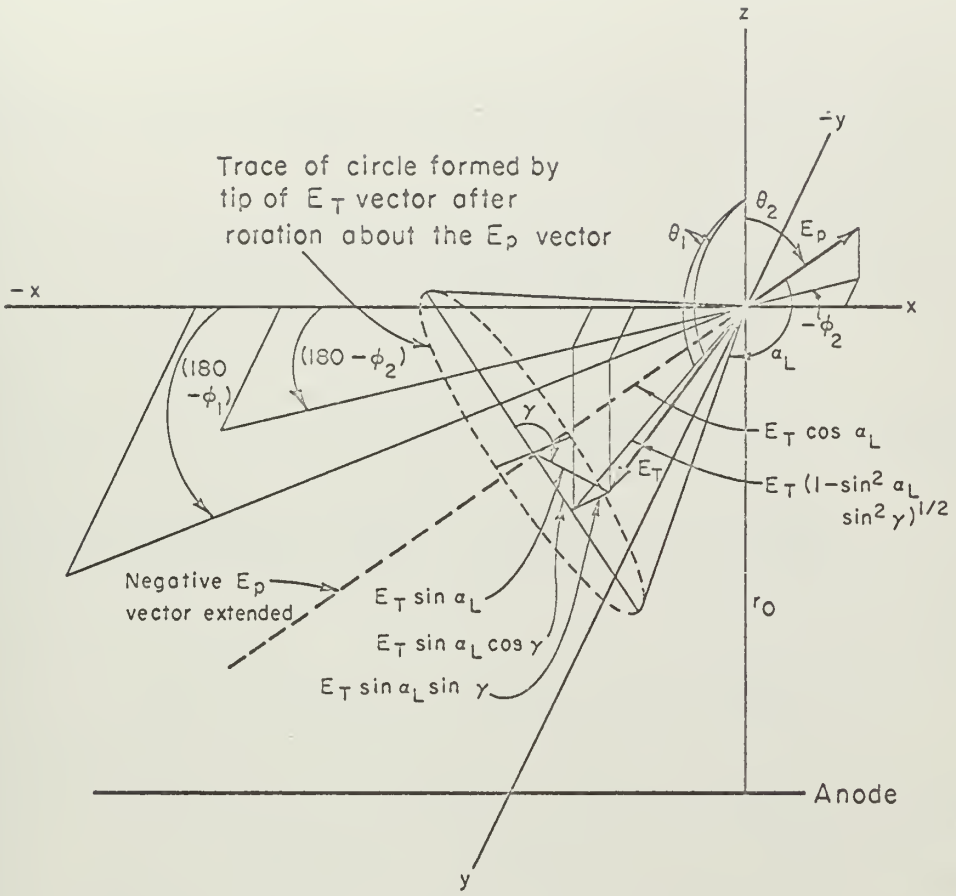

Note: Vector E_T shown exaggerated in size with respect to E_p for clarity of angular relationships.

MU-37201

Fig. 13. Determining Relationship Between θ_2 and θ_1, and ϕ_2 and ϕ_1

If we likewise were to consider the perpendicular projection of the tip of the E_T vector to the (E_P, z) plane we can readily determine that since this projection is perpendicular to the (E_P, z) plane, it must of necessity be parallel to x - y plane. We may therefore compute the incremental angle between ϕ_1 and ϕ_2, and determine a relationship between them. The incremental angle is

$$\cos^{-1} \left[\frac{E_T \left(1 - \sin^2 \alpha_L \sin^2 \gamma\right)^{1/2}}{E_T} \right]$$

Therefore, the relationship between ϕ_1 and ϕ_2 can be expressed as

$$(180 - \phi_1) = (180 - \phi_2) - \cos^{-1} \left[\left(1 - \sin^2 \alpha_L \sin^2 \gamma\right) \right]^{1/2}$$

or

$$\phi_1 = \phi_2 \pm \cos^{-1} \left[\left(1 - \sin^2 \alpha_L \sin^2 \gamma\right)^{1/2} \right]$$

where the negative sign of the square root is taken for $0 < \gamma < \pi$ and the positive square root is taken for $\pi < \gamma < 2\pi$

α_L is a constant determined by fixed E_P and E_N

ϕ_2 is arbitrary

Having now established a relationship between θ_1 and θ_2, ϕ_1 and ϕ_2 through the constant angle α_L and the rotational angle γ, let us now proceed to determine $r_1(r_0, E_T, \theta_1, \phi_1)$.

Referring to Fig. 14, the same procedure can be followed as was used for the computation of $r_2(r_0, E_P, \theta_2, \phi_2)$ in Fig. 10. We arrive at

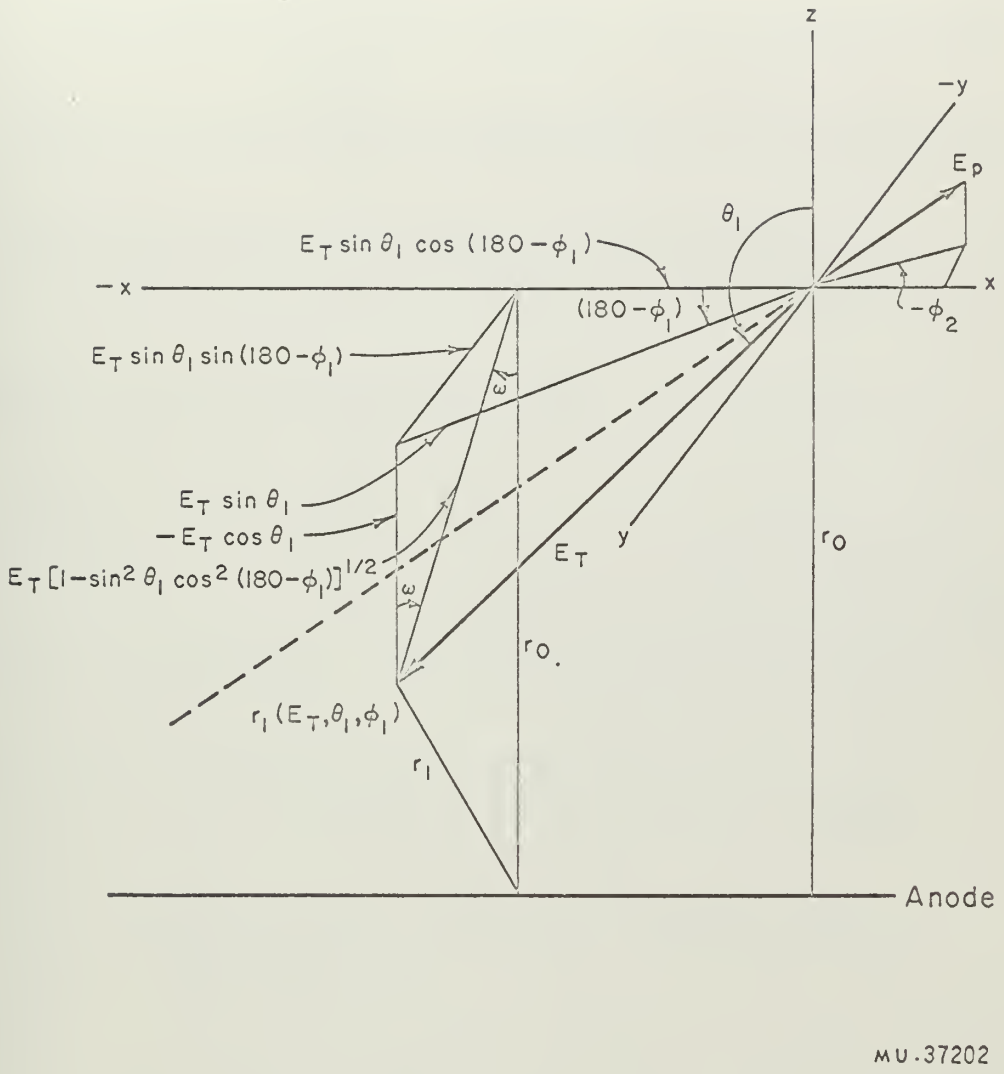

Fig. 14. Determination of $r_1(r_0, E_T, \theta_1, \phi_1)$

the relationship

$$r_1^2 = r_0^2 + E_T^2 \left[1 - \sin^2 \theta_1 \cos^2 (180 - \phi_1)\right] - 2 r_0 E_T \left[1 - \sin^2 \theta_1 \cos^2 (180 - \phi_1)\right]^{1}$$

but from Fig. 14, $\cos \omega = \dfrac{E_T \cos \theta_1}{E_T \left[1 - \sin^2 \theta_1 \cos^2 (180 - \phi_1)\right]^{1/2}}$

substituting this value into the above relationship we find that

$$r_1 = \sqrt{r_0^2 + E_T^2 \left[1 - \sin^2 \theta_1 \cos^2 (180 - \phi_1)\right] - 2 r_0 E_T \cos \theta_1} \qquad (15)$$

The possibility of a "skew" condition must likewise be considered in case of the E_T vector. The length (ℓ_T) must be determined and substituted into Eq. 16. The partial derivative of r_1 with respect to $\ell(E_T)$ must be taken and set equal to zero,

thus:

$$\frac{\partial r_1}{\partial \ell(E_T)} = \frac{1}{2} \left[r_0^2 + \ell(E_T)^2 \left[1 - \sin^2 \theta_1 \cos^2 (180 - \phi_1)\right] - 2 r_0 \ell(E_T) \cos \theta\right.$$

$$\cdot \left[2 \ell(E_T) \left[1 - \sin^2 \theta_1 \cos^2 (180 - \phi_1)\right] - 2 r_0 \cos \theta_1\right] = 0$$

Solving for ℓ_T we find that

$$\ell_T = \frac{r_0 \cos \theta_1}{\left[1 - \sin^2 \theta_1 \cos^2 (180 - \phi_1)\right]} \qquad (1$$

for $0 < \ell_T < \ell(E_T)$

substituting this value back into Eq. 16 and calling this closest point of approach r_3, we find that

$$r_3 = \sqrt{r_0^2 + \frac{r_0^2 \cos^2\theta_1 \left[1 - \sin^2\theta_1 \cos^2(180 - \phi_1)\right]}{\left[1 - \sin^2\theta_1 \cos^2(180 - \phi_1)\right]^2} - \frac{2 r_0^2 \cos^2\theta_1}{\left[1 - \sin^2\theta_1 \cos^2(180 - \phi_1)\right]}}$$

or (18)

$$r_3 = r_0 \sqrt{1 - \frac{\cos^2\theta_1}{\left[1 - \sin^2\theta_1 \cos^2(180 - \phi_1)\right]}}$$

Summarizing the calculations for radial distances from the center wire, given E_N, E_P, and r_0 we must calculate four additional radial distances for each E_P, E_T vector pair.

$$E_T = E_N + Q - E_P \tag{9}$$

$$r_0 = r_0$$

$$r_2 = \sqrt{r_0^2 + E_P^2 \left[1 - \sin^2\theta_2 \cos^2(-\phi_2)\right] + 2 r_0 E_P \cos\theta_2} \tag{11}$$

$$r_4 = r_0 \sqrt{1 - \frac{\cos^2\theta_2}{\left[1 - \sin^2\theta_2 \cos^2(-\phi_2)\right]}} \tag{13}$$

(only necessary to compute r_4 where $\frac{\pi}{2} \leq \theta_2 < \pi$ and $0 < \ell_P < E_P$)

$$r_1 = \sqrt{r_0^2 + E_T^2 \left[1 - \sin^2\theta_1 \cos^2(180 - \phi_1)\right] - 2 r_0 E_T \cos\theta_1} \tag{16}$$

$$r_3 = r_0 \sqrt{1 - \frac{\cos^2\theta_1}{\left[1 - \sin^2\theta_1 \cos^2(180 - \phi_1)\right]}} \tag{18}$$

and:

$$\theta_1 = 180 - \theta_2 \pm \sin^{-1}\left[\frac{\sin\alpha_L \cos\gamma}{\left(1 - \sin^2\alpha_L \sin^2\gamma\right)^{1/2}}\right] \quad \text{where } \cos\alpha = -\frac{(2E_T + Q)}{2\sqrt{3 E_T E_P}} \tag{14}$$

The sign of the incremental angle is as follows: plus for $-\frac{3}{2}\pi < \gamma < \frac{\pi}{2}$, minus if $\frac{\pi}{2} < \gamma < \frac{3\pi}{2}$

$$\phi = \phi_2 \mp \cos^{-1} \left[1 - \sin^2 \alpha_L \sin^2 \gamma\right]^{1/2} \qquad (15$$

The sign of the incremental angle is taken as negative for $0 < \gamma < \pi$ and positive for $\pi < \gamma < 2$.

It has thus been shown that all possible combinations of radial distances from the center wire can be calculated in terms of known E_N, E_P, and r_0 in terms of θ_2, ϕ_2, γ, and α_L.

If r_0, r_1, r_2, r_3, and r_4 are calculated for a given event, and the maximum and the minimum radial distances taken as the positions of the most distant electron, r_f, and the nearest electron r_n to reach the central counting wire, we now have the distances to substitute into the equation for determining rise time.

Deuteron radial distances

For the reaction involving deuterons, there is an analogous relationship to the proceeding if we replace E_P with E_{D2}, E_T with E_{D2}, and α_L with the relationship: (see Appendix B)

$$\cos\alpha_L = - \frac{(Q_{n,d} + E_{D2} + E_{D1})}{4\sqrt{E_{D1}\ E_{D2}}} \qquad (19)$$

thus, given E_N, E_{D2}, and r_0

$$E_{D1} = E_N - E_{D2} + Q_{n,d} \tag{20}$$

$$r_0 = r_0$$

$$r_2 = \sqrt{r_0^2 + E_{D2}^2 \left[1 - \sin^2 \theta_2 \cos^2 (-\theta_2)\right] + 2 r_0 E_{D2} \cos \theta_2} \tag{21}$$

$$r_4 = r_0 \sqrt{1 - \frac{\cos^2 \theta_2}{\left[1 - \sin^2 \theta_2 \cos^2 (-\phi_2)\right]}} \tag{22}$$

(only necessary to compute r_4 when $\frac{\pi}{2} < \theta_2 < \pi$ and $0 < \ell_{D2} < \ell(E_{D2})$

$$r_1 = \sqrt{r_0^2 + E_{D1}^2 \left[1 - \sin^2 \theta_1 \cos^2 (180 - \phi_1)\right] - 2 r_0 E_{D1} \cos \theta_1} \tag{23}$$

$$r_3 = r_0 \sqrt{1 - \frac{\cos^2 \theta_1}{\left[1 - \sin^2 \theta_1 \cos^2 (180 - \phi_1)\right]}} \quad 0 < \ell_{D1} < \ell(E_{D1}) \tag{24}$$

and $$\theta_1 = 180 - \theta_2 \pm \sin^{-1} \left[\frac{\sin \alpha_L \cos \gamma}{\left[1 - \sin^2 \alpha_L \sin^2 \gamma\right]^{1/2}} \right] \tag{25}$$

The sign of the incremental angle is as follows: plus for $\frac{-3\pi}{2} < \gamma < \frac{\pi}{2}$, minus if $\frac{\pi}{2} < \gamma < \frac{3}{2}$ and $\phi_1 = \phi_2 \mp \cos^{-1} \left[(1 - \sin^2 \alpha_L \sin^2 \gamma)\right]^{1/2}$ (26)

where the incremental angle is positive for $\pi \quad \gamma < 2 <$ and negative for $0 < \gamma < \pi$.

6. Development of the probability function (P_R) for the replacement of pulses removed by rise time discrimination.

We have now developed a means whereby the rise time of any valid pulse (i.e. not a recoil) can be determined for any possible energy distribution and spatial configuration of the ^3He (n, p)T and the ^3He(n, d)D reaction. If we were to vary E_P, r_0, cos θ, ϕ, and γ over all possible ranges,* a tabulation of rise times t_r can be made for each incoming neutron energy. Before this tabulation can be accomplished however, three additional conditions must be considered.

(1) The volume probability of an event occurring at a distance r is greater at points that are distant from the anode. In Fig. 15 below, an end view of the counter tube is shown. The volume probability g(r) of a reaction occurrence at r within a differential element dr is:

$$g(r)dr = \frac{2\pi r\, dr}{\pi b^2} = \frac{2r\, dr}{b^2}$$

where b is the radius of the cathode.

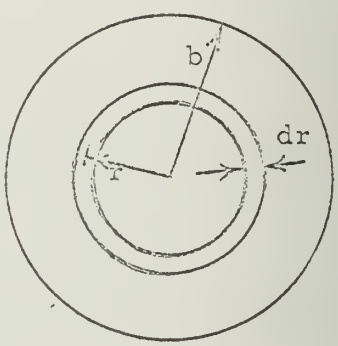

Fig. 15. Volume probability in the radial direction.

*E_P will vary from $E_{P\,max}$ to $E_{P\,min}$ for a set neutron energy. Any energy within these limits is equally possible. Cos θ is selected as a variable since the selection of θ would result in undue weighting of the rise times near the polar angles. A discussion of these factors is included in Appendix C. It is assumed that the applied voltage is held constant in the

Therefore, events occurring at various distances r from the centerline of the counter must be weighted in accordance with their volume probability.

(2) Thus far, the finite size of our tube has not been considered in the determination of rise times. It becomes obvious that some of the energy vectors will intersect the walls of the cylinder, and that the ionizing tracks will be stopped short of their full length. In this case a pulse of lower energy and rise time will result. An additional constraint must therefore be placed upon the calculations of the various r's (i.e. r_1, r_2, r_3, r_4) in the preceding section, viz, if any of the r's exceeds b, then the pulse must be considered as a "short pulse." Short pulses will be divided into two possibilities:

(a). The radial component of the track lengths is still sufficient to cause the pulse rise time to be above the rise time discriminator level t_r'. This will cause a count to be registered in a lower energy channel. The rise time is computed using b as r_f. This type of pulse will be designated as a "wall effect pulse" (W. E. P.) and will be totaled separately.

(b) The radial component of the track lengths is insufficient to cause a pulse to be registered in any energy channel. The rise time will be computed however, using b as the maximum of the r's and catalogued in the appropriate rise time channel.

For "bookkeeping" purposes it is necessary that the above two possibilities for "short pulses" be catalogued in the same energy channel appropriate to the $(E_N + Q)$ considered for a pulse that goes full length

in the track medium. They are not to be catalogued in the energy channel corresponding to their reduced length. Wall effects are separately remov and if these degenerate pulses were removed twice, it would distort the spectrum.

Each time the rise time discriminator setting is changed the above two possibilities for "short pulses" must be recomputed.

(3) To compare the rise time spectrum from the (n, p) and (n, d) reaction it is necessary that the two reactions have a common reference conditions. This common reference condition can be met if it is stipulated that the number of rise time situations considered for each incoming neutron ener be the same. The variables for the rise time spectrum (for a set neutron energy E_N, fixed rise time discriminator setting, and fixed applied voltag are: three angles ($\cos\theta$, ϕ, and γ), distance r_0, and an energy distributio of E_p. The angle variations are identical for each case considered, the variation of r_0 will be identical, but the E can vary from an $E_{p\ max}$ to $E_{p\ min}$, the values of which are dependent on the energy of the incoming neutron. We must therefore consider in our tabulations that an identical number of energy increments (not identical energy increments) be taken between $E_{p\ max}$ and $E_{p\ min}$ regardless of the energy of the incoming neutron. Note that since only a ratio is eventually desired, this condition merely increases the numerator and denominator of the ratio by a constan factor.

All three of the above conditions are likewise applicable to the deuter reactions, as shown in the following discussion.

Table I. Number of (n, p) Pulses for Various Rise Times at Energy $(E_N + Q)$

r (cm)	$\frac{r}{b^2}$	Number of wall effect pulses	N(WEP) $\times \frac{r}{b^2}$	Number of pulses with 1 μsec rise time	N(1 μsec) $\times \frac{r}{b^2}$	Number of pulses having 2 μsec rise time	N(2 μsec) $\times \frac{r}{b^2}$	. . .	Number of pulses having 30 μsec rise time	N(30 μsec) $\times \frac{r}{b^2}$
r_a										
r_b										
r_c										
r_d										
.										
.										
.										
b										
			$\sum_{r=0}^{r=b} N(WEP) \cdot \frac{r}{b^2}$		$\sum_{r=0}^{r=b} N(1\,\mu sec) \cdot \frac{r}{b^2}$		$\sum_{r=0}^{r=b} N(2\,\mu sec) \cdot \frac{r}{b^2}$			$\sum_{r=0}^{r=b} N(30\,\mu sec) \cdot \frac{r}{b^2}$

A tabulation of the number of occurrences of pulses having the same rise time for each $(E_N + Q)$ channel can now be formed. This can be accomplished in the following manner (see Table I): For each $(E_N + Q_{n,p})$ channel, i.e. the energy of the incoming neutron plus the $Q_{n,p}$ of the reaction, a reaction site r_a is selected. The energy distribution of the particles produced by the reaction is varied in a number of energy increments from $E_{P\ max}$ to $E_{P\ min}$. Note that the total energy available is constant at $(E_N + Q)$ since we have not varied the energy of the incoming neutron. The three angular relations are also varied over all possible configurations. For each energy increment, and for each angular configuration, the pulse rise time is calculated and tabulated. The number of pulses that have rise times at 1 μsec, 2 μsec, etc. are summarized and multiplied by the weighting function $\frac{r}{b^2}$. The reaction site is moved a small radial distance outward and the process is repeated. This tabulation continues until the reaction site is an infinitesimal distance from the cathode. The volume weighted number of pulses of the same rise time is then totaled;

$$\sum_{\text{all counts}} \cdot dr = \left[\sum_{r=0}^{r=b} N(\text{WEP}) \cdot \frac{r}{b^2} + \sum_{r=0}^{r=b} N(1\,\mu\text{sec}) \frac{r}{b^2} + \sum_{r=0}^{r=b} N(2\,\mu\text{sec}) \frac{r}{b^2} + \ldots + \sum_{r=0}^{r=b} N(30\,\mu\text{sec}) \frac{r}{b^2} \right] \cdot dr$$

where dr can be any constant and is added merely to remove the dimensiona dependence of cm^{-1}. For finite differences in r, the interval between the

r_a and r_b could be selected.

The above tabulation is repeated for all values of $(E_N + Q)$ from $E_N = 0$, to $E_N = 14.0$ MeV. Note that because of the previously imposed conditions, that the summation of all the counts for each $(E_N + Q)$ tabulation are equal.

Tabulating the $^3He(n, p)T$ and the $^3He(n, d)D$ reactions separately, we can construct a matrix for each reaction which is a tabulation of the number of events having identical rise times in each energy channel. Such a matrix is shown in Table II.

An identical tabulation to Table II would be constructed for the (n, d) reaction.

The (n, p) and (n, d) tabulations could be directly combined, but the reactions are not equally probable. However, if we multiply all the entries of the (n, d) tabulation by a factor that is proportional to their relative probabilities, then we could directly add the corresponding elements in the two matrices to obtain a combined matrix of rise time vs. $(E_N + Q)$. Such a factor is available to us in the form of the cross sections of the two reactions, $\sigma_{n, p}(E_N)$ and $\sigma_{n, d}(E_N)$. (Note that these are the cross sections of $\sigma(E_N)$ and not $\sigma(E_N + Q)$.) The combined matrix would appear as shown in Table III.

Therefore the percentage of counts removed per energy channel is equal to the sum of the counts to the left of the rise time cutoff (see Table III) divided by the total number of counts in that energy channel.

Table II. Weighted Number of (n, p) Events Having Identical Rise Times

Energy of product particles	$\sum_{r=0}^{r=b} N(1\ \mu\text{sec})\frac{r}{b^2}\cdot dr$	$\sum_{r=0}^{r=b} N(2\ \mu\text{sec})\frac{r}{b^2}\cdot dr$	. . .	$\sum_{r=0}^{r=b} N(30)\ \mu\text{sec})\frac{r}{b^2}\cdot dr$	$\sum_{r=0}^{r=b} N(\text{WEP})\frac{r}{b^2}\cdot dr$	$\sum_{r=0}^{r=b} \text{All counts}\cdot dr$
$E_{N1}+Q$						
$E_{N2}+Q$						
$E_{N3}+Q$						
.						
.						
.						

Table III. Combined Weighted Number of Events (n, p) and (n, d) Having Identical Rise Times

Energy of product particles	$\sum_{r=0}^{r=b} N(1\,\mu\text{sec})\frac{r}{b^2}\cdot dr$	$\sum_{r=0}^{r=b} N(2\,\mu\text{sec})\frac{r}{b^2}\cdot dr$	. . .	$\sum_{r=0}^{r=b} N(t'_r\,\mu\text{sec})\frac{r}{b^2}\cdot dr$	. . .	$\sum_{r=0}^{r=b} N(30\,\mu\text{sec})\frac{r}{b^2}\cdot dr$	$\sum_{r=0}^{r=b} N(\text{WEP})\frac{r}{b^2}\cdot dr$	$\sum_{r=0}^{r=b} \text{All counts}\cdot dr$
$E_{N1}+Q$								
$E_{N2}+Q$								
$E_{N3}+Q$								
.								
.								
.				←Rise Time Cutoff				

If the percentage of counts removed is designated as "P_R," then the percentage of counts that were counted is $(1 - P_R)$. Thererore, considerir the raw spectrum that is received as output from the multichannel analyze and designating the counts from any individual $(E_N + Q)$ channel as C_N, we can say $(1 - P_R)C_{RN} = C_N$ or $C_{RN} = \frac{C_N}{(1 - P_R)}$, where C_{RN} is the valid counts we would have received without rise time discrimination.

A"P_R" can be computed for each $(E_N + Q)$ energy channel of the multi-channel analyzer, and after correction we will obtain the corrected neutro spectrum with the rise time discrimination removed.

7. Discussion of error introduced by assumption of linear dependence of electron velocity and (E/P).

It has previously been assumed (Section II-B.1) that the mobility of the electrons in the gas medium is a constant value and that the velocity of the electrons in their inward drift towards the anode varies directly as the (E/P) value, i.e. $v = m \cdot E/P$. This relationship appears to be a reasonable approximation in the regions where the field gradient E varies slowly. It can be seen from Fig. 3 that from the cathode, to about a distance of 1.0 cm from the anode, this condition of a slowly varying (E/P) holds quite true. At distances closer than 1.0 cm from the anode, the field gradient increases rapidly, becoming higher the closer the anode is approached. At regions very close to the anode, gas multiplication takes place, and an "electron avalanche" is produced.

The region of interest for electron migration time calculations,

however, is the region between the radius where gas multiplication begins (i.e. a few mean free paths of the anode--or as deseribed by Wilkinson,[23] "a distanee from the wire surface of the order of its diameter") and the region where the field gradient begins its rapid assent (i.e. about 1.0 cm radius).

First, it is known that the mobility of electrons is not a constant value over unlimited variations of E/P. At some value for eaeh eomponent gas, a saturation eondition is reaehed whereby further increase in E/P does not result in an inerease in eleetron drift velocity--and in fact, the veloeity may even decrease with inereasing E/P. These saturation effects are probably the result of eleetron collisions with gas moleeules that are no longer purely elastic, and a portion of the eleetron's kinetie energy is imparted to the gas molecule in an inelastic eollision. The probability of an inelastic eollision apparently increases with increasing electron kinetie energy, but the inereased energy losses due to the inelastie collisions cause the drift and agitational velocities to remain at a constant (or nearly contant) value. In the ease of krypton, this terminal velocity is reached at an E/P value of 1.5 volts/cm · cm^{-1} Hg[20] when the krypton has 1/2% CO_2 intermixed. English and Hanna[20] attribute this peak velocity as the result of the "Ramsauer Effeet." On the other hand, no such terminal velocity peak has been reported either in pure He,[24] or in ^3He-CO_2 mixtures.[11,19] In addition, the veloeity vs. E/P curves that are available from various experimenters do not go beyond an E/P value

of more than 6.0 volts/cm · cm^{-1} Hg for krypton,[20] and 10.0 volts/cm · cm^{-1} Hg[11,24] for ^3He, whereas the E/P value varies from 0.75 to over 190 volts/cm · cm^{-1} Hg in our counter, in the region under consideration. It is thus impossible (at present) to even estimate the electron drift velocity in the inner 1.0 cm radius of the counter tube.

Quantitatively, we can say that the electron velocity in this region will be considerably less than the value we have assumed. This phenomenon of smaller and slowly changing velocity is due to the saturation effects of the $Kr-CO_2$ mixture--and probably an identical effect from the $^3He-CO_2$ mixture that occurs at an E/P value higher than those reported.

Let us now examine the effects of this uncertainty of electron velocity in this region in our counter tube. Equation 5 states that the rise time of a pulse is equal (for a specified applied voltage) to a constant times the differences in the squares of two radii, i.e.

$$t_r = \text{const.} \cdot \left(r_f^2 - r_n^2 \right) \qquad (5.$$

We have likewise pointed out that for tracks that occur entirely within the region where E/P varies slowly, that we may consider the "rise time" as the time that it takes the furthest electron to migrate to a radius equal to that of the original position of the nearest electron.

Let us now go back to the determination of our original setting of the rise time discriminator. The value of the rise time discrimination t_r' was determined by solving Eq. 5a with the values $r_f = b$ and

$r_n = b - \ell_{^3He}(\frac{3}{4} E_N)$. Once this value has been determined, we can interpret Eq. 5a as the area between two concentric circles of radii r_f and r_n.

Fig. 16. Interpretation of rise time values as a constant area.

The total area between the circles remains a constant, i.e.

$$\pi(r_f^2 - r_n^2) = \pi t_r' \frac{2 m P}{V_0 \ell n \frac{r_c}{r_a}}$$

when $r_n = 0$, this expression reduces to:

$$r_{f(min)} = \sqrt{\frac{t_r' \; 2 m P}{V_0 \ell n \frac{r_c}{r_a}}} \qquad (5b)$$

Where $r_{f(min)}$ is the outer radius of the "dead volume," and any tracks that lie completely within the cylinder bounded by $r_{f(min)}$, they are rejected by rise time discrimination. From the above discussion we realize that $r_{f(min)}$ is not as large as calculated in Eq. 5b, due to the uncertainty of the electron migration velocity in the region $r_a < r < 1.0$ cm, since the velocity tends to be considerably less than the linear relationship originally assumed in a high E/P region. For a 14.0 MeV neutron, which produces a 10.5 MeV maximum ^3He recoil, we find that

t'_r = 6.1 usec and $r_{f(min)}$ = 2.7 cm (for V_0 = 5500 V). Since $r_{f(min)}$ (actual) is less than the value calculated for a fixed t'_r, the "dead volume" of our counter is less than calculated. The question of "how much less" is one that cannot at present be analytically solved. It has been previously stated that it was considered that the linear dependence of velocity with the (E/P) factor was valid at regions r> 1.0 cm. If the $r_{f(min)}$ (actual) is not less than 1.0 cm, then our assumptions are still valid for those events whose tracks lie entirely in the active volume beyond 1.0 cm radius.

We have assumed that the probability of a reaction occurring in any unit volume of the gas medium is identical. The volume enclosed by the 1.0 cm radius comprises only 4% of the total sensitive volume. The track orientations can likewise be completely at random, and so the probability of a track having any portion of its length in the volume enclosed by a 1.0 cm radius is dependent upon the disintegration particle energies, the reaction site, and the orientation of the reaction particles. While the probability of passing into this "inner wall" region can be computed in a manner similar to the probability of a particle striking the outer wall (see Section II-C), there is no way to relate this probability to the rise time spectrum, since electron velocities are unknown in the region--also every accepted count will be registered as a "full energy count." In addition, even if the tracks of the charged particles do enter into the region of the "dead volume," their total radial orientation may be such

that the pulse rise time is greater than t_r', and the counts will be registered.

It can thus be concluded that:

(a) Pulses that are the result of tracks lying completely inside the "dead volume" will be excluded due to rise time discrimination, regardless of energy and orientation. (4% of the active volume.)

(b) Tracks that lie completely outside the "dead volume" may, or may not, be counted due to rise time discrimination. Those pulses above a minimum energy that were removed due to track orientation can be mathematically replaced.

(c) Those tracks that have some portion of the length within the "dead volume" may, or may not be counted. The actual rise time of these pulses will be larger than the calculated rise time, but the rise time discriminator setting will be the same as in (a) and (b) above. This means that more counts of each energy would be registered than would be indicated by our theory (i.e. more counts because more pulses would have longer rise times and thus more would escape rejection due to rise time discrimination.)

The magnitude of the error introduced by (c) above is unknown, and its effects must await the comparison of the final spectrum as developed from our counter with a spectrum obtained by other means from the same source. It is not anticipated that this error will be large.

II-C DEVELOPMENT OF A PROBABILITY FUNCTION FOR THE UNFOLDING OF THE WALL EFFECTS.

The development of a probability function to remove the wall effects wa primarily developed by Brown, and then extended by Wang. The overall development is quite long, being in general the substance of two theses, and only certain aspects will be presented herein along with a correction to Wangs "Wall Effects Function". For a complete derivation of the entire series of probability functions, readers are referred to Ref. 9 and 16. The notation of Brown and Wang will be continued in this paper to aid persons who are interested in development of these functions, but in general these functions will only be presented and identified in their final form.

1. Wall Effects

The sensitive volume of the proportional counter tube was previously identified in Fig. 1. Within this sensitive volume of length L and radius b, let us select a reaction site at r, and assume that the track length of charged particles is ℓ. For the analysis, the whole gas filled volume (not just the sensitive volume) may be considered to be divided into four regions which will be identified in our subsequent discussion.

a. Region A

Region A is the core of the sensitive volume defined by radius of $b - \ell$ and length $L - 2\ell$ as shown in Fig. 17

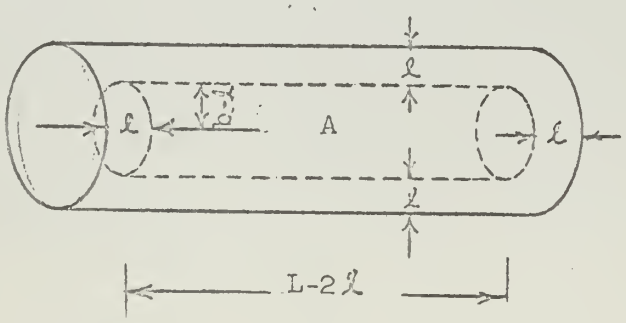

(17)

Figure 17-Region A

It is clear that only tracks of full size can be found in this region. Therefore, the probability $P_A(\rho)$ per unit track length that a track will have a length between ρ and $\rho + d\rho$ in this region is :

$$P_A(\rho)d\rho = \delta(\rho - \ell)d\rho$$

For a single reaction happening in region A the probability is

$$\int_0^\infty P_A(\rho)d\rho = \int_0^\infty \delta(\rho - \ell)d\rho = 1 \qquad (4)$$

b. Region B

Region B is the hollow cylindrical volume with an inner radius of $b - \ell$, an outer radius of b, and a length $L - 2\ell$, as in Fig. 18

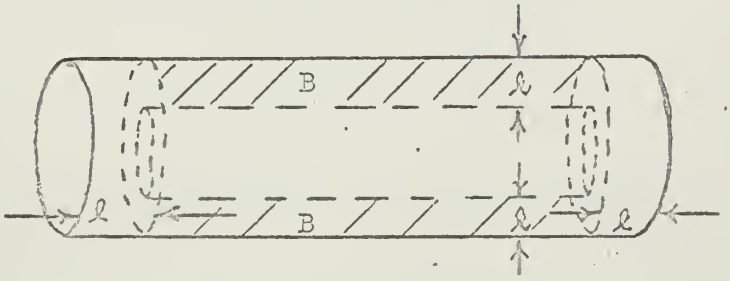

(4)

Figure 18 - Region B

For region B, Wang classifies the track length into two categories:

Case 1

For a single reaction in this region, those tracks not intersecting the wall will have a length ℓ, the full sized track. The probability, $P_{B1}(\rho)$, per unit track length that a track will have a length between ρ and $(\rho + d\rho)$ in this region is :

$$P_{B1}(\rho)d\rho = F_{B1}(\rho)\,\delta(\rho - \ell) \qquad (4)$$

where the factor $F_{B1}(\rho)$ represents the fractional area of a sphere with

radius ℓ centered at (0,0,0) that falls inside the sensitive volume.

Referring to Fig. 19, it is seen that the fractional surface area of the sphere inside the cylinder is

$$F_{B1}(\rho) = \frac{4\pi\ell^2 - \int_S \ell^2 \sin\theta \, d\theta \, d\phi}{4\pi\ell^2} = 1 - \frac{1}{2}\int_{\theta_1}^{\theta_2} \sin\theta \, d\theta$$

where S = spherical surface area outside of the cylinder.

Brown makes an approximation that the transition from θ_2 to θ_1 along the line of intersection between the sphere and cylinder can be represented by the $\sin^2\phi$, and he concludes that:

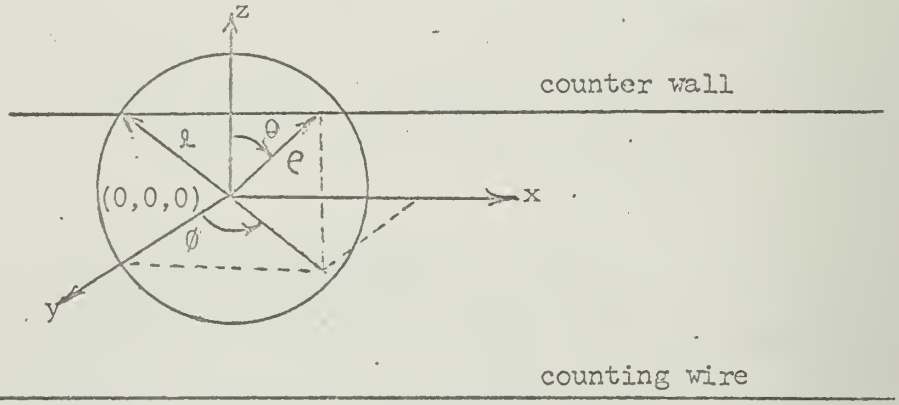

Figure 19 Intersection of a Sphere and a Cylinder

$$F_{B1}(\rho) = 1 + \frac{1}{4}\left[\left(\frac{b^2 - \ell^2}{2\ell}\right)\cdot\frac{1}{r} + \left(\frac{b}{\ell} - 2\right) - \left(\frac{3}{2\ell}\right)\cdot r\right] \qquad (+$$

$$\therefore \quad P_{B1}(\rho)d\rho = 1 + \frac{1}{4}\left[\left(\frac{b^2 - \ell^2}{2\ell}\right)\cdot\frac{1}{r} + \left(\frac{b}{\ell} - 2\right) - \left(\frac{3r}{2\ell}\right)\right]\delta(\rho - \ell)\,d\rho \qquad (+$$

Case 2.

Those tracks that do interest the detector wall will lose a portion of their length. The probability of hitting the wall is then the spherical surface outside the cylinder i.e.

$$F_{B2}(r) = -\frac{1}{4}\left[\left(\frac{b^2 - \rho^2}{2\rho}\right)\frac{1}{r} + \left(\frac{b}{\rho} - 2\right) - \frac{3}{2\rho}\cdot r\right]$$

Then the variation over ρ gives $P_{B2} = (\rho, r)$

$$P_{B2} = (\rho , r) = F_{B2} (\rho , r)$$

$$\frac{\partial}{\partial \rho} (F_{B2}(\rho , r)) = P_{B2} (\rho , r) d\rho$$

$$= - \frac{1}{4} \left\{ - \left[\frac{b^2 - \rho^2}{2 \rho^2 r} \right] - \frac{2\rho}{2\rho r} - \frac{b}{\rho^2} + \frac{3r}{2\rho^2} \right\} d\rho$$

$$= \frac{1}{8} \left\{ \frac{1}{r} \cdot \left[\frac{b^2}{\rho^2} + 1 \right] + \frac{2b}{\rho^2} - \frac{3r}{\rho^2} \right\} d\rho$$

c. Region C

Regions C are the portions of the sensitive volume of distance ℓ from the ends of the sensitive volume, as in Fig. 20

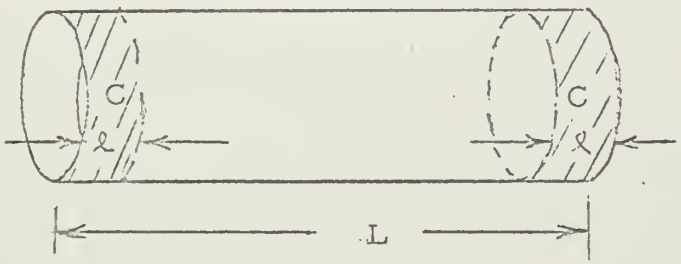

Figure 20 - Region C

The track can be classified into two different cases.

Case 1

For a simple reaction in this region, the probability of having a full track length is

$$P_{C1} (\rho) d\rho = F_{C1} (\rho) \delta (\ell - \rho) d\rho$$

$$F_{C1} (\rho) = \frac{4\pi \ell^2 - \iint_{SC} \sin \alpha \, d\alpha \, d\beta}{4\pi \ell^2} = 1 - \frac{1}{2} \int_{\alpha} \sin \alpha \, d\alpha$$

$$= 1 - \frac{1}{2} \left[\cos \alpha \right]_{\cos^{-1} \left(\frac{z}{\ell} \right)}^{0}$$

$$= 1 - \frac{1}{2}\left[1 - \frac{z}{\ell}\right] = \frac{1}{2}\left(1 + \frac{z}{\ell}\right) \quad (4)$$

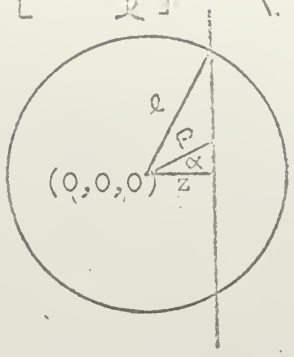

Figure 21 - Region C
Intersection of Sphere with Active Volume

Case 2

The probability of having a curtailed track length is (4)

$$P_{Cz}(\rho)\, d\rho = \left(\frac{1}{2} \sin\alpha\, d\alpha\right) \times 2$$

since $\cos\alpha = \frac{z}{\rho}$, $\sin\alpha\, d\alpha = \left(\frac{z}{\rho^2}\right) d\rho$, therefore

$$P_{C2}(\rho)\, d\rho = \frac{z}{\rho^2}\, d\rho \qquad \text{if } z < \rho$$

$$= 0 \qquad \text{if } z > \rho$$

d. Region D

Region D are the portions of the gas filled volume beyond the sensitive volume, as in Fig. 22 .

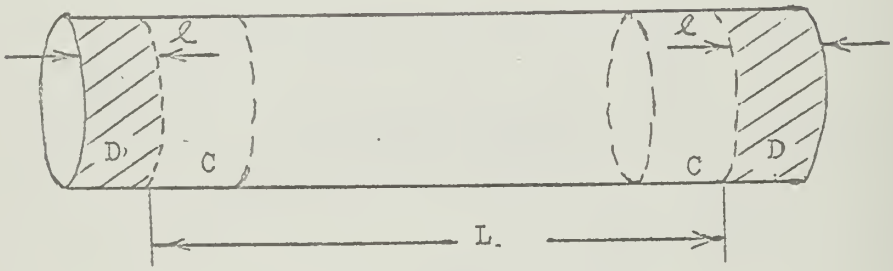

(4)

Figure 22 - Region D

Nuclear reactions occurring at sites outside the sensitive volume can also cause energy to be deposited inside the sensitive volume of the counter.

If the probability of depositing energy from a track length inside the sensitive volume per unit track length of ρ is $P_D(\rho)$ then:

$$P_D(\rho)d\rho = \frac{1}{2}\sin\alpha\, d\alpha \times 2$$

$$\text{but } \cos\alpha = -\frac{z}{\rho - \ell}$$

$$\text{therefore } \sin\alpha\, d\alpha = -\frac{z}{(\ell - \rho)}\, d\rho \text{ for } \ell > \rho, \text{ and}$$

$$P_D(\rho)d\rho = \frac{z\, d\rho}{(\ell - \rho)^2} \text{ for } (\ell - z) \geq \rho \geq 0 \qquad (++)$$

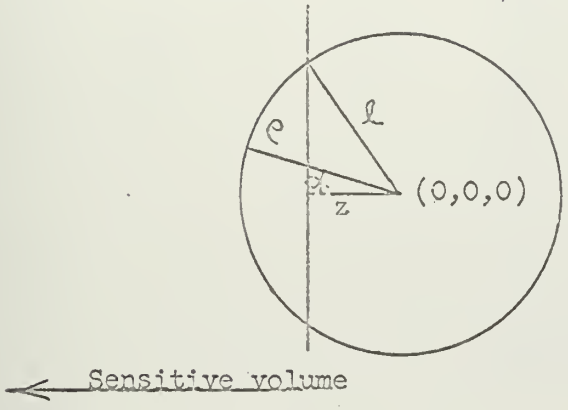

Figure 23-Region D; Track Lengths Inside Sensitive Volume

e. Summary of the General Wall Analysis

For an arbitrary track length ℓ the gas-filled volume can be divided into four regions, as in Fig. 24

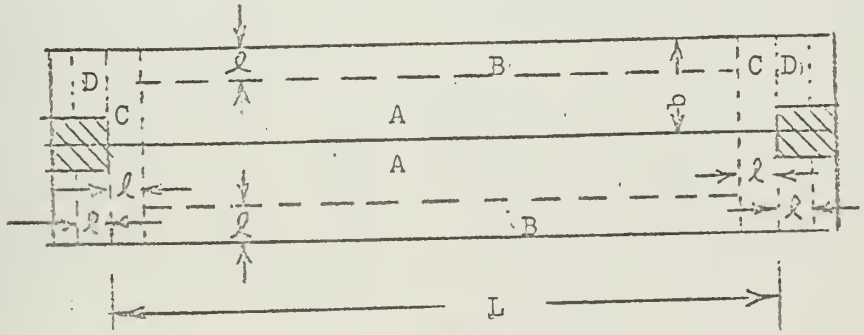

(++)

Figure 24: Summary of Counter Regions

The probabilities per unit track length that a track will have a length between ρ and $(\rho + d\rho)$ in each region are listed in Table IV.

Table IV. Probability functions for different regions of the counter.

Region	Probability of giving full track length	Probability of giving partial track length due to wall effect
A	$p_A(\rho) = \delta(\rho - \ell)$	
B	$p_{B1} = \left\{1 + \frac{1}{4}\left[\left(\frac{b^2 - \ell^2}{2\ell}\right)\frac{1}{r} + \left(\frac{b}{\ell} - 2\right) - \frac{3r}{2\ell}\right]\right\}\delta(\rho - \ell)$	$p_{B2}(\rho) = \frac{1}{8}\left\{\left(\frac{b}{\rho}\right)^2 \cdot \frac{1}{r} + \frac{1}{r} + \frac{2b}{\rho^2} - \frac{3r}{\rho^2}\right\}$
C	$p_{C1} = (1 + \frac{Z}{\ell})\ \delta(\rho - \ell)$	$p_{C2}(\rho) = \frac{Z}{\rho^2}$ for $Z < \rho$ $= 0$ $Z > \rho$
D	-	$p_{D2}(\rho) = \frac{Z}{(\ell - \rho)^2}$ for $(\ell - Z) \geq \rho \geq 0$

f. The probability, $P(E \rightarrow E_i)$, per unit energy that reaction products of energy E will deposit energy E_i inside the sensitive volume due to the wall effect

According to the foregoing analysis, now, if we assume that the pulse height is proportional to the energy deposited inside the sensitive volume, then it is reasonable to assume, for the first-order approximation, that

$$E = K,$$

$$E_i = K\rho,$$

$$E_b = Kb,$$

$$E_L = KL,$$

where K is some proportionality constant that will be cancelled out shortly. Therefore

$$P(E \rightarrow E_i) = K' p(\ell \rightarrow \rho),$$

where K' is another proportionality constant. For the whole counter

$$p(\ell \rightarrow \rho) = \int_{b-\rho}^{b} p_{B2}(\rho, r) g_1(r)dr + \int_0^{\rho} p_{C2}(\rho, z) g_2(z)dz + \int_0^{\ell-\rho} p_{D2}(\rho, z) g_3(z)dz.$$

From Subsec. II-D.1b.

$$p_{B2}(\rho) = \frac{1}{8}\left\{\left(\frac{b}{\rho}\right)^2 \cdot \frac{1}{r} + \frac{1}{r} + \frac{2b}{\rho^2} - \frac{3r}{\rho^2}\right\}, \quad p_{C2} = \frac{z}{\rho^2}, \quad p_{D2} = \frac{z}{(\ell-\rho)^2},$$

and the volume fractions are, respectively,

$$g_1(r)dr = \frac{2\pi r\,dr}{\pi b^2} = \frac{2r\,dr}{b^2},$$

$$g_2(z)dz = g_3(z)dz = \frac{dz}{L},$$

Therefore:

$$p(\ell-\rho) = \frac{1}{8}\int_{b}^{b}\left\{\left[\left(\frac{b}{\rho}\right)^{2}+1\right]\frac{1}{r}+\frac{2b}{\rho^{2}}-\frac{3r}{\rho^{2}}\right\}\frac{2r\,dr}{b^{2}} +$$

$$\int_{0}^{\rho}\frac{z}{\rho^{2}}\cdot\frac{dz}{L} + \int_{0}^{\ell-\rho}\frac{z}{(\ell-\rho)^{2}}\cdot\frac{dz}{L}$$

$$p(\ell-\rho) = \frac{1}{2b} + \frac{1}{2L} + \frac{1}{2L} = \frac{1}{2b} + \frac{1}{L}$$

and since $p(\ell\rightarrow\rho)d\rho = P(E\rightarrow E_i)dE$

then $$P(E \rightarrow E_i) = \frac{1}{2E_b} + \frac{1}{E_L} \qquad (27)$$

Where E_b is the energy width of the particle in question, and E_L is the energy length. Note that this is the probability or fraction of giving a track of energy E_i due to the wall effect. Surprisingly, this probability turns out to be constant independent of the energy of the incoming neutron.*

2. Probability of a Track Not Hitting the Container Envelope

Brown and Wang derive expressions for the average laboratory energy of the various particles in a plane perpendicular to the counting wire. The expressions cannot be analytically resolved, so numerical integration is performed on these expressions and the resultant energies are then approximated by use of the following formula:

$$E_P^{\perp} = 0.505\,E_N + 0.450 \qquad (+)$$

* Wang's more complicated probability function is due to the improper selection of limits of integration for region C and the approximation utilized in determination of $P_{B2}(\rho)\,d\rho$.

$$E_T^{\perp} = 0.340\ E_N + 0.150 \qquad (\dagger)$$

$$E_D^{\perp} = 0.42\ E_N - 1.27 \qquad (\dagger)$$

Where the designation $E^{\perp}$ indicates the average laboratory energy in a plane perpendicular to the anode resulting from a neutron of energy E_N. All units are in MeV.

From these expressions of particle energy, the probability that a simultaneously emitted proton and triton, or a pair of deuterons, will not hit the walls of the containing vessel are derived. Using the notation of Wang,

$f_1(E)$ = probability that a proton-triton will not hit the wall

$f_5(E)$ = probability that the deuterons will not hit the wall

$$f_1(E) = f_{1p}(\vec{E}^{\perp}) \cdot f_{1T}(E)(1 - \bar{\mu}_T^2)^{1/2} \qquad (28)\ (\dagger)$$

where $f_{1p}(\vec{E}^{\perp})$ ≡ the probability that a proton track will not hit the wall*

f_{1T} ≡ the probability that a triton track will not hit the wall

$(1 - \bar{\mu}_T^2)^{1/2}$ = a factor added to account for the forward track component of the triton.

$$\bar{\mu}_T = \left(\frac{3E_N}{3E_N + 4Q_{n,p}}\right)^{1/2} \quad \text{where } Q_{n,p} = 0.764 \text{ (MeV)}$$

$$f_{1p}(\vec{E}^{\perp}) = \left[1 - \frac{2}{\pi}\left\{\frac{\ell_p}{2b}\left[1 - \left(\frac{\ell_p}{2b}\right)^2\right]^{1/2} + \sin^{-1}\left(\frac{\ell_p}{2b}\right)\right\}\right] \qquad (29)\ (\dagger)$$

$$f_{1T}(\vec{E}^{\perp}) = \left[1 - \frac{4}{\pi}\left(\frac{\ell_T}{2b}\right)\right] \qquad (30)\ (\dagger)$$

* Both Brown and Wang calculate two different values for $f_{1p}(\vec{E}^{\perp})$ and equate them for energy boundary conditions of their tubes. In our case, the energy boundary conditions (because of a larger size tube and greater filling pressure) are such that we do not ever reach the conditions that Brown and Wang encountered. (i. e. the E_{crit} for our tube is at 17.0 MeV which is above the designed maximum of 14.0 MeV)

where ℓ_{L_p} = length of proton track in the gas mixture for a proton of energy E_p.

and ℓ_{T_L} = length of triton track in the gas mixture for a triton of energy E_T.

$$f_5(E) = \left[1 - \frac{4}{\pi}\left(\frac{\ell_D}{2b}\right)\right]\left[1 + (1 - \bar{\mu}_D^2)^{1/2}\right] \qquad (31)$$

where $\bar{\mu}_D = \dfrac{x_D}{(1 + x_D^2)^{1/2}}$

and $x_D = \left(\dfrac{E_N}{3E_N + 4Q_{n,d}}\right)^{1/2}$, $Q_{n,d} = 3.24$ (MeV)

ℓ_D = length of a deuteron track in the gas mixture for a deuteron of energy E_D.

The above nomenclature and designation will be used in subsequent sections.

D. Combination of the Two Probability Factors to Reconstruct the Original Neutron Spectrum.

The original purpose of our neutron spectrometer was to accurately portray a neutron spectrum in the energy range from essentially 0.1 MeV to 14.0 MeV. The spectrometer operation was such however, that in order to remove the more numerous recoil pulses which were smeared across the energy spectrum from $(\frac{3}{4} E_N)_{max}$ to zero, advantage was taken of the differences in pulse rise times between valid pulses and recoil events. The removal of the recoil pulses, however, was not without its disadvantages. It was discovered that to obtain a neutron spectra without recoils, it is necessary to forgo all information at the lower energies since the track lengths of lower energy pulses were shorter than the maximum energy recoil pulse. These lower energy pulses were thus removed with the recoils. In addition, the orientation of the tracks of a valid event may be such that the radial components are less than the minimum required to produce a pulse that exceeds the rise time minimum cut off.

The loss of the lower energies of the neutron spectrum is unfortunate, and a means to overcome this deficiency has yet to be devised. A means to effect the replacement of the higher energy pulses that were removed due to their specific orientations within the counting tube has been developed and presented earlier in this report. The probability function (P_R) can be directly applied to the raw spectrum from the multichannel analyzer to replace "rise time removed" pulses in this situation.

The other portion of the problem in the determination of a reconstructed neutron spectrum has to do with the removal of the wall and end effects. As mentioned earlier, this problem was essentially solved by Brown and extended by Wang. Modification to Wang's probability function have been made, and the revised probability function $P(E \rightarrow E_i)$ has been previously presented.

What remains to be accomplished is to present a computer program outline of the means to unfold the various effects and to arrive at a complete neutron spectrum.

For the purposes of this section and to add clarity to the computer program, it is considered that the following subroutines have already been accomplished:

(a) Assume that the raw spectrum has been corrected for rise time discrimination. The raw counts in each $(E_N + Q)$ channel have been divided by the probability function $(1-P_R)$ and the revised channel counts are now designated C_{RN}.

(b) The counter efficiency has been calculated, and an energy dependent value of the efficiency can be shown in the various reaction cross-sections. The efficiency of the counter was developed by Wang to be a function of (a) the nuclear cross sections, (b) the counter dimensions, and (c) the gas pressures.

$$\eta_{n,p}(E_N) = N_{^3He}\, \sigma_{n,p}(E_N) D\ f_1(E_N) \qquad \dagger$$

where

$N_{^3He}$ = number of ^3He atoms/cm^3 of sensitive volume at filling pressure

$\sigma_{n,p}(E_N)$ = ^3He (n,p)T cross section (see Fig. 2)

D = Effective thickness of the detector for 4π geometry

$$= \frac{\text{Total sensitive volume}}{\text{effective area}}$$

where sensitive volume of sphere = sensitive volume of cylinder

$$\frac{4}{3}\pi R^3 = \pi b^2 L$$

or

$$R = \left(\frac{3}{4} b^2 L\right)^{1/3}$$

thus effective area $= \pi R^2 = \pi\left(\frac{3}{4} b^2 L\right)^{2/3}$

$$\therefore \quad D = \frac{\pi b^2 L}{\pi\left(\frac{3}{4} b^2 L\right)^{2/3}} = \left(\frac{4}{3}\right)^{2/3} b^{2/3} L^{1/3} \qquad \dagger\dagger$$

$f_1(E_N)$ = Probability the proton or triton will not hit the wall

A similar expression can be written for the efficiency of the ^3He (n,d)D reaction

$$\eta_{n,d}(E_N) = N_{^3He}\, \sigma_{n,d}(E_P) D\ f_5(E_N)$$

where the notation is similar to the above

It can be seen that the efficiency can be reflected in a new cross-section notation such that:

$$\sigma_{n,p}(E_N)^* \equiv N_{^3He}\, D\, \sigma_{n,p}(E_N) = \frac{\eta_{n,p}(E_N)}{f_1(E_N)}$$

where $\sigma_{n,p}(E_N)^*$ is the cross section that has been corrected for the efficiency of the counter.

and

$$\sigma_{n,d}(E_N)^* \equiv N_{^3He}\, D\, \sigma_{n,d}(E_N) = \frac{\eta_{n,d}(E_N)}{f_5(E_N)}$$

where $\sigma_{n,d}(E_N)^*$ is the cross section of the $^3He(n,d)D$ reaction that has been counted for the physical efficiency of the counter.

Assume now that the higher energy rise time discrimination removal counts have been replaced, and the cross sections have been corrected for the counter efficiency as indicated above. A computer program to unfold the wall effects and to calculate the resultant true neutron spectrum could be as follows:

(1) Let $E_{j'} = E_j - Q_{n,p}$

where $E_{j'}$ = Actual neutron energy

E_j = Registered neutron energy

(2) Let $A_{j'}$ = Number of neutrons of energy $E_{j'}$

$E_{j'} \neq E_j$

(3) Let C_{RN} = Number of counts registered in top energy channel of the multichannel analyzer (after correction for rise-discrimination)

(4) $C_{RN} = A_{N'}\, \sigma_{n,p}(E_{N'})^*\, f_1(E_N)$

(5) Solve for $A_{N'}$

$$A_{N'} = \frac{C_{RN}}{\sigma_{n,p}(E_{N'})^*\, f_1(E_N)}$$

(6) $$C_{R(N-1)} = A_{(N-1)'}\ \sigma_{n,p}(E_{N-1})'^{*}f(E_{N-1}) + A_{N'}\ \sigma_{n,p}(E_{N'})^{*}\cdot \left[1-f_1(E_N)\right] \cdot P_P\left(E_N \rightarrow E_{(N-1)}\right)$$

where $P_P(E_N \rightarrow E_{(N-1)})$ is the probability that an (n,p) event from channel E_N will be registered in channel $E_{(N-1)}$ $P(E_N \rightarrow E_i) = \frac{1}{2\bar{E}_b} - \frac{1}{E_L}$

(7) Solve for $A_{(N-1)'}$

(8) Repeat this procedure until we reach channel $A_{(N-j)'}$

where:

$$A_{(N-j)'} = \frac{C_{R(N-j)} - \sum_{i=0}^{i=j-1} A_{(N-i)'}\ \sigma_{n,p}(E_{(N-i)'})^{*}\left[1-f_1(E_{(N-i)})\right] P_P(E_{N-i} \rightarrow E}{\sigma_{n,p}(E_{(N-j)'})^{*} f_1(E_{(N-j)})}$$

(9) Let $E_{N-j-1} = E_N - (Q_{n,p} - Q_{n,d})$ and the deuterons begin to appear.

i. e. $E_{registered} = E_N - (0.764 + 3.27) = E_{N'} - 3.27$

(10) $$C_{R(N-j-1)} = A_{(N-j-1)'}\ \sigma_{n,p}(E_{(N-j-1)'})^{*} f_1(E_{(N-j-1)}) + \sum_{i=0}^{i=j} A_{(N-i)'}\,c$$

$$(E_{(N-i)'})^{*}\left[1-f_1(E_{(N-i)})\right] \cdot P_P\left(E_{(N-i)} \rightarrow E_{(N-j-1)}\right) + A_{N'}\ \sigma_{n,d}(E_{(N')})^{*}$$

$f_5(E_{(N-j-1)})$. The last term in this expression indicates the deuteron effects from $E_{N'}$ and $f_5(E_{(N-j-1)})$ = the probability that the deuterons of energy $E_{(N-j-1)}$ will not hit the wall.

(11) Solve for $A_{(N-j-1)'}$

$$A_{(N-j-1)'} = C_{R(N-j-1)} - \sum_{i=0}^{i=j} A_{(N-i)'}\ \sigma_{n,p}(E_{(N-i)'})^{*}\left[1-f_1(E_{(N-i)})\right]\cdot$$

$$P_P\left(E_{(N-i)} \rightarrow E_{(N-j-1)}\right) - A_{N'}\ \sigma_{n,d}(E_{N'})^{*} f_5(E_{(N-j-1)})$$

divided by $\sigma_{n,p}(E_{(N-j-1)'}) * f_1(E_{(N-j-1)})$

(12) Then in general:

$$A_{(N-j-1-k)'} = C_R\,(N-j-1-k) - \sum_{i=0}^{i=j+k} A_{(N-i)'}\,\sigma_{n,p}(E_{(N-i)'})^{*}\cdot \left[1-f_1\,(E_{(N-i)})\right]\cdot P_P\,(E_{(N-i)} \rightarrow E_{(N-j-1-k)}) - A_{(N-k)'}\,\sigma_{n,d}\,(E_{(N-k)'})^{*}\cdot f_5\,(E_{(N-j-1-k)}) - \sum_{i=0}^{i=k-1} A_{(N-i)'}\,\sigma_{n,d}\,(E_{(N-i)'})^{*}\left[f_6\,(E_{(N-j-1-k)})\right]\cdot P_d\,(E_{(N-j-1-i)} \rightarrow E_{(N-j-1-k)})$$

divided by $\sigma_{n,p}\,(E_{(N-j-1-k)'})^{*}\; f_1\,(E_{(N-j-1-k)})$

where $P_d\,(E_{(N-j-1-i)} \rightarrow E_{(N-j-1-k)})$ is the probability of a deuteron having scattering from a higher energy channel into channel $E_{(N-j-1-k)}$ and $f_6\,(E_{(N-j-1-k)})$ = the probability that the deuterons having energy $E_{(N-j-1-k)}$ will intersect the wall $= \left[1-f_5\,(E_{(N-j-1-k)})\right]$

(13) This procedure is followed until the spectrum is unfolded to the lowest energy channel that has escaped rise time discrimination.

(14) The unfolded spectrum

$$A_{N'},\ A_{(N-1)'},\ A_{(N-2)'},\ A_{(N-3)'}\cdots\cdots A_{(N-j-1-k)}\ \cdots\cdots$$

is then the neutron spectrum corrected for (a) rise time discrimination, (b) wall effects, and (c) counter efficiency.

E. Random Probability Inversion Matrix

The foregoing sections have considered in detail the computations necessary to change the raw energy spectra to a neutron spectra by the removal of the rise time discrimination effects, the wall and end effects, and corrections for the spectrometer efficiency.

Unfortunately, as can also be seen from the foregoing sections, the number of computations necessary to remove these various effects and corrections is exceedingly large. There are four position variables, two independent energy variables (one reaction particle variable, one incoming neutron variable), risetime discriminator setting, and an applied voltage condition--a total of 8 variables. The number of variables and constraints on individual computations make their solution by analytic means virually an impossibility, and even when considered for high speed computing machines, the number of computations involved would require several hours of machine time. It was therefore decided that in order to compute an "inversion matrix" which could be applied to the "raw spectra" output of the multichannel analyzer recourse must be made to a "random probability method being that it will require only a comparatively small amount of electronic computing machine time, and in addition will permit computation of all corrections to the raw spectra simultaneously, as well as elimination of several assumptions that previously were necessary to apply to the more general case.

The random probability analysis for our counter has been developed

by means of a FORTRAN PROGRAM having the code name "CATMAN." An outline of the random probability analysis is presented below:

(1) A neutron of a specific energy E_N (selected as the maximum neutron energy that our counter is expected to detect) comes into the counting tube. The direction of the incoming neutron is selected at random, and since the detector is to have a 4π response, this direction may be completely arbitrary.

(2) The neutron passes into the volume of the tube (not necessary to limit this to the "active volume" between the field tubes) and transits a distance into the gas medium. Since each unit volume is presumed to have an equal probability of a reaction occurring in that volume, the position of the event is selected at random by a "random number generator" which determines both longitudinal distance along the anode wire, and radial position r_0.

(3) An event occurs at a radius r_0 from the counter center line and at some length ℓ along the counter length. The event can be either a $^3He(n,p)T$ reaction, or a $^3He(n,d)D$ reaction. The probability of the type of reaction is based on the ratio of the cross sections at the energy of the incoming neutron to the sum of their cross sections, i.e. the probability of a $^3He(n,p)T$ reaction is:

$$\frac{\sigma_{n,p}(E_N)}{\sigma_{n,p}(E_N) + \sigma_{n,d}(E_N)},$$

and the probability of a $^3He(n,d)D$ reaction is:

$$\frac{\sigma_{n,d}(E_N)}{\sigma_{n,p}(E_N) + \sigma_{n,d}(E_N)}.$$

(4) The reaction particles are assumed to have isotropic distribution in the center of mass system of coordinates, and the direction of one of the reaction particles is selected at random (three dimensional selection based on ϕ_{cm}, $\cos\theta_{cm}$, and equal but opposite momentum vectors). The energy of the particles in the CM system is divided among the particles as follows:

$$\left.\begin{aligned} E_{P\,cm} &= \frac{3}{4}\left(\frac{3}{4}E_N + Q_{n,p}\right) \\ E_{T\,cm} &= \frac{1}{4}\left(\frac{3}{4}E_N + Q_{n,p}\right) \end{aligned}\right\} {}^3He(n,p)\text{ reaction}$$

$$\left.E_{D1\,cm} = E_{D2\,cm} = \frac{1}{2}\left(\frac{3}{4}E_N + Q_{n,d}\right)\right\} {}^3He(n,d)D\text{ reaction}$$

(5) The reaction is converted into the Laboratory system of coordinates, and the energy of the various particles is computed in the Laboratory system. Note that any energy between a maximum and a minimum Laboratory energy is equally probable and can occur for the proton and triton particles. Likewise, if $\frac{3}{4}E_N > |Q_{n,d}|$ (threshold energy), the two deuteron particles will vary between a maximum and minimum Laboratory energy with equal probabilities. (From Appendix C.) The Laboratory energies are determined by the random selection of ϕ_{cm} and $\cos\theta_{cm}$.

(6) The length of track of the various Laboratory particle energies are computed by the relationships previously presented.

(7) The track lengths and orientations are then compared to the reaction site to determine if any portion of the tracks has intercepted the walls

of the tube, and/or has a portion of its length in the gas volume determined by the perpendicular radial projections of the interior ends of the field tubes and the end walls (end effects).

(8) If the track of one of the particles intersects the wall or the end portion of the counter, the portion of the energy represented by the track that is physically within the active volume is calculated. Note that this energy is not directly proportional to the track length since the energy deposition is not linear (see Fig. 5). The energy deposited in the active volume is equal to the total energy of the particle minus the energy represented by the length of track that passes outside the active volume (if the same gas mixture were present outside the container). This conclusion can be drawn from the concept that after a charged particle has lost a certain amount of energy, it still has the same length of path to travel as an identical particle that begins its life with an energy equal to the reduced energy of the particle in question.

(9) The various $r_{(1, 2, 3, 4)}$ values (radial components of track lengths) are calculated to determine rise times, with the condition that an appropriate constraint be placed on those tracks that intersect the walls of the tube, or pass into the end regions.

(10) The rise time of the pulse is then determined, based on the time that it takes for the nearest (r_n) and most distant electron (r_f) to reach the anode.

$$t_r = \frac{1}{2m} \frac{P}{V_0} \ln \frac{r_c}{r_a} \left[r_f^2 - r_n^2 \right]$$

(11) A weighting frunction is applied to the result to account for the greater volume probability at points more distant from the anode.

$$g(r)dr = \frac{2r}{b^2}\ dr$$

where r is the reaction site selected in (3) above.

(12) The weighted pulse is catalogued by energy ($E_N + Q$), rise time, and reduced energy (if applicable).

(13) Steps 1 through 12 are repeated several thousand times for the same incoming neutron energy. The probability of the various particles not hitting the wall is computed. $f_1(E)$, the probability of the proton-triton tracks not hitting the wall, and $f_5(E)$, the probability of the deuteron combinations not hitting the wall, are calculated after "weighting" for volume probability considerations. The probability of causing a pulse in a lower energy channel $P(E \rightarrow E_i)$ is likewise calculated from the track length-energy relationship described in step 8, after the volume probability function has been applied. All three of these probability functions are combined into a new probability function $P_n(E \rightarrow E_i)$ for the spectrum unfolding procedures.

(14) The energy of the incoming neutron is reduced by one energy unit, and steps 1 through 13 repeated.

(15) The energy of the incoming neutron is reduced in successive steps until the lowest value of interest is obtained, or until the length of track of the charged particles are less than the length required to escape rise time discrimination.

(16) The weighted number of counts in their respective energy channels are totaled and accounted for, as explained in the preceding section. A matrix arrangement can then be compiled and corrected for the efficiency of the counter. The matrix arrangement could appear as:

$$\begin{bmatrix} C_1 \\ C_2 \\ \cdot \\ \cdot \\ \cdot \\ C_n \end{bmatrix} = \begin{bmatrix} a_{11} & a_{12} & a_{13} \cdots\cdots a_{1n} \\ a_{21} & a_{22} & a_{23} \cdots\cdots a_{2n} \\ \cdot & & \\ \cdot & & \\ \cdot & & \\ a_{n1} & a_{n2} & a_{n3} \cdots\cdots a_{nn} \end{bmatrix} \times \begin{bmatrix} A_1 \\ A \\ \cdot \\ \cdot \\ \cdot \\ A_n \end{bmatrix}$$

Counts registered in each energy increment for random probability analysis.

a_{ij} = fraction of neutrons of energy j that are counted at energy i.

Total neutrons sent into each energy range.

(17) The problem now resolves itself into determining an inversion matrix whereby we can calculate the original neutron spectra from the counts registered in each energy channel of the multichannel analyzer, i.e. to compute an inversion matrix such that:

$$\begin{bmatrix} A_1 \\ A_2 \\ A_3 \\ \cdot \\ \cdot \\ A_N \end{bmatrix} = \begin{bmatrix} b_{11} & b_{12} & b_{13} \cdots\cdots\cdots b_{1n} \\ b_{21} & b_{22} & b_{23} \cdots\cdots\cdots b_{2n} \\ \cdot & & \\ \cdot & & \\ \cdot\cdot & & \\ b_{n1} & b_{n2} & b_{n3} \cdots\cdots\cdots b_{nn} \end{bmatrix} \times \begin{bmatrix} C_1 \\ C_2 \\ \cdot \\ \cdot \\ \cdot \\ C_{(N-1)} \\ C_N \end{bmatrix}$$

Neutron Spectra — Inversion Matrix — Raw Counts from Multichannel Analyzer

(18) Note that in steps 16 and 17 we have referred to a matrix arrangement and an inversion matrix for our illustration. The actual matrices, if they were to be constructed, would be an array of 500 x 500 or more, and would be difficult, if not impossible, to invert. Instead of actually constructing these matrices, the computer would solve this problem by a subtraction-division process similar to that explained in the preceding section II (D).

(19) The complete random probability analysis in FORTRAN language (with appropriate comment cards) is included in Appendix E.

III. CONCLUSIONS AND PRESENT STATUS OF PROJECT

At the present time, the ^{3}He neutron spectrometer described herein as under development, has not been tested. The electronic circuitry for the rise time discrimination however has been constructed and operated, using the small ^{3}He tube used by Wang. This tube is filled with 10 atmospheres of ^{3}He (no heavy stopping gas), has only a 15/16 in. inside diameter, and an energy width E_b of only 0.5 MeV and an energy length E_L of 2.5 MeV[16] for protons.* The intrinsic tube efficiency (due to the small size) however is extremely low, even at these moderate energies, and it was not considered that the expense of developing an inversion matrix was warranted.

The "inversion matrix" for the larger tube that is on order from the Texas Nuclear Corporation, has essentially been completed, and the "random probability program" (CATMAN) which is used to generate the "inversion matrix" has been completed.

Future work in the development of this ^{3}He spectrometer could lie in some means of electronically comparing the rise time of pulses to the pulse magnitude (energy) to determine if the pulse should be "gated" into the multichannel analyzer. This comparison feature would be in lieu of a set value (t_r') for the rise time discriminator circuitry, and would enable the registering of those valid low energy pulses which are now

*These figures have been recalculated in this report, since Wang made an error in the density of ^{3}He on pages 87 et seq. of Reference 16.

automatically eliminated because their short track lengths cannot overcome the rise time discriminator setting. The rise time setting would then be some function of energy, i.e. $t_r'(E)$. This improvement would enable the spectrometer to still differentiate between valid pulses and recoils without sacrificing all low energy valid pulses in the process. It seems somewhat paradoxical that efforts should be made to extend the range to energies in the neighborhood of 1.0 MeV from the upper energies when the original work of Batchelor[3] was aimed at extending the range of his spectrometer beyond 1.0 MeV from the lower energies by eliminating the ^{3}He recoils.

A subsequent report ~~(Part II)~~ will be written by the Health Physics Group of the Lawrence Radiation Laboratory, Berkeley concerning the actual functioning of the ^{3}He neutron spectrometer, and departures (if any) from the predicted operational characteristics.

ACKNOWLEDGMENTS

This work was conducted under the guidance of Dr. Roger Wallace of the Lawrence Radiation Laboratory, Berkeley, and the author wishes to thank him for his support and encouragement.

The author also wishes to acknowledge the help of Mr. William F. Dempster of the Lawrence Radiation Laboratory Mathematics and Computing Services Division for his aid in the development of the computer program and for his general assistance. Mr. Roger M. Brown of the Lawrence Radiation Laboratory Physics Technical Support Group constructed the electronics and should be thanked for this task and his interest in the project.

The author was financially supported during his period of residence at the University of California, by the U. S. Navy, and the material support for the project was supplied under the auspices of the U. S. Atomic Energy Commission.

Finally, the author wishes to acknowledge the assistance of Mrs. Ellen Cimpher and Mrs. Mary Long, for the typing of this manuscript.

REFERENCES

1. R. Batchelor, Neutron Energy Measurements with a Helium-3 Filled Proportional Counter, Proc. Physic Society (London) A65, 674 (1952).

2. S. D. Bloom, E. Reilly, and B. J. Toppel, A High Pressure Proportional Counter for Fast Neutron Spectroscopy, Brookhaven National Laboratory Report, BNL-358 (T-66) (1955).

3. R. Batchelor, R. Aves, and T. H. R. Skyrme, Helium-3 Filled Proportional Counter for Neutron Spectroscopy, Review of Scientific Instruments 26, 1037 (November 1955).

4. R. Batchelor and G. C. Morrison, Helium-3 Neutron Spectrometer, Fast Neutron Physics, Marion and Fowler, Eds., Pt 1, pp 413-39, Interscience Publishers (John Wiley and Sons), New York, (1960).

5. Alden R. Sayres, Interaction of Neutrons with ^{3}He, Pegram Nuclear Physics Laboratories, CU (PNPL)-200 (1960).

6. A. Sayres, D. Lister, and D. Lightbody, Angular Distributions and the Total Cross Section for the N^{15} (p,n)O^{15} Reaction, Bulletin, American Physical Society 6, 26 (1961).

7. J. M. Freeman and D. West, Studies of $_{10}$(p,n) Reactions with a ^{3}He Ion Chamber and Some New Levels of Ne^{19}, Nuclear Physics 38, 89 (1962)

8. W. Brown and L. Passell, A Helium-3 Neutron Spectrometer with Extended Energy Range. Part 1: Design and Development of the Spectrometer, University of California Lawrence Radiation Laboratory Report, UCRL-6911 Pt. 1 (1962).

9. W. K. Brown, A Helium-3 Neutron Spectrometer with Extended Energy Range. Part 2: Method of Energy-Range Extension, University of California Lawrence Radiation Laboratory Report, UCRL-6911 Pt. 2 (1962).

10. A. Sayres and M. Coppola, ^{3}He Neutron Spectrometer Using Pulse Rise-time Discrimination, Review of Scientific Instruments, 35, 431-437 (1964).

11. J. L. Friedes and R. E. Chrien, Design of ^{3}He-Filled Fast Proportional Counters, The Review of Scientific Instruments, 35, 469-472 (1964).

12. A. I. Abramov, A Miniature Ionization Chamber with a ^{3}He Pressure of 4 Atmos, Instruments and Experimental Techniques, pp 570-571, translated from Pribory i Tekhnika Eksperimenta (Russian) 4 pp 56-57 (July-August 1959)

13. B. V. Rybakov and V. A. Sidorov, Nuclear Reaction Method, Fast Neutron Spectroscopy, N. A. Vlasov, Ed., pp 32-35,38, (Supplement no. 6 of the Soviet Journal of Atomic Energy),(1958), translated by Consultants Bureau Inc., New York (1960)

14. A. R. Sayres, K. W. Jones, C. S. Wu, Interaction of Neutrons with ^{3}He, Physical Review 122, 1853 (1961).

15. W. K. Brown, A Method of Extending the Energy Range of the ^{3}He Neutron Spectrometer, Nuclear Instruments and Methods 26, pp 1-6, (1964).

16. Hsien-Tsan Wang, Inversion Matrix for a Helium-3 Fast Neutron Spectrometer, University of California Lawrence Radiation Laboratory Report, UCRL-10770 (1963).

17. Theodore Elink-Schuurman (Assistant Manager for Technical Planning, Texas Nuclear Corporation, Austin, Texas, June 15, 1965) private communication.

18. R. Batchelor and K. Parker, Neutron Cross Sections of ^{3}He in the Energy Range 0.001 eV-14 MeV, 1963 Interim Revision, AWRE Report No.O-78/64, (August 1964).

19. O. K. Harling, Detector Time Jitter in ^{3}He and BF_3 Proportional Counters, Nuclear Instruments and Methods, 34,141-145 (1965).

20. W. N. English and G. C. Hanna, Grid Ionization Chamber Measurements of Electron Drift Velocities in Gas Mixtures, Canadian Journal Physics 31, 768-797 (1953).

21. Hans H. Staub, Fundamental Principles of Particle Detection, Experimental Nuclear Physics Vol. 1, E. Segre, Ed., pp 1-47 (John Wiley and Sons, Inc., New York) (1953).

22. G. Friedlander, J. W. Kennedy, and J. M. Miller, Nuclear and Radiochemistry, 2nd Edition pp 94-98 (John Wiley and Sons, New York) (1964).

23. D. H. Wilkinson, Ionization Chambers and Counters, (Cambridge University Press, England) (1950).

24. J. C. Bowe, Drift Velocity of Electrons in Nitrogen, Helium, Neon, Argon, Krypton, and Xenon, Physical Review 117 , 1411 (1960).

25. W. R. Mills, R. L. Caldwell, and I. L. Morgan, Low Voltage ^{3}He-Filled Proportional Counter for Efficient Detection of Thermal and Epithermal Neutrons, The Review of Scientific Instruments 33, 866-868 (1962).

26. Texas Nuclear Corporation, Technical Specifications B4/2-2 Series 9300 Texlium Detectors, Austin 17, Texas.

27. A. L. Cockroft and S. C. Curran, The Elimination of the End Effects in Counters, Review of Scientific Instruments 22, 37 (1951).

28. W. Franzen and L. W. Cochran, Pulse Ionization Chambers and Proportional Counters, Nuclear Instruments and their Uses, A. H. Snell, Ed., Vol. 1 pp 3-77 (John Wiley and Sons, Inc., New York) (1962).

29. D. West, Energy Measurements with Proportional Counters, Progress in Nuclear Physics Vol. 3, O. R. Frisch, Ed., (Academic Press Inc., New York) pp 22-24 (1953).

30. D. J. Hughes and R. B. Schwartz, Neutron Cross Sections, Brookhaven National Laboratory Report BNL-325 2nd Edition, (1958).

31. F. L. Ribe, $^{6}Li\ (n,\alpha)^{3}H$ Cross Section as a Function of Neutron Energy, Physical Review 103 pp 741-748 (1956).

32. R. E. Shamu, The Disintegration of Neon and Krypton by Neutrons, Nuclear Physics 31, 166-176 (1962).

33. Brookhaven National Laboratory Report, Neutron Cross Sections, Vol. 1 Z = 1 to 20, 2nd Edition, Supplement no. 2, BNL-325 TID-4500, 32 Edition (1964).

34. F. J. Vaughn, W. L. Imhof, R. G. Johnson, and M. Walt, Total Neutron Cross Sections of Helium, Neon, Argon, Krypton, and Xenon, Physical Review 118, 683-686 (1960).

35. Lawrence Radiation Laboratory Counting Handbook, Nuclear Instrumentati Group, Eds., UCRL-3307 (Rev. 2) June 5, 1964.

Appendix A. DESIGN OF EXPERIMENTAL APPARATUS

1. Design of the ^{3}He proportional counter tube

a. Previously constructed ^{3}He proportional counters.

The design of the helium-3 proportional counter tube was completed after an extensive search of the technical literature. To aid in the selection of the counter tube parameters, a summary of comparative sizes, gas compositions, filling pressures, and other pertinent data on all ^{3}He proportional counters and ionization chambers constructed to date was tabulated (Table A1). The data necessary to complete Table I is not reported, but it is apparent that a variety of heavy monotonic gases and stabilizing gases have been employed by experimenters. Counter dimensions and shapes have likewise been somewhat varied.

b. Lawrence Radiation Laboratory usage requirements

This ^{3}He proportional counter will ultimately be used for radiation surveys by the Health Physics Department at the Lawrence Radiation Laboratory. The objective of this counter therefore, is to be capable of detecting and accurately evaluating neutron spectra of energies to about 14.0 MeV regardless of the neutron source direction. It is likewise necessary that the apparatus be capable of being readily transported and placed in relatively inaccessible locations. The usage requirements thus consist essentially of: (1) 4π resolution, (2) relatively small size, (3) the high voltage requirements remain within the capacities of existing Laboratory equipment, i.e. less than 6000 volts (an additional consideration that was imposed).

c. Design variables

In the design of a proportional counter, the designer has essentially five variables that are available to him, viz: shape (geometry), dimensions of the container (cathode), dimensions of the anode, gas composition and pressure, and applied voltage. It is to be noted that once a design has been fixed, the only variable available to the experimenter is the applied voltage. Unfortunately, the five variables each effect the final properties of the counter and are essentially inter-related.

d. Design parameters

TABLE A-1

Physical Characteristics of ^{3}He Proportional Counters and Ionization Chambers Reported in the Technical Literature

Type counter	Counter shape	Cathode radius (in.)	Anode radius (in.)	Effective length (in.)	Operating voltage (volts)	Gas multiplication	Energy range (MeV)	Filling Gas (atmospheres) at STP							Experimenter, Date, and Reference
								He	Stopping gas			Stabilizing gas			
								(^{3}He)	A	Kr	Xe	CO_2	CH_4	N_2	Total Pressure
Prop.	Cyl.	1.5		11.0			0-1.0	.071 (.0071)			1.45				1.52	R. Batchelor (1952) Ref. 1
Prop.	Cyl.	1.0625	.002	4.79	2600	~10	0-1.2	0.355 (0.355)		2.16		.0237			2.54	Batchelor, Aves, and Skyrme (1955) Ref. 3
Prop.	Cyl.	1.965	.0025	5.51	6000-8000		0-5.0	(1.0 cc) @ STP	6-10						6-10	Bloom, Reilly, and Topple (1955) Ref. 2
Prop.	Cyl.	1.0625	.002	4.79	4400	~10	0-2.5	1.355 (1.355)		4.46			.0066		5.84	Batchelor and Morrison (1960) Ref. 4
Prop.	Cyl.	0.9375	.002	9.00			0-17.5	(0.976) (0.01335) (0.992) (0.0501)		4.0 4.25 4.0 4.25		.0418 .0445 .0418 .0445			5.02 4.32 5.03 4.34	A. R. Sayres (1960) Ref. 5
Prop.	Cyl.	0.980	.001	6.00	2450	4-5	7.0	(1.09)		4.50		.0106			5.60	W.K. Brown (1962) Ref. 8, 9
Prop.	Cyl.	0.480	.001	4-12	~1200			(1-10)				small amount			1-10+	Mills, Caldwell, and Morgan (1962) Ref. 25. Wang (1963) Ref. 16
Prop.	Cyl.	0.480	.001	6.0	~1900			(2)		4.0		small amount			6+	Texas Nuclear Corp. (1964) Ref. 26
Prop.	Cyl.	0.480	.003		2100			(10)				?			10+	J. L. Friedes and R. E. Chrien (1964) Ref. 11
		0.480	.003		920			(2)				?			2+	
		0.480	.001		1050			(6)				?			6+	
		0.3125	.006		5000			(9.7)				0.3			10	
		0.3125	.005		5000			(9.7)				0.3			10	
Prop.	Cyl.	2.00	.004	15.0			8.1	(1.0)		4.0			.01		5.01	Sayres and Coppola (1964) Ref. 10

TABLE A-1 (cont.)

Type counter	Counter shape	Cathode radius (in.)	Anode radius (in.)	Effective length (in.)	Operating voltage (volts)	Gas multiplication	Energy range (MeV)	Filling Gas (atmospheres) at STP							Experimenter, Date, and Reference
								He	Stopping gas			Stabilizing gas			Total Pressure
								(^{3}He)	A	Kr	Xe	CO_2	CH_4	N_2	
Prop.	Cyl.	0.4375	.0025	10.0	4000	450		5.5 (?)				0.61			6.11
		0.4375	.0025	10.0	2500	11		5.5 (?)				0.611			6.11
		0.4375	.0025	10.0	5000	93		9.02 (?)				1.00			10.02
		0.4375	.0025	10.0	4000	42		11.64 (?)				0.61			12.25
		0.4375	.0025	10.0	2400	32		5.805 (?)				0.305			6.11
		0.4375	.0025	10.0	750	1.0		5.93 (?)						(BF_3) 0.66	6.59
		0.4375	.0025	10.0	1000	1.2		5.93 (?)						(BF_3) 0.66	6.59
		0.4375	.0025	10.0	2000	2.4		5.93 (?)						(BF_3) 0.66	6.59
		0.4375	.0025	10.0	3000	8		5.93 (?)						(BF_3) 0.66	6.59
		0.4375	.0025	10.0	4200	15		5.93 (?)						(BF_3) 0.66	6.59
		0.4375	.0025	10.0	4500	390		8.71 (?)					0.97		9.68
		0.4375	.001	6.0	1000	100		5.92 (?)				?	?	?	5.92
Ion	Cyl.	~1.375	~0.14	9.25	6000			2.7 (2.7)		3.8			0.07		6.57	Freeman and West (1962) Ref. 7
Ion	Sphere	3.94	0.295	N.A.			0.1-1.0	0.46 (0.46)	2.5					0.118	3.08	N. P. Glazkov (1957) Rev. 13
Ion	Sphere	0.511	.0197	N.A.	>1600		0.2-0.8	2.5-4	2.5-4					0.1-0.16	5.1-8+	A. I. Abramov (1958) Rev. 12

In addition to the three usage requirements, there exist several mechanical and electrical requirements that the counter must fulfill. These requirements are:

(1.) To fulfill the 4π requirement, the filling gas must be capable of completely stopping maximum energy product particles within the active volume of the container.

(2.) The wall thickness of the container must be sufficient to contain the filling gases under pressure.

(3.) The gas fillings must not provide competing reactions that can be mistaken for bona-fide events. Recombination should be minimal.

(4.) Gas multiplication to some degree is necessary to overcome electrical noise, and to obtain independence from the reaction site within the counter.

(5.) "Jitter-time" (the time it takes for an electron at a point on the cathode to migrate to the anode) must be relatively small, and within the resolving capabilities of the associated electronics.

(6.) Electric field distortion must be minimized, and field gradient at equal distances from the anode should be equal.

(7.) Electrical breakdown and "Corona discharge" must be eliminated.

e. Effect of design variables on design parameters

The changing of any design variable has a profound effect on the design parameters. The interdependence of the parameters to several variables makes any proportional counter a compromise. The changing of the variables has an effect upon the parameters as follows:

(1.) Shape (geometry)--effects: 4π response; field gradient distribution (thus "jitter time"); space charge distribution.

(2.) Dimensions of the cathode--effects: amount, pressure, and composition of the filling gas; field gradients (thus "jitter time").

(3.) Dimension of the anode--effects: field gradient ("jitter time" and gas amplification); corona discharge.

(4.) Gas composition and pressure--effects: stopping power; jitter time; gas amplification; competing nuclear events; relative cross sections of the composite gas.

(5) Applied voltage--effects: field gradient (thus jitter time and gas multiplication); corona effect.

f. Selection of the appropriate design variables

(1) The geometry selected was a cylindrical proportional counter. A cylinder was selected instead of a sphere, due to the adverse effect of a concentration of positive space charges near the anode after the occurrence of gas multiplication. While this condition likewise exits in a cylindrical proportional counter, the space charge effects are distributed over the length of the anode wire and are not concentrated at a single point as in a spherical configuration. It was also considered that the resolving time lag would be less (thus the counting rate higher) and multiplication more uniform in a cylindrical chamber. This selection, however, necessitated some sacrifice of the 4π response of the proportional counter--a deficiency that was partially overcome by increasing the gas pressure. The field gradient distribution is radial along a central axis in a cylindrical tube, except near the ends, instead of a direct radial distribution as in a spherical chamber. The end distortion of the field gradient of the cylinder can be eliminated, however, through the use of appropriately designed field tubes.[27]

(2) The dimensions of the cathode were arbitrarily selected to be a maximum outside radius of 2.0 in. and an active length of 15.0 in. These dimensions were considered to be about the maximum that would meet both the portability requirement and still maintain a reasonable field gradient (thus jitter time) near the outer portions of the tube's radius. It is to be noted that the tube size, which has been dictated by practical consideration likewise limits selections of the amounts, pressures, and composition of the filling gases. The thickness of the cathode walls is determined by the filling pressures.

(3) Gas composition and filling pressures

(3.a.) The gas composition must be such that:

(3.a.1) The reaction particles from a 14.0 MeV incident neutron will be stopped in a diameter of the cylinder. This will to a certain measure restore a portion of the 4π geometry resolution.

(3.a.2) The electron migration through the gas mixture should be sufficiently

rapid that extremely long jitter-times are not encountered.

(3.a.3) Competing nuclear events are minimized.

(3.a.4) A stabilizing gas be employed to absorb photon produced from bremsstrahlung during gas multiplication and to prevent spurious pulses.

(3.a.5) The gas multiplication (which is a function of the pressure) be sufficient to provide a pulse that is both proportional to the energy of the incident neutron and sufficient to mask electrical noise. A gas multiplication of at least 10 is considered desirable.[28,29]

(3.b.) The selection of the gas composition was dictated by several factors.

(3.b.1) The cross section of the $^{3}He(n,p)T$ reaction decreases by a factor of 10 for neutrons at 0.1 MeV to 11 MeV.[18] It was decided that some compensation for this decrease in cross section should be made if neutrons of higher energies are to be detected in meaningful numbers. This reduction in efficiency at higher energies is likewise compounded by the fact that since the higher energy product particles will travel further in the gas medium, their chances of intersecting a wall are increased and thus the probability of the production of a full energy count is decreased. It was considered that two atmospheres of ^{3}He would compensate somewhat for this loss of efficiency at higher energies.

(3.b.2) Helium-3 is a gas with relatively low stopping power for charged particles. A heavy monotonic gas must be added to insure that the charged particles stop within the diameter of the cylinder. Previous experimenters have used argon, krypton, and xenon for this purpose. Argon was rejected in this design for two reasons: First, the pressures of argon necessary to stop a charged particle are greater than those of either Kr or Xe for the same energy. Secondly, the $A(n,\alpha)S^{33}$ reaction becomes significant above about 2.2 MeV.[2,30] Pulses due to this reaction can be removed by rise time discrimination, but the reaction data is incomplete and at higher energies an argon (n,p) reaction occurs. The disintegration cross section at a single energy of 14.0 MeV has been measured for argon, krypton, and xenon and found to greater for argon than either Kr and Xe.[31] (The disintegration particles produced are not however identified in reference 31.)

Xenon was likewise rejected due to the uncertainty of the type of

disintegration particles produced, and absence of data concerning the disintegration cross section at intermediate energies. The rejection of xenon was difficult since the heavier of the noble gases would have required smaller filling pressures than either argon or krypton.

Krypton was thus selected to be the "stopping gas". Unfortunately, krypton likewise has a disintegration cross section (tentatively identified as an (n,p) reaction by Shamu[32]) which produces a scattering of disintegration particle energies over the entire energy distribution, the main portion lying in the 4-8 MeV region.[31,32] No attempt will be made to remove the protons produced from krypton disintegration from the resultant spectrum due to the uncertainty of their energy distribution.

Having selected a helium-3, krypton mixture it was necessary to determine the appropriate filling pressures. This was accomplished by a trial and error method of computation based upon determining the length of track of a proton having the energy of the average cosine of scattering angle (Lab System)from a 14.0 MeV incident neutron. When the length of track was equal to the radius of the cylinder, it was considered that the pressure requirement had been met, and that a configuration that could approach the desired 4π resolution had been accomplished. It was found that 10 atmospheres of krypton plus 2 atmospheres of ^{3}He met this condition.

(3.b.3) A stabilizing gas was considered essential and 0.5% CO_2 was selected for this purpose. Carbon dioxide was selected in lieu of methane which has been successfully utilized by Batchelor,[3] Freeman and West,[7] and Sayres[10] in their most recent counters. The reason for this change is that our counter is designed to evaluate neutron spectra to 14.0 MeV (considerably above the energies evaluated by previous experimenters), and it was considered that the introduction of a source of additional recoil protons (from the methane) into the tube would provide unnecessary complications--especially in view of the additional proton background due to the krypton disintegrations (which was not a problem at lower neutron energies).

(3.b.4) For comparison purposes, the cross-sections of the various gas reactions are plotted in Fig. A1 as a function of neutron energy. The cross section for the CO_2 was obtained by adding the energy dependent

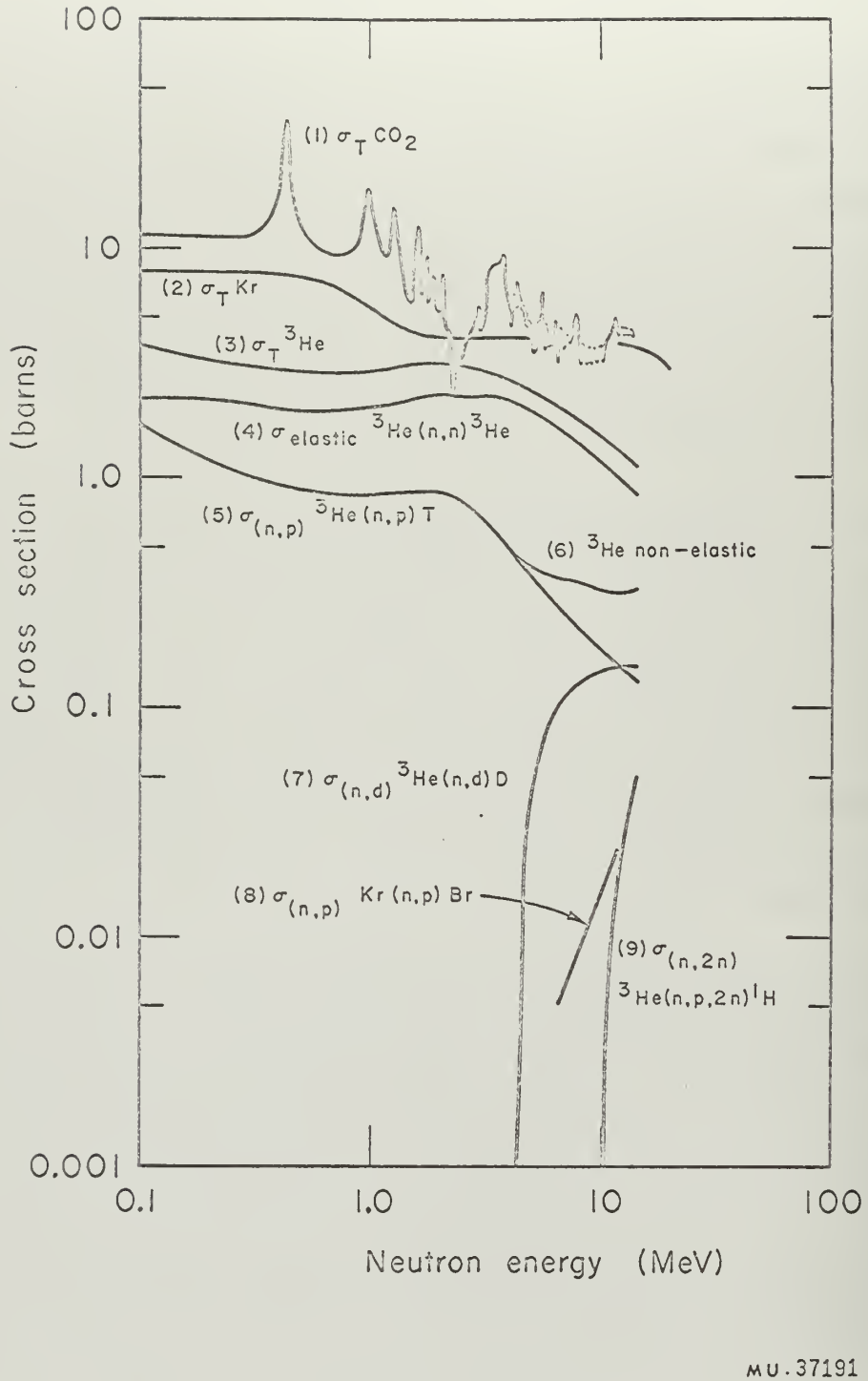

Fig. A1. Neutron Reaction Cross Sections

Source of Data

(1) Calculated from σ_T(E) carbon + σ_T(E) oxygen (Ref. 33)
(2) Ref. 34
(3-7) Ref. 18
(8) Ref. 32
(9) Ref. 18

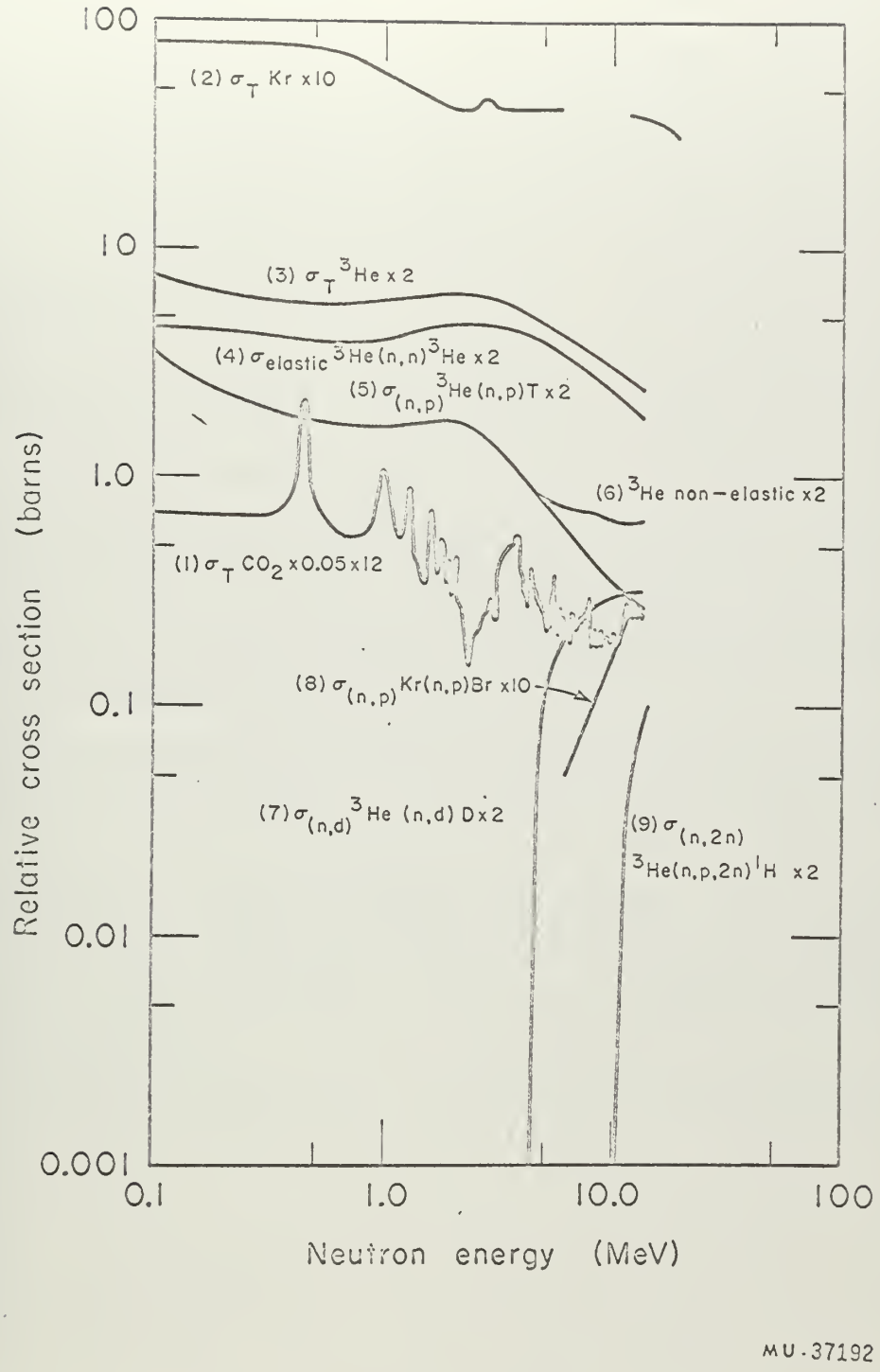

Fig. A2. Relative Neutron Reaction Cross Sections in a Gas Mixture of 10 Atmos Kr, 2 Atmos ^{3}He, and 0.5% CO_2

total cross section of carbon to twice the total cross section of oxygen. In addition, a relative plot of the cross sections is presented to display the collision probabilities "seen" by a neutron as it enters the tube (Fig. A2). It should be noted that the disintegration cross section of the krypton at 10 atmospheres pressure becomes a factor of major consideration at higher energies, and probably will determine the upper energy limit of further refinement on this type counter.

(3.b.5) The dimensions of the anode were now considered and several applie voltage and wire size combinations were attempted. Jitter time was calculated by use of a "weighted" electron mobility factor (presented on page 19) and found to vary from 18-22 μseconds for applied voltages of 6000-5000 volts. The gas multiplication was calculated from extrapolations of Brown's data[8] and found to be approximately 10-15 for the above range of voltages, using a 3 mil diameter wire. The jitter time is considerably longer than desired, but increasing the wire size (for fixed cathode dimension and filling pressure) decreases the gas multiplication and does not appreciably decrease the jitter time in the voltage ranges considered. The jitter time is relatively insensitive to changes in applied voltages, therefore if we seek to reduce the jitter time, the only feasible method is to reduce the diameter of the counter and increase the gas filling pressure. This alternative is undesirable since an increase in gas pressure would increase the relative disintegration cross section of the krypton--a problem that is already larger than negligible proportions.

(3.b.6) We must therefore accept the fact that the counter will be comparatively slow, and design the electronics accordingly.

2. Design of the Associated Electronic Components

a. Design Parameters

The electronic components of the ^3He proportional counter must be designed to meet several requirements. The majority of these requirements are common to proportional counters in general, however there exist several unique problems associated with the broad range of rise times of the pulses (essentially 3-22 μsec is our region of interest). The design parameters include:

(1) The pulse produced by an ionizing event must be linearly amplified and be capable of accurately portraying the energy of the ionizing event.

(2) The electronics must have a low signal to noise ratio.

(3) The high voltage supply must be well stabilized, since variations in the high voltage will cause a direct variation in the pulse height.

(4) The electronics must be capable of distinguishing between a desired event and an undesired event (recoil).

(5) The electronics must be sensitive to the relatively large range of rise times, and to accomodate pulses that vary in both energy and rise time.

(6) Provision must be made to permit variation in: the high voltage supply, the counter field tube settings, the rise time discriminator setting, and the time constants of the double differentiating network.

b. Electronic design

(1) A block diagram of the electronics arrangement constructed to meet the above parameters is indicated below. The basic arrangement of components is similar to that described by Sayres and Coppola[10] with the exception of a new Peak Sampler Unit and a Time to Height Converter Unit which were designed and constructed by Mr. R. M. Brown of the LRL Physics Technical Support Group. The purpose of the Peak Sampler Unit is to provide a gating to the Multichannel Analyzer at a time when the pulse has reached its maximum value.

(2) To explain the operation of the electronics, consider the formation of a pulse in the proportional counter as the result of a collision of a neutron with one of the contained gas molecules (^3He, Kr, CO_2). The

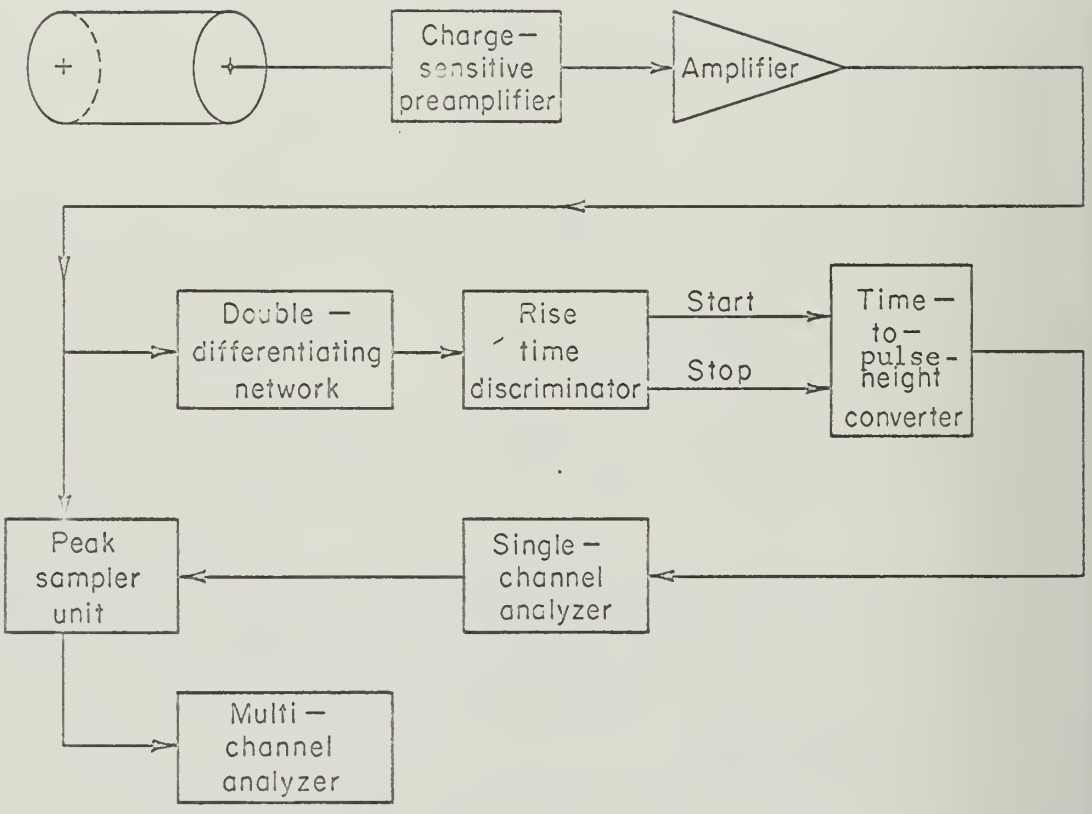

Fig. A3. Block Diagram of Electronic Components for Rise-Time Discrimination

collision may result in either a desired event, i. e. disintegration of the ^{3}He nucleus, or an undesired event--the production of a recoil.

(2.a.) The electrons that were liberated as the charged particle (s) transit the gas are accelerated by the electrical field gradient and a charge is deposited on the anode. The size of the charge is dependent upon the energy of the particles that are stopped within the gas medium, and the amount of gas multiplication in the area surrounding the anode. (For gas multiplication above about 10, the energy spectrum is undistorted by the position of the ionizing event within the tube[29] providing, that saturation of positive ions in the sheath surrounding the anode has not been achieved.) The electrical pulse begins to accumulate when the first electron reaches the anode, and reaches a maximum when the last electron finally arrives at the center wire. Depending upon the type of event, the initial energy of the incoming neutron, the radial distance from, and the resulting track orientations with respect to the anode, this charge build-up period may vary from a fraction of a micro second to as much as 22 μseconds for a given voltage gradient distribution within the counter. The actions of the following component units begin when the first charge begins to appear on the anode, and continue until all the charge has been collected.

(2.b.) The incoming pulse is amplified through a charge sensitive Preamplifier and an Amplifier.

(2.c.) The pulse is sent into two parallel channels after leaving the Amplifier. One portion of the still rising pulse is sent directly to the Peak Sampler Unit where it accumulates to a maximum--at which time it is either "gated" into the Multichannel Analyzer, or is discarded.

(2.d.) The other portion of the pulse is sent to a Double Differentiating Circuit (figure A-4) where an output pulse is obtained whose duration is dependent upon the rise time of the input pulse. (As an approximation, the output pulse from this unit represent the "rate of rise time" since simple RC circuits are not true differentiators.) The time between base line crossings of the doubly differentiated pulse is thus related to the rise time.[10] The exact relationship between the differentiating time constants and the rise time is not critical since we are only interested in setting a discriminator value which eliminates all pulses having a

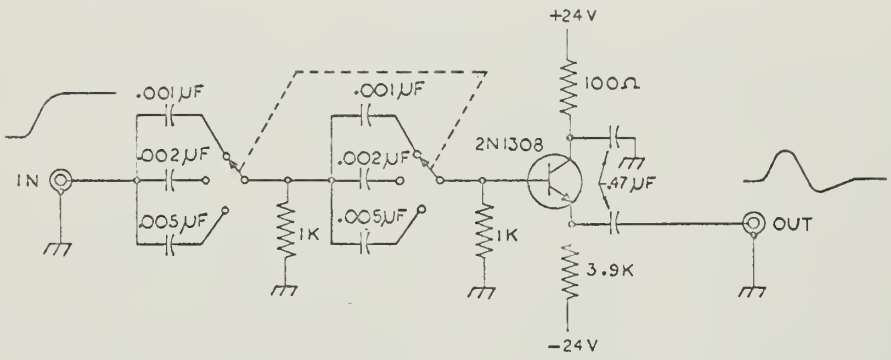

FIG. A4

DOUBLE DIFFERENTIATOR

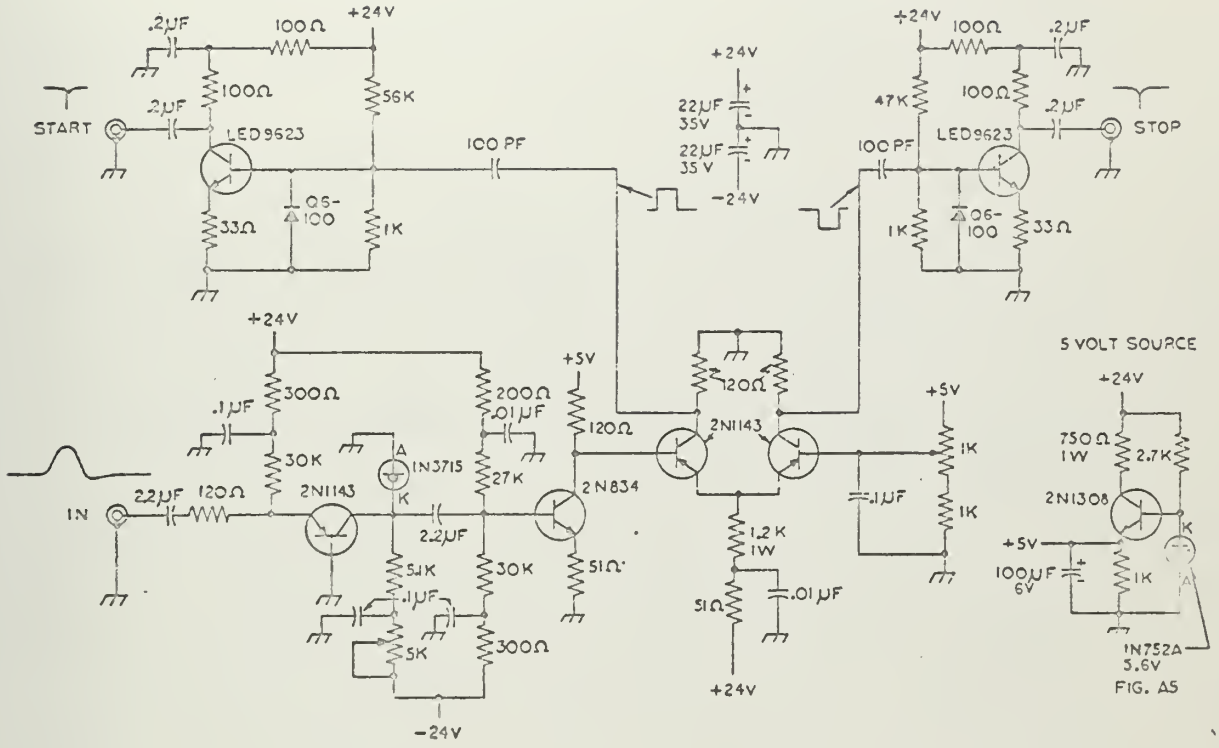

FIG. A5

RISE TIME DISCRIMINATOR CIRCUITRY

rise time less than a predetermined value, and retaining those that have a rise time greater than this value. The calibration of the rise time circuitry is accomplished by utilizing a signal generator with pulses of known rise times. The shape of the input and output pulses are shown on Fig. A-4. The differentiating time constants are equal to each other at each of the three settings (1, 2, and 5 μsec), and can be varied depending upon the desired output. The counter normally operates with the differentiating time constants set at 2.0 μsec. For an analysis of low energy spectra, the differentiating time constants are set at 1.0 μsec, and at the higher 5.0 μsec time constant when we are primarily interested in the higher end of the energy spectra.

(2.e.) The output of the Double Differentiating Circuit is directed to a unit called a "Pulse Height Discriminator". The purpose of this unit is to convert the input pulse to a square wave, and from this square wave to generate a "start pulse" and a "stop pulse" as the input double differentiated pulse crosses the zero potential axis. The electronic arrangement for this component is shown in Fig. A-5 along with the circuitry necessary to produce the 5 volt bias source.

(2.f.) The "start pulse" and the "stop pulse" are then directed to a Time-to-Height-Converter unit. A block discription and a pulse formation diagram is displayed in Fig. A-6. The "start pulse" sets the Bistable Multivibrator thus initiating the ramp generator (consisting of a constant current source charging a capacitor). The charging process continues until it is stopped by the action of the "stop pulse". The "stop pulse" is fed into a Monostable Multivibrator which produces a 2.5 μsec output pulse. This pulse turns off the constant current source, and thus terminates the charging process. The height of the ramp at the point where it is terminated determines the height of the 2.5 μsec wide output pulse. The capacitor is rapidly discharged, and the Start Multivibrator is reset for the next pulse. The output of the Time-to-Height Converter is thus a pulse of magnitude such tat it is directly related to the zero cross of the double differentiating circuit output--thus directly related to the pulse rise time. The pulse width of 2.5 μsec is of no significance other than a convenient width for the following components. A circuit diagram of the Time-to-Height Converter is shown in Fig. A-7.

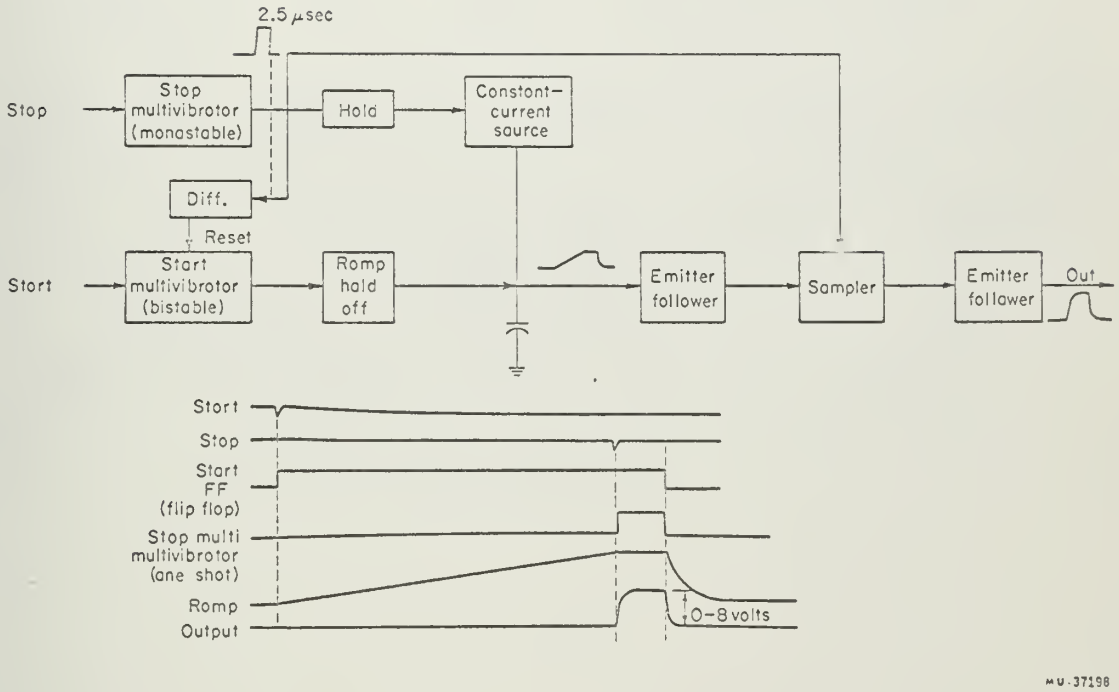

Fig. A6. Block Diagram of Time to Height Converter

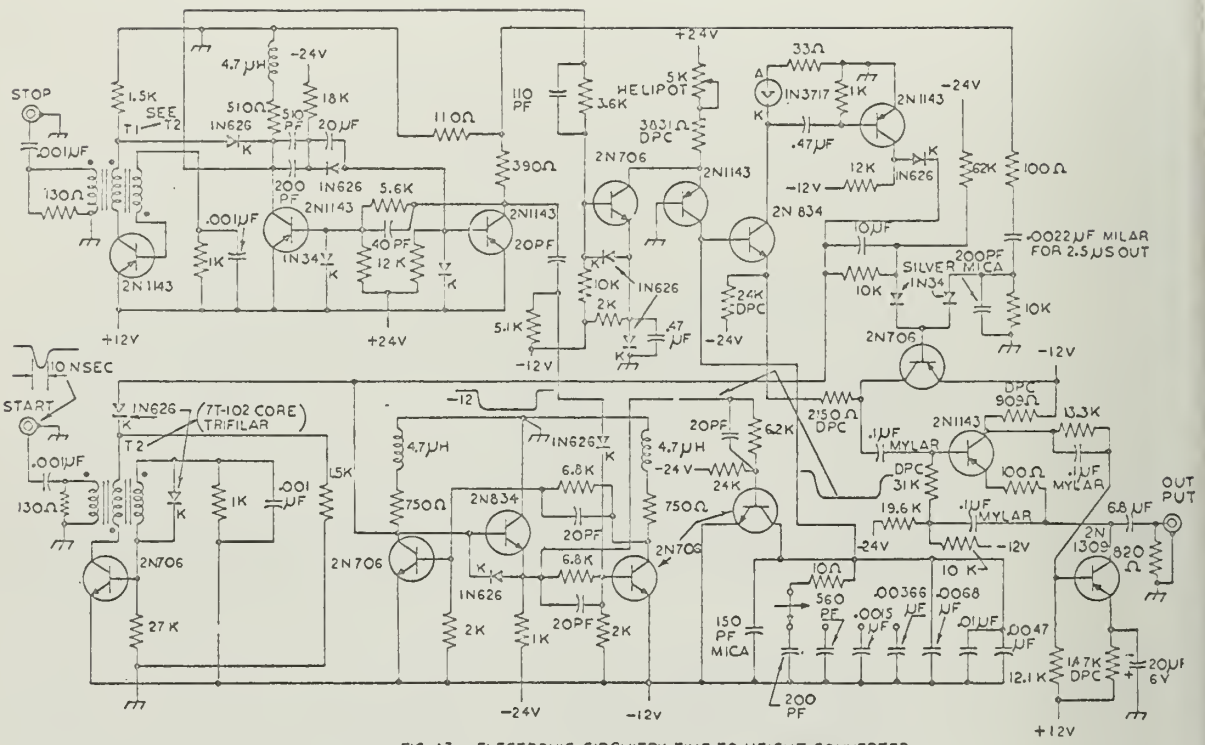

FIG A7 ELECTRONIC CIRCUITRY, TIME TO HEIGHT CONVERTER

(2.g.) The output of the Time-to-Height Converter is then sent to a Single Channel Analyzer (Fig. A-8). The Single Channel Analyzer can be set to accept all pulses above a certain height (time) or to accept pulses on a window basis. The analyzer settings are adjustable. Numbers on Fig. A-8 refer to standard LRL drawings .* The Single Channel Analyzer produces an output pulse only if the input amplitude is within the window setting.

(2.h.) The output pulses of the Single Channel Analyzer (rise times within desired ranges) are then passed to the trigger input of the Peak Sampler Unit (Fig. A-9). The original pulse has been building up to a maximum and when the "trigger signal" arrives from the Single Channel Analyzer, the pulse is gated into the Multi-Channel Analyzer. If the "trigger signal" does not enter the Peak Sampler Unit, the pulse is led to ground.

* Data on the units of Fig. A-8 can be found in Reference 35.

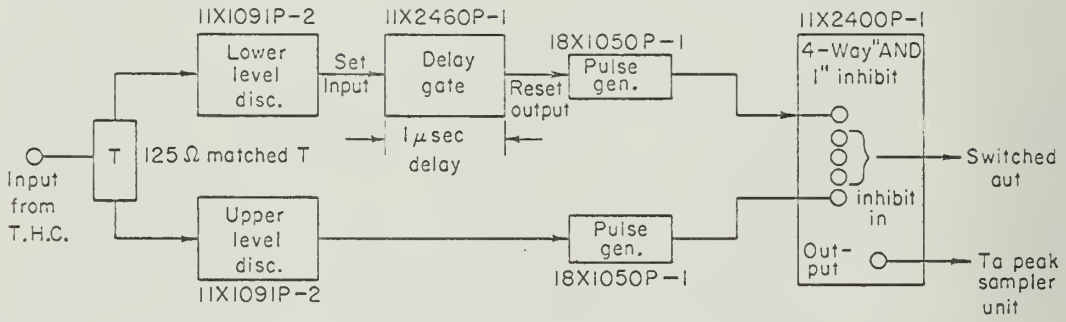

Note: Numbers refer to standard LRL drawing numbers

Fig. A8. Block Diagram, Single Channel Analyzer Unit

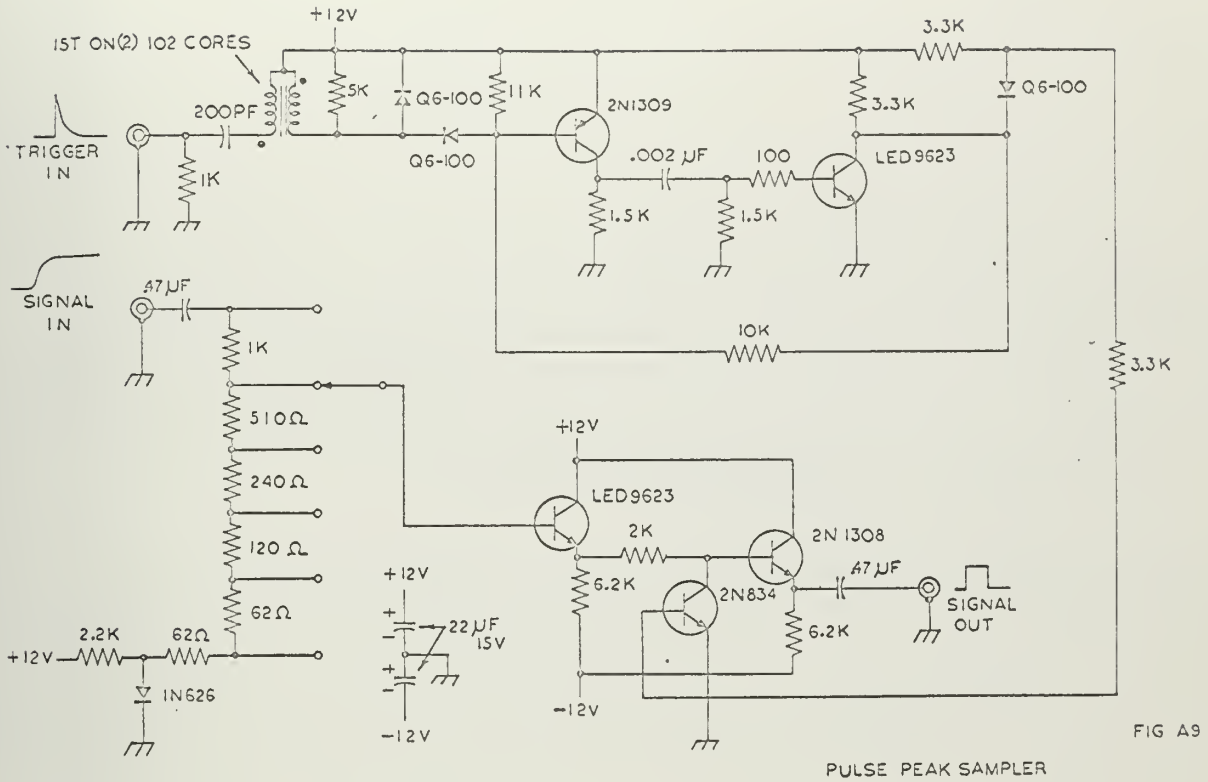

FIG A9

PULSE PEAK SAMPLER

Appendix B. Nuclear Reaction Dynamics

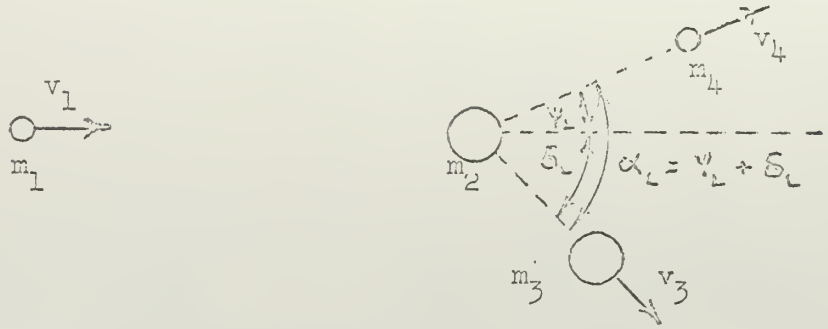

Consider the general case of a particle of mass m_1 and v_1 colliding with a particle of mass m_2 assumed to be at rest. Particle m_2 absorbs the collision. After the reaction, particles m_3 and m_4 with velocities v_3 and v_4 leave the reaction site at angles δ_L and Ψ_L respectively. Utilizing non-relativistic dynamics, the laboratory system of coordinates, and mass numbers of masses, we can write the three general equations for the conservation of momentum and energy.

a. Conservation of Momentum:

$$m_1 v_1 = m_3 v_3 \cos \delta_L + m_4 v_4 \cos \Psi_L \qquad \text{(B-1)}$$

$$0 = m_3 v_3 \sin \delta_L - m_4 v_4 \sin \Psi_L \qquad \text{(B-2)}$$

b. For the Conservation of Energy:

$$\frac{1}{2} m_1 v_1^2 + Q = \frac{1}{2} m_3 v_3^2 + \frac{1}{2} m_4 v_4^2 \qquad \text{(B-3)}$$

where Q is the energy equivalent corresponding to the mass difference (in non-relativistic particles) between the initial masses (before collision) and the resulted masses (after collision). i.e.

$$Q = (m_1 + m_2) - (m_3 + m_4) \qquad \text{(B-4)}$$

Note that Q may be positive or negative. Q values are tabulated and are readily available, or may be calculated by using Eq. (B-4)

Equations (B-1), (B-2), and (B-3) may also be written in terms of energy by making use of the relationship $E = \frac{1}{2} mv^2$ of $mv = \sqrt{2\ Em}$

Thus equations (B-1), (B-2), and (B-3) (after clearing of the constant $\sqrt{2}$ factor in Eqs. (B-1) and (B-2)) becomes:

$$\sqrt{m_1 E_1} = \sqrt{m_3 E_3} \cos \delta_L + \sqrt{m_4 E_4} \cos \psi_L \qquad \text{(B-1.a.)}$$

$$0 = \sqrt{m_3 E_3} \sin \delta_L - \sqrt{m_4 E_4} \sin \psi_L \qquad \text{(B-2.a.)}$$

$$E_1 + Q = E_3 + E_4 \qquad \text{(B-3.a.)}$$

In the following analysis, we shall work with energies rather than velocities. Note that by the simultaneous solutions of the above three equations, we may eliminate any two parameters.

Case I Simple Scattering

Let us first consider the case of simple scattering wherein $m_1 = m_3$ and $m_2 = m_4$. It is readily seen from Eq. (B-4) that in this case $Q = 0$. It is desirable to derive an expression for the energy imparted to the stationary target m_2 in terms of the incident particle energy. Making the above mass substitutions into Eqs. (B-1.a.) and (B-2.a.) transposing the last term of Eqs. (B-1.a.) and either term in (B-2.a.), squaring both equations and adding we can eliminate the angle δ_L to obtain

$$m_1 E_1 - 2\sqrt{m_1 m_2 E_1 E_4} \cos \psi_L + m_2 E_4 = m_1 E_3$$

Solving Eq. (B-3.a.) for E_3 and substituting this value into the above relationship, one obtains:

$$m_1 E_1 - 2\sqrt{m_1 m_2 E_1 E_4} \cos \psi_L + m_2 E_4 = m_1 (E_1 - E_4)$$

or:

$$-2\sqrt{m_1 m_2 E_1 E_4} \cos \psi_L + m_2 E_4 = - m_1 E_4$$

$$E_4 (m_1 + m_2) = 2\sqrt{m_1 m_2 E_1 E_4} \cos \psi_L$$

squaring both sides and solving for E_4 yields:

$$E_4 = \frac{4\, m_1\, m_2}{(m_1 + m_2)^2}\, E_1 \cos^2 \psi_L \qquad \text{(B-5)}$$

Therefore, the energy of the recoil particle is dependent upon (a) the masses the incident particle and target particles, (b) the energy of the incident particle, and (c) the scattering angle the target particle makes to the direction of the incident particle. For a maximum recoil it is obvious that a head-on collision $(\psi_L = 0)$ will impart the maximum energy to the recoil particle.

Our counter is designed to analyze neutrons of energies approaching 14.0 MeV. It is of interest to determine the maximum energy that can be imparted to a potential recoil particle. In this case, let us assume that $\psi_L = 0$. Using the atomic masses of the neutron and the Helium-3 nucleus, and the chemical atomic weights for krypton, carbon, and oxygen respectively, we can substitute these values into Eq. (B-5) to obtain:

	Maximum Recoil Energy General	for 14.0 MeV neutron
1. E_{max} ^{3}He recoil	$0.75\ E_N$	10.5 MeV
2. E_{max} carbon recoil	$0.284\ E_N$	3.95 MeV
3. E_{max} oxygen recoil	$0.222\ E_N$	3.11 MeV
4. E_{max} krypton recoil	$0.0466\ E_N$	0.65 MeV

Case II - ^{3}He (n,p)T reaction

In the case of the ^{3}He (n,p)T reaction we can write the equations for conservation of momentum and energy as follows: Let us identify m_1 and E_1 as a neutron having mass of unity and energy E_N; mass m_2 will be the ^{3}He molecule having a mass of 3; we shall designate m_3 as the triton having a mass of 3 and energy E_T; the proton having a mass of unity will replace m_4 and will have an energy E_p. Making these substitutions into Eqs. (B-1.a.), (B-2.a.), and (B-3.a.) yields:

$$\sqrt{E_N} = \sqrt{3\ E_T} \cos \delta_L + \sqrt{E_P} \cos \psi_L \qquad \text{(B-1.b.)}$$

$$0 = \sqrt{3\,E_T}\,\sin\delta_L + \sqrt{E_P}\,\sin\psi_L \qquad \text{(B-2.b.)}$$

$$E_N + Q_{n,p} = E_T + E_P \qquad \text{(B-3.b.)}$$

It will be of interest in the determination of rise times for us to have an expression for the angle α_L between the proton vector E_P and the triton vector E_T. This expression can be obtained by squaring Eqs. (B-1.b.) and (B-2.b.) and adding the two equations. This yields:

$$E_N = 3\,E_T + 2\sqrt{3\,E_T\,E_P}\;(\cos\psi_L\;\cos\delta_L - \sin\psi_L\,\sin\delta_L) + E_P$$

Recognizing that the bracketed term is equal to: $\cos(\psi_L + \delta_L) = \cos\alpha_L$, we can solve for $\cos\alpha_L$

$$\cos\alpha_L = \frac{E_N - 3\,E_T - E_P}{2\,(3\,E_T\,E_P)^{1/2}}$$

The solution of equation (B-3.b.) for E_N and the substitution into the expression for $\cos\alpha_L$ yields:

$$\cos\alpha_L = -\frac{(Q_{n,p} + 2E_T)}{2\sqrt{3\,E_T\,E_P}} \qquad \text{(B-6)}$$

Note that α_L is always obtuse since $Q_{n,p}$ is a positive quantity.

$$Q_{n,p} = 0.764 \text{ MeV}$$

The $\sin\alpha_L$ will also be of interest in our computations. This can be easily derived using the Pythagorean Theorem to produce

$$\sin\alpha = \frac{\sqrt{4E_T\,(2\,E_P - E_T) - Q_{n,p}^2}}{2\sqrt{3\,E_T\,E_P}} \qquad \text{(B-7)}$$

Case III ^{3}He(n,d)D Reaction

In a dueteron producing reaction, let us identify the general case as follows: E_N and unity are again substituted for E_1 and m_1; m_2 is the ^{3}He molecule of mass 3; E_{D1} and mass 2 are assigned as E_3 and m_3; and E_{D2}

and mass 2 are utilized for E_4 and m_4. Substitution of these values into Eqs. (B-1.a.), (B-2.a), and (B-3.a.) yields:

$$\sqrt{E_N} = \sqrt{2\,E_{D1}}\ \cos\theta_L + \sqrt{2\,E_{D2}}\ \cos\psi_L \qquad \text{(B-1.c.)}$$

$$0 = \sqrt{2\,E_{D1}}\ \sin\theta_L + \sqrt{2\,E_{D2}}\ \sin\psi_L \qquad \text{(B-2.c.)}$$

$$E_N + Q_{n,d} = E_{D1} + E_{D2} \qquad \text{(B-3.c.)}$$

We are again interested in the angle α_L between the two deuteron vectors. Proceeding as in the previous case we find that

$$\cos\alpha_L = \frac{E_N - 2\,E_{D1} - 2\,E_{D2}}{4\sqrt{E_{D1}\,E_{D2}}}$$

Solving (B-3.c.) for E_N and substitution into the value for $\cos\alpha_L$

$$\cos\alpha_L = -\frac{\left(Q_{n,d} + E_{D2} + E_{D1}\right)}{4\sqrt{E_{D1}\,E_{D2}}} \qquad \text{(B-8)}$$

Note that if $E_{D1} + E_{D2} = Q_{n,d}$ (which is negative), then $\alpha_L = \frac{\pi}{2}$. If $E_{D1} + E_{D2} < Q_{n,d}$, α_L is acute; and if $E_{D1} + E_{D2} > Q_{n,d}$, α_L is obtuse.

$Q_{n,d}$ = - 3.27 MeV and is threshold at 4.36 MeV

At threshold $\alpha_L = 0$

The sin of α_L can be determined as in case II

$$\sin\alpha_L = \frac{\sqrt{16\,E_{D1}\,E_{D2} - \left(Q_{n,d} + E_{D1} + E_{D2}\right)^2}}{4\sqrt{E_{D1}\,E_{D2}}} \qquad \text{(B-9)}$$

APPENDIX C

DISTRIBUTION OF ENERGY AND ANGULAR DEPENDENCE IN SPHERICAL COORDINATES

A. Reason for the Variation of Cos Θ rather than Θ in Determination of Rise-Time Probability Function.

In spherical coordiantes, an element of surface area is determined as portrayed in the attached sketch. Assume a radius of unity.

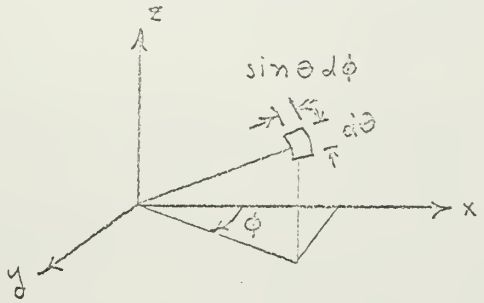

$$dA = \sin \Theta \, d \phi \, d \Theta = -d \phi \, d (\cos \Theta) \qquad (C\text{-}1)$$

If we wish to cover every possible element of the area of the sphere, we can see that the differential area is not composed of merely dΘ and dϕ, but dΘ and sin Θdϕ. Varying just Θ and ϕ would place undue emphasis on the polar regions where the sine of Θ varies slowly with Θ. Therefore, we must vary ϕ and cos Θ to obtain uniform distribution of the tips of our energy vectors over all possible configurations.

B. Probability of a Lab Energy Particle Having an Energy E_L after Interaction.

Given: A particle of mass m_1 with energy E_{1L} strikes a particle of mass m_2 at rest. Product particles are m_3 and m_4 with added energy Q.

To Find: What is the energy of m_3 in the Lab system of coordinates.

This problem is similar to the relationships developed in Appendix "B", however it will be shown that any distribution of energy of the product

particles is equally probable within a maximum and minimum energy rang

Notation: m = mass

E = energy = $\frac{1}{2} mv^2$

P = momentum = mv

v = velocity

ϕ = azimuthal angle

θ = polar angle

subscript x, y, z = components of vector quantities in x, y, or z directio

subscript 1,2,3,4= particle identification

subscript L, cm = coordinate system; L≡ Laboratory system, cm≡ center of mass system

Select the coordinates of the cm system so that the z axis is along the direction of $|\overrightarrow{v_{1L}}|$

$$E_{1L} = \frac{1}{2} m_1 |\overrightarrow{v_{1L}}|^2 \quad \text{or}$$

$$|\overrightarrow{v_{1L}}| = \sqrt{\frac{2E_{1L}}{m_1}}$$

$$|\overrightarrow{P_{1L}}| = m_1 |\overrightarrow{v_{1L}}| = 2 m_1 E_{1L}$$

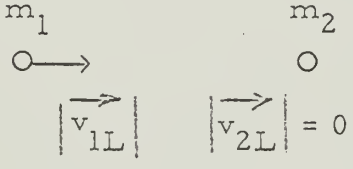

Laboratory system before collision.

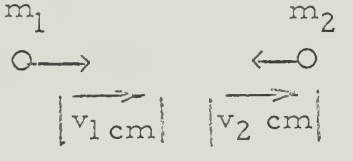

Center of mass system before collision.

$$|\overrightarrow{P_{cm}}| = |\overrightarrow{P_{1\,cm}}| + |\overrightarrow{P_{2\,cm}}| + |\overrightarrow{P_{3\,cm}}|$$

$$|\overrightarrow{v_{cm}}| = \frac{m_1}{m_1 + m_2} |\overrightarrow{v_{1L}}|$$

$|\overrightarrow{v_{1\,cm}}| = |\overrightarrow{v_{1L}}| - |\overrightarrow{v_{cm}}|$ but $|\overrightarrow{v_{1L}}|$ and $|\overrightarrow{v_{cm}}|$ are parallel

$$\therefore |\overrightarrow{v_{1\,cm}}| = |\overrightarrow{v_{1L}} - \overrightarrow{v_{cm}}| = |\overrightarrow{v_{1L}}| \left[1 - \frac{m_1}{m_1 + m_2}\right] = |\overrightarrow{v_{1L}}| \left[\frac{m_2}{m_1 + m_2}\right]$$

and $$|\overrightarrow{v_{2\,cm}}| = |\overrightarrow{v_{2L}} - \overrightarrow{v_{cm}}| = -|\overrightarrow{v_{1L}}| \left[\frac{m_1}{m_1 + m_2}\right]$$

$\therefore E_{(tot.\ before\ cm)} \equiv$ Total energy available in the cm system before collision

$$E_{(tot.\ before\ cm)} = \frac{1}{2} m_1 |\overrightarrow{v_{1\,cm}}|^2 + \frac{1}{2} m_2 |\overrightarrow{v_{2\,cm}}|^2$$

$$= \frac{1}{2} \frac{m_1 m_2}{m_1 + m_2} |\overrightarrow{v_{1L}}|^2 = E_{1L} \left(\frac{m_2}{m_1 + m_2}\right)$$

and $$E_{(tot.\ after\ cm)} = E_{tot.\ before\ cm} + Q \equiv E'$$

$$\therefore E' = E_{1L} \frac{m_2}{m_1 + m_2} + Q \qquad (C\text{-}2)$$

but, $$E' = \frac{|\overrightarrow{P_{3\,cm}}|^2}{2 m_3} + \frac{|\overrightarrow{P_{4\,cm}}|^2}{2 m_4}$$

and since in the cm system, $|\overrightarrow{P_{3\,cm}}| = -|\overrightarrow{P_{4\,cm}}|$

$$E' = \frac{|\overrightarrow{P_{3\,cm}}|^2}{2} \cdot \left[\frac{1}{m_3} + \frac{1}{m_4}\right]$$

solving for $|\overrightarrow{P_{3\,cm}}|$

$$|\overrightarrow{P_{3\,cm}}| = \sqrt{\frac{2 m_3 m_4 E'}{m_3 + m_4}}$$

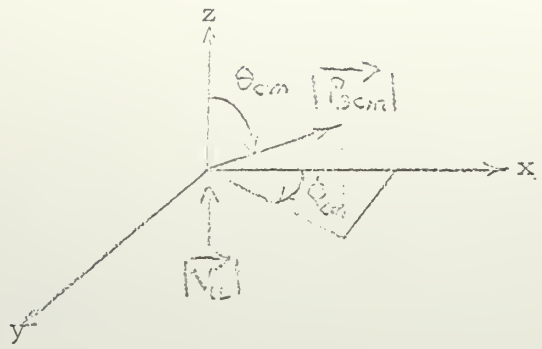

$$P_{3x\ cm} = \left|\vec{P}_{3\ cm}\right| \cos\ (90-\theta)_{cm} \cos\ \phi_{cm} = \left|\vec{P}_{3\ cm}\right| \sin\ \theta_{cm} \cos\ \phi_{cm}$$

$$P_{3y\ cm} = \left|\vec{P}_{3\ cm}\right| \cos\ (90-\theta)_{cm} \sin\ \phi_{cm} = \left|\vec{P}_{3\ cm}\right| \sin\ \theta_{cm} \sin\ \phi_{cm}$$

$$P_{3z\ cm} = \left|\vec{P}_{3\ cm}\right| \cos\ \theta_{cm}$$

but:

$$P_{3\ xL} = P_{3x\ cm}$$

$$P_{3\ yL} = P_{3y\ cm}$$

$$P_{3\ zL} = m_3 \left[\frac{P_{3z\ cm}}{m_3} + v_{z\ cm}\right] \quad \text{but the last term in brackets} = \left|\vec{v}_{c.m.}\right|$$

$$P_{3zL} = m_3\left(\frac{\left|\vec{P}_{3\ cm}\right|}{m_3} \cos\ \theta_{cm} + \frac{m_1 \left|\vec{v}_{1L}\right|}{(m_1 + m_2)}\right)$$

$$= \cos\ \theta_{cm} \sqrt{\frac{2\ m_3\ m_4\ E'}{(m_3 + m_4)}} + \frac{m_3 \sqrt{2m_1\ E_{1L}}}{(m_1 + m_2)}$$

$$\left|\vec{P}_{3L}\right|^2 = P_{3xL}^2 + P_{3yL}^2 + P_{3zL}^2$$

$$= \left|\vec{P}_{3\ cm}\right|^2 \left\{\sin^2\ \theta_{cm}\ \cos^2\ \phi_{cm} + \sin^2\ \theta_{cm}\ \sin^2\ \phi_{cm}\right\} +$$

$$\cos^2\ \theta_{cm} \left(\frac{2m_3\ m_4\ E'}{m_3 + m_4}\right) + \frac{2m_1\ m_3^2\ E_{1L}}{(m_1 + m_2)^2} + \frac{4\ m_3 \cos\ \theta_{cm}}{(m_1 + m_2)} \sqrt{\frac{m_1 m_3\ m_4\ E_{1L}\ E'}{(m_3 + m_4)}}$$

$$\left|\vec{P}_{3L}\right|^2 = \frac{2 m_3 m_4 E'}{(m_3 + m_4)} + \frac{2 m_1 m_3^2 E_{1L}}{(m_1 + m_2)^2} + \frac{4 m_3 \cos\theta_{cm}}{(m_1 + m_2)} \sqrt{\frac{m_1 m_3 m_4 E_{1L} E'}{(m_3 + m_4)}}$$

$$E_{3L} = \frac{\left|\vec{P}_{3L}\right|^2}{2 m_3} = \frac{m_4 E'}{(m_3 + m_4)} + \frac{m_1 m_3 E_{1L}}{(m_1 + m_2)^2} + \frac{2 \cos\theta_{cm}}{(m_1 + m_2)} \sqrt{\frac{m_1 m_3 m_4 E_{1L} E'}{(m_3 + m_4)}}$$

Substituting for E' from equation C-2 and regrouping yields:

$$E_{3L} = E_{1L}\left(\frac{m_2 m_4}{(m_1 + m_2)(m_3 + m_4)} + \frac{m_1 m_3}{(m_1 + m_2)^2}\right) + \frac{m_4 Q}{(m_3 + m_4)} + \frac{2 \cos\theta_{cm}}{(m_1 + m_2)} \sqrt{\frac{m_1 m_3 m_4 E_{1L}\left(\frac{m_2 E_{1L}}{m_1 + m_2} + Q\right)}{(m_3 + m_4)}} \qquad (C\text{-}3)$$

Note that E_{3L} is composed of two parts:

(a) A constant value dependent only on the energy of the incoming particle.

(b) A variable that is dependent on the cosine of the scattering angle θ in the center of mass system.

In part A of this appendix, we discussed the fact that in spherical coordinates, the parameter to vary to insure complete coverage of a spherical surface was the cosine of the polar angle and not the angle. We can therefore conclude that since the cosine of θ_{cm} can vary, any value is equally probable between -1 and +1. Thus the Lab energy of the product particle is equally likely to have any energy between a maximum determined by $\cos\theta_{cm} = 1$ and a minimum of $\cos\theta_{cm} = -1$.

If $m_1 = 1$, $m_2 = 3$, $m_3 = 1$, $m_4 = 3$ as in the $He^3(n,p)T$ reaction, equation C-3 becomes for the proton particle:

$$E_{PL} = \left[\frac{5}{8} E_{NL} + \frac{3}{4} Q_{n,p} + \frac{\cos \theta_{cm}}{4} \sqrt{\frac{9}{4} E_{NL}^2 + 3 E_{NL} Q_{n,p}} \right] \quad \text{(C-4)}$$

If $m = 1$, $m_2 = 3$, $m_3 = 3$, $m_4 = 1$ for the triton

$$E_{TL} = \left[\frac{3}{8} E_{NL} + \frac{1}{4} Q_{n,p} + \frac{\cos \theta_{cm}}{4} \sqrt{\frac{9}{4} E_{NL}^2 + 3 E_{NL} Q_{n,p}} \right] \quad \text{(C-5)}$$

The total energy in the Lab system of coordinates $E_{NL} + Q_{n,p} = E_{pL} + E_{TL}$

$$E_{NL} + Q_{n,p} = \left[\frac{5}{8} E_{NL} + \frac{3}{4} Q_{n,p} + \frac{\cos \theta_{cm}}{4} \sqrt{\frac{9}{4} E_{NL}^2 + 3 E_{NL} Q} \right] +$$

$$\left[\frac{3}{8} E_{NL} + \frac{1}{4} Q_{n,p} - \frac{\cos \theta_{cm}}{4} \sqrt{\frac{9}{4} E_{NL}^2 + 3 E_{NL} Q} \right]$$

Since the scattering angles in the c.m. system are equal and opposite

$$E_{NL} + Q_{n,p} = E_{NL} + Q_{n,p}$$

If $m_1 = 1$, $m_2 = 3$, $m_3 = m_4 = 2$ as in the case for the $He^3(n,d)D$ reaction, equation C-3 becomes for deuteron 1

$$E_{D\,1L} = \frac{1}{2} \left(E_{NL} + Q_{n,d} \right) + \frac{\cos \theta_{cm}}{2} \sqrt{\frac{3}{4} E_{NL}^2 + E_{NL} Q_{n,d}} \quad \text{(C}$$

Deuteron #2 is equal to deuteron #1, except that when adding to determine total energy, the sign of one of the scattering angles must be reversed.

Appendix D. Derivation of Field Strength and Voltage Equipotential Equations for Coaxial Cylindrical Geometry

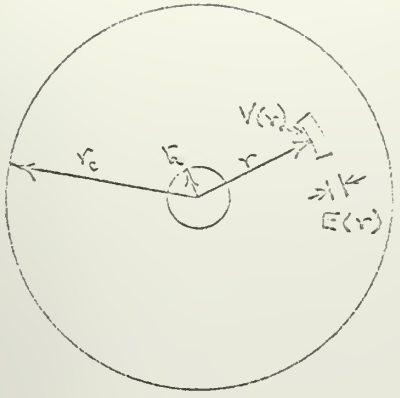

$E(r)$ = voltage gradient at any radial position r.

$V(r)$ = voltage at any radial position r

r_c = radius of the cathode

r_a = radius of the anode

V_o = applied potential to the anode

0 = applied potential to the cathode

$$E = -\text{grad } V$$

thus $$\nabla^2 V = 0$$

Boundary conditions: (1) $V(r_a) = V_o$

(2) $V(r_c) = 0$

in cylindrical geometry

$$\frac{1}{r}\left(\frac{\partial}{\partial r}\left(r\frac{\partial V}{\partial r}\right)\right) = 0$$

$$r\frac{\partial V}{\partial r} = C_1$$

$$\frac{\partial V}{\partial r} = \frac{C_1}{r}$$

$$V = C_1 \ln r + C_2$$

Applying the B. C.

$$V(r_a) = C_1 \ln r_a + C_2 = V_o \qquad \text{(B. C. no. 1)}$$

$$V(r_c) = C_1 \ln r_c + C_2 = 0 \qquad \text{(B. C. no. 2)}$$

Solving the above two equations to determine C_1 and C_2 we obtain

$$V(r) = \frac{V_o}{\ln \frac{r_a}{r_c}} \cdot \ln r - \frac{V_o}{\ln \frac{r_a}{r_c}} \ln r_c$$

or

$$V(r) = \frac{V_o}{\ln \frac{r_c}{r_a}} \cdot \ln \frac{r_a}{r}$$

but $E(r) = -\text{grad } V(r)$

$$E(r) = \frac{V_o}{r \ln \frac{r_c}{r_a}}$$

Appendix E

Random Probability Analysis

CATMAN

```
$IBFTC CATMAN
C       THIS PROGRAM DETERMINES THE RESPONSE OF A PARTICULAR NEUTRON
C       PROPORTIONAL COUNTER BY MONTE CARLO METHODS.  THE COUNTER IS A
C       CYLINDER WITH AN AXIAL WIRE FOR THE ANODE.  THERE IS A DEAD
C       SECTION AT EACH END OF THE CYLINDER WHERE ELECTRONS IONIZED BY
C       THE PASSAGE OF A CHARGED PARTICLE CANNOT REACH THE ANODE.  IN
C       THE CASE OF A PARTICLE TRACK THAT ORIGINATES IN THE LIVE PART
C       OF THE CYLINDER AND PASSES TO THE DEAD REGION, THE EFFECT IS AS
C       IF THE CYLINDER END WALL IS AT THE BOUNDARY BETWEEN THE TWO
C       REGIONS.  HOWEVER, A TRACK MIGHT ORIGINATE IN THE DEAD REGION
C       AND PASS TO THE LIVE REGION, IN WHICH CASE IT ONLY DEPOSITS
C       ENERGY ALONG THAT PART OF THE TRACK WHICH IS IN THE LIVE REGION.
C       IF THE EVENT DEPOSITS ENERGY IN THE LIVE REGION IT IS COUNTED
C       IN THE CHANNEL THAT CORRESPONDS TO THE ENERGY DEPOSITED, UNLESS
C       THE RISE TIME IS LESS THAN THE TIME SETTING.  THE RISE TIME IS
C       THE TIME BETWEEN THE FIRST AND LAST ELECTRONS HITTING THE ANODE.
C       THE RISE TIME =     CONSTANT X (R1**2 - R0**2)  WHERE R1 AND
C       R0 ARE THE DISTANCES FROM THE ANODE OF THE FARTHEST AND THE
C       NEAREST ELECTRONS.  THE CONSTANT DEPENDS ON THE PHYSICAL DATA
C       FOR THE COUNTER.  TO GENERATE RANDOM EVENTS, A POINT FOR THE
C       REACTION SITE IS RANDOMLY CHOSEN IN THE VOLUME OF THE CYLINDER.
C       THE DIRECTION OF THE NEUTRON IS ALSO RANDOMLY CHOSEN.  THE
C       NEUTRON COLLISION WITH A HELIUM-3 NUCLEUS MAY YIELD A PROTON -
C       TRITON PAIR OR A DEUTERON - DEUTERON PAIR.  THE CHOICE IS MADE
C       RANDOMLY AFTER PROPER CONSIDERATION OF THE RELATIVE CROSS
C       SECTIONS.  SUPPOSE PROTON - TRITON IS CHOSEN.  THE DIRECTION
C       OF THE PROTON IN THE C.M. SYSTEM IS CHOSEN RANDOMLY.  THE
C       MOMENTA AND TRITON DIRECTION ARE THEN DETERMINED BY ENERGY AND
C       MOMENTUM CONSERVATION, AND ALL QUANTITIES ARE TRANSFORMED TO
C       THE LAB SYSTEM.  IT IS NOW POSSIBLE TO DETERMINE IF EITHER
C       PARTICLE HAS PASSED INTO A WALL OR THE DEAD SPACE, AND IF SO,
C       HOW MUCH ENERGY IS LOST.  THE RISE TIME IS FOUND, AND IF IT IS
C       MORE THAN THE MINIMUM, THE EVENT IS COUNTED.  THEN WE START
C       AGAIN FROM THE BEGINNING, ETC.  WE USE CGS UNITS THROUGHOUT.
      DIMENSION ENER(600),ERG(600),EL(600,4),ELL(600,4),EEL(600,4),KJ(3)
     1 ,WTSM(100),ELMAX(4),ELSP(4),SIGNP(600),SIGND(600),RPAIR(600),
     2  LOST(100),A1(2),A2(2),A3(2),A4(2),A5(2),A6(2),A7(2),A8(2),
     3  CHAN(600),COUNTS(600,3),CPITP(600,3),CNORM(600,3),WTLST(100)
      DIMENSION TOTAL(100),LCHN(600)
      EQUIVALENCE (A1(2),ENER,LCHN),(A2(2),ERG),(A3(2),EL),(A4(2),ELL),
     1  (A5(2),EEL),(A6(2),SIGND),(A7(2),RPAIR),(A8(2),SIGNP)
      READ(2,1)  NCHANS,NTABS,NENS,IFTEST,IFPLOT,NUTRNS,VOLTS,TIME,ELOW,
     1        EHIGH
      WRITE(3,1) NCHANS,NTABS,NENS,IFTEST,IFPLOT,NUTRNS,VOLTS,TIME,ELOW,
     1        EHIGH
    1 FORMAT(5I5,I10,F10.0,E10.3,2F5.3,E15.6)
C       NCHANS IS THE NUMBER OF CHANNELS. NTABS IS THE NUMBER OF
C       TABULATIONS OF THE RANGE AND CROSS SECTION DATA. NENS IS THE
C       NUMBER OF NEUTRON ENERGIES TO RUN. IF IFTEST .NE. 0 WE PRINT
C       NEARLY ALL VARIABLES AFTER EACH EVENT. IF IFPLOT .NE. 0 WE
C       PUNCH CARDS SUITABLE FOR INPUT TO THE PROGRAM THAT PLOTS THE
C       RESULTS. NUTRNS IS THE NUMBER OF NEUTRONS TO GENERATE. VOLTS IS
C       THE COUNTER VOLTAGE. TIME IS THE RISE TIME SETTING. ANRAD IS
C       THE ANODE RADIUS. CATRAD IS THE CATHODE RADIUS. CYLENG IS HALF
C       THE CYLINDER LENGTH. YMAX IS HALF THE LIVE REGION LENGTH. PRESS
C       IS THE PRESSURE. PMM IS THE PROTON MASS. TMM IS THE TRITON MASS
```

```
C         DM IS THE DEUTERON MASS.  ENM IS NEUTRON MASS. HE3M IS HELIUM-
C         3 MASS. ELVOLT IS ONE ELECTRON-VOLT IN ERGS. ENLIM IS THE MAX.
C         ENERGY OF THE CHANNELS. QND IS THE DEUTERON REACTION ENERGY.
C         QNP IS THE PROTON-TRITON REACTION ENERGY. DIFMIN IS THE MINIMUM
C         DIFFERENCE BETWEEN THE SQUARE OF THE MAX. RADIUS AND THE SQUARE
C         OF THE MIN. RADIUS SO THAT THE RISE TIME IS LONG ENOUGH. SIGNP
C         IS THE PROTON-TRITON REACTION CROSS SECTION. SIGND IS THE
C         DEUTERON REACTION CROSS SECTION. RPAIR IS THE PROTON RANGE IN
C         AIR DATA.  THE CROSS SECTIONS ARE IN BARNS (10.**(-24) CM.**2).
      ENTABS = FLOAT(NTABS)
      ANRAD = .015*2.54
      CATRAD = 1.965*2.54
      CAT2 = CATRAD**2
      CATMAN = CATRAD - ANRAD
      CYLENG = 8.5*2.54
      YMAX = 7.5*2.54
      PRESS = 12.005*76.
      HEPRES = 2.
      PMM = 1.67248E-24
      TWM = 5.02208E-24
      DM = 3.34728E-24
      ENM = 1.6748E-24
      HE3M = 5.01976E-24
      ELVOLT = 1.60207E-12
      ENLIM = 15.E6*ELVOLT
      ERANGE = ENLIM - 1.E6*ELVOLT
      QND = -3.27E6*ELVOLT
      QNP = .764E6*ELVOLT
      TFACTR = PRESS*ALOG(CATRAD/ANRAD)/(2.*.721E6*VOLTS)
      TEMP = 293.16
      DIFMIN = TIME/TFACTR
      READ(2,2) (SIGNP(I),I = 1,NTABS)
      READ(2,2) (SIGND(I),I = 1,NTABS)
      READ(2,2) (RPAIR(I),I = 1,NTABS)
    2 FORMAT(8F10.0)
      A1(1) = 0.
      A2(1) = 0.
      A6(1) = 0.
      A7(1) = 0.
      A8(1) = 2.*SIGNP(1) - SIGNP(2)
      SPACNG = ENLIM/ENTABS
      SRECIP = ENTABS/ENLIM
      RCHNWD = FLOAT(NCHANS)/ENLIM
      CALL CLOCKI(TIM1)
      CALL LENGTH(NTABS,ENLIM,ENER,ERG,RPAIR,EL,ELMAX,ELSP,ELL,EEL)
      CALL CLOCKI(TIM2)
C         CLOCKI IS A LIBRARY ROUTINE TO PROVIDE TIMING INFORMATION.
      DO 160 NEUEN = 1,NENS
      EN = ERANGE*(ELOW + FLOAT(NEUEN)*(EHIGH - ELOW)/FLOAT(NENS))
      INTERP = INT(ENTABS*EN/ENLIM)
      PART = (EN - ERG(INTERP))*SRECIP
      SIGP = SIGNP(INTERP) + PART*(SIGNP(INTERP+1) - SIGNP(INTERP))
      SIGD = SIGND(INTERP) + PART*(SIGND(INTERP+1) - SIGND(INTERP))
C         EN IS THE NEUTRON ENERGY.  SIGP IS THE P-T REACTION CROSS
C         SECTION.  PNEUTL IS THE NEUTRON MOMENTUM IN THE LAB, AND PNUTCM
C         IS IN THE C.M. SYSTEM. VCMSYS IS THE VELOCITY OF THE C.M.
C         SYSTEM.  ETCM IS THE TOTAL ENERGY IN C.M.
```

```
      SIGTOT = SIGP + SIGD
      CHOICE = SIGP/SIGTOT
     .WTFCTR = .6025*PEPRES*273.16*SIGTOT*(2.*CYLENG)*CATMAN*3.14159265/
     1      (22400.*TEMP)
      PNEUTL = SQRT(2.*ENM*EN)
      VCMSYS = PNEUTL/(ENM + HE3M)
      PNUTCM = PNEUTL - VCMSYS*ENM
      ENCM = PNUTCM**2/(2.*ENM)
      PHE3CM = VCMSYS*HE3M
      EHCM = PHE3CM**2/(2.*HE3M)
      ETCM = ENCM + EHCM
      LOST(NEUEN) = 0
      WTLST(NEUEN) = 0.
      WTSW(NEUEN) = 0.
      TOTAL(NEUEN) = 0.
      DO 16 I = 1,NCHANS
      CHAN(I) = 0.
   16 CONTINUE
      NEUTRN = 0
   17 NEUTRN = NEUTRN + 1
C        STATEMENT 17 BEGINS THE RANDOM GENERATION LOOP (SEE STATEMENT
C        140 BELOW).  WE CAN CONSIDER ALL EVENTS TO OCCUR TO THE RIGHT
C        OF THE CENTER OF THE CYLINDER (IMAGINING THE CYLINDER TO LIE
C        HORIZONTALLY) BECAUSE OF SYMMETRY.  THIS IS SIMPLER BECAUSE THEN
C        NO TRACK CAN REACH AS FAR AS THE LEFT END SINCE AT 15 MEV OR
C        LESS, ALL TRACKS ARE SHORTER THAN XMAX.  THE END WALL EFFECT IS
C        THEN DUE ONLY TO THE RIGHT END.  TO CHOOSE THE REACTION SITE AT
C        RANDOM IN THE CYLINDER VOLUME WE CHOOSE HP, THE HORIZONTAL
C        POSITION MEASURED TO THE RIGHT FROM THE CENTER, AND R, THE
C        RADIAL DISTANCE FROM THE CENTER AXIS.  THE REACTION SITES ARE
C        NOT UNIFORM IN THE VOLUME SINCE THERE IS MORE VOLUME IN R TO
C        R+DR FOR LARGE R THAN FOR SMALL R.  SINCE WE ARE CHOOSING THE
C        VALUE OF R UNIFORMLY, WE MUST APPLY A WEIGHT TO CORRECT THE
C        DISTRIBUTION.  SINCE THE VOLUME IN THE INTERVAL DR IS DIRECTLY
C        PROPORTIONAL TO R, THE WEIGHT MUST BE PROPORTIONAL TO R.  THEN
C        WHEN AN EVENT IS COUNTED, WE DO NOT ADD 1 TO THE PROPER CHANNEL
C        BUT WE ADD THE WEIGHT.  IN ORDER TO COMPARE THE RESPONSE
C        SPECTRA FOR SEVERAL NEUTRON ENERGIES IT WOULD HAVE BEEN
C        NECCESARY TO USE A WEIGHT ANYWAY BECAUSE THE TOTAL REACTION
C        CROSS SECTION VARIES WITH NEUTRON ENERGY.  WT IS THE WEIGHT.
C        WTFCTR IS (NUMBER OF HELIUM ATOMS/CC)*(LENGTH OF CYLINDER)*PI*
C        (RADIUS OF CYLINDER (CORRECTED FOR SOLID ANODE))*(TOTAL CROSS
C        SECTION).  IMAGINE A COORDINATE SYSTEM AT THE REACTION SITE
C        WITH Y-AXIS PARALLEL TO THE ANODE AND Z-AXIS ALONG A RADIAL
C        LINE FROM THE ANODE.  WE CHOOSE A NEUTRON DIRECTION RELATIVE TO
C        THIS SYSTEM BY CHOOSING AZIMUTHAL ANGLE, PHI, AT RANDOM AND
C        COSINE OF THE POLAR ANGLE, CTH, AT RANDOM.  IT IS NECCESARY TO
C        PICK THE COSINE AT RANDOM TO GET A UNIFORM DIRECTIONAL
C        DISTRIBUTION.  THE C.M. SYSTEM IS IMAGINED TO HAVE X-AXIS
C        PARALLEL TO THE NEUTRON DIRECTION.
      HP = CYLENG*RGEN(UGH)
      R = CATMAN*RGEN(UGH) + ANRAD
      R2 = R*R
      WT = WTFCTR*R
      TOTAL(NEUEN) = TOTAL(NEUEN) + WT
      PHI = 6.2831853*RGEN(UGH)
      CCSPHI = COS(PHI)
```

```
      SINPHI = SIN(PHI)
      CTH = 2.*RGEN(UGH) - 1.
      STH = SQRT(1. - CTH**2)
      IF(RGEN(UGH) .GT. CHOICE) GO TO 18
C        CHOICE IS THE FRACTION OF EVENTS THAT ARE PROTON-TRITON EVENTS.
C        IF A NUMBER RANDOMLY CHOSEN BETWEEN 0 AND 1 IS .GT. CHOICE, WE
C        PICK THE DEUTERON CASE.  IN THIS CASE WE MERELY SUBSTITUTE THE
C        DEUTERON MASS FOR THE PROTON AND TRITON MASSES AND 0ND FOR THE
C        REACTION ENERGY.
      PM = PMM
      TM = TMM
      Q = QNP
      KASE = 0
      GO TO 19
   18 PM = DM
      TM = DM
      Q = QND
      KASE = 2
   19 PPCM = SQRT(2.*(ETCM + Q)*PM*TM/(PM + TM))
      PHIP = 6.28318531*RGEN(UGH)
      CTHP = 2.*RGEN(UGH) - 1.
      STHP = SQRT(1. - CTHP**2)
      XPCM = PPCM*STHP*COS(PHIP)
      YPCM = PPCM*STHP*SIN(PHIP)
      ZPCM = PPCM*CTHP
      XMA = XPCM*STH - ZPCM*CTH
      ZMB = ZPCM*STH + XPCM*CTH
      XMB = XMA*COSPHI - YPCM*SINPHI
      YMB = XMA*SINPHI + YPCM*COSPHI
C        PPCM IS THE PROTON MOMENTUM IN C.M.  XMB,YMB,ZMB, ARE THE X,Y,Z
C        COMPONENTS OF PROTON MOMENTUM IN A COORDINATE SYSTEM THAT IS
C        PARALLEL TO THE LAB SYSTEM, BUT MOVING WITH THE C.M.  NOTE THAT
C        THE COMPONENTS OF TRITON MOMENTUM IN THIS SYSTEM MUST BE THE
C        NEGATIVES OF XMB,YMB,ZMB.
      VCSYSX = VCMSYS*STH*COSPHI
      VCSYSY = VCMSYS*STH*SINPHI
      VCSYSZ = VCMSYS*CTH
      PLABXP = PM*VCSYSX + XMB
      PLABYP = PM*VCSYSY + YMB
      PLABZP = PM*VCSYSZ + ZMB
      PLABXT = TM*VCSYSX - XMB
      PLABYT = TM*VCSYSY - YMB
      PLABZT = TM*VCSYSZ - ZMB
      PLXP2 = PLABXP**2
      PLZP2 = PLABZP**2
      XPZP = PLXP2 + PLZP2
      PLABP2 = XPZP + PLABYP**2
      PLABP = SQRT(PLABP2)
      PLXT2 = PLABXT**2
      PLZT2 = PLABZT**2
      XPZT = PLXT2 + PLZT2
      PLABT2 = XPZT + PLABYT**2
      PLABT = SQRT(PLABT2)
      EP = PLABP2/(2.*PM)
      ET = PLABT2/(2.*TM)
C        EP AND ET ARE THE PROTON AND TRITON ENERGIES IN THE LAB.  PLENG
C        AND TLENG ARE THE TRACK LENGTHS.  XP,YP,ZP ARE THE X,Y,Z
```

```
C         COORDINATES OF THE TIP OF THE PROTON TRACK IN A SYSTEM WITH
C         ORIGIN AT THE CYLINDER CENTER, Y-AXIS ALONG THE ANODE, AND
C         Z-AXIS PARALLEL TO THE RADIAL LINE FROM ANODE TO REACTION SITE.
      INTP = INT(SRECIP*EP)
      INTT = INT(SRECIP*ET)
      PARTP = (EP - ERG(INTP))*SRECIP
      PARTT = (ET - ERG(INTT))*SRECIP
      PLENG = EL(INTP,KASE*1) +PARTP*(EL(INTP+1,KASE*1)-EL(INTP,KASE*1))
      TLENG = EL(INTT,KASE*2) +PARTT*(EL(INTT+1,KASE*2)-EL(INTT,KASE*2))
      RATIOP = PLENG/PLABP
      RATIOT = TLENG/PLABT
      XP = PLABXP*RATIOP
      YP = PLABYP*RATIOP + HP
      ZP = PLABZP*RATIOP + R
      XPSQ = XP*XP
      ZPSQ = ZP*ZP
      RP2 = XPSQ + ZPSQ
      XT = PLABXT*RATIOT
      YT = PLABYT*RATIOT + HP
      ZT = PLABZT*RATIOT + R
      XTSQ = XT*XT
      ZTSQ = ZT*ZT
      RT2 = XTSQ + ZTSQ
      YPMHP = YP - HP
      YTMHP = YT - HP
      YWALL = YMAX - HP
      IF(RP2 .GT. CAT2) ALPHA = R*(SQRT(CAT2*XPZP/R2-PLXP2)-PLABZP)/
     1      (XPZP*RATIOP)
      IF(RT2 .GT. CAT2) BETA = R*(SQRT(CAT2*XPZT/R2-PLXT2)-PLABZT)/
     1      (XPZT*RATIOT)
C         ALPHA AND BETA ARE THE FRACTIONS OF PROTON AND TRITON TRACK
C         LENGTHS THAT REMAIN INSIDE THE CYLINDER WALL.  THE PROGRAM FROM
C         HERE TO STATEMENT 120 DETERMINES IF THE RISE TIME IS BIG ENOUGH
C         AND IF SO, WHAT ENERGY TO COUNT.  GENERALLY, THE TRACKS ARE
C         SKEW LINES RELATIVE TO THE ANODE AND THE MINIMUM DISTANCE MUST
C         BE FOUND TO GET THE RISE TIME.  YMINR IS THE Y COORDINATE OF THE
C         POINT OF MINIMUM DISTANCE IN THE LAB SYSTEM WITH ORIGIN AT THE
C         REACTION SITE.
      IF(HP .GT. YMAX) GO TO 60
      IF(YP .LE. YMAX) GO TO 24
      IF(RP2 .LE. CAT2) GO TO 20
      YCUT = YPMHP*ALPHA
      IF(YCUT .LE. YWALL) GO TO 25
   20 R2WALP = ((R*PLABYP + PLABZP*YWALL)**2 + PLXP2*YWALL**2)/PLABY2**2
C         R2WALP IS THE SQUARE OF THE DISTANCE FROM ANODE TO THE POINT
C         WHERE THE PROTON TRACK GOES THRU THE LIVE SPACE-DEAD SPACE WALL
      IF(PLABZP .GE. 0.) GO TO 22
      YMINR = -PLABY2*PLABZP*R/XPZP
      IF(YMINR .GT. YWALL) GO TO 21
      RMIN2P = PLXP2*R2/XPZP
      RMAX2P = AMAX1(R2,R2WALP)
      GO TO 23
   21 RMIN2P = R2WALP
      RMAX2P = R2
      GO TO 23
   22 RMIN2P = R2
      RMAX2P = R2WALP
```

```
   23 TIPP = (1. - YWALL/YPMHP)*PLENG
      GO TO 39
   24 IF(RP2 .LE. CAT2) GO TO 31
   25 IF(PLABZP .GE. 0.) GO TO 27
      RMIN2P = PLXP2*R2/XPZP
      GO TO 28
   27 RMIN2P = R2
   28 RMAX2P = CAT2
      TIPP = (1. - ALPHA)*PLENG
C        TIPP IS THE LENGTH OF THE END OF PROTON TRACK THAT IS OUTSIDE
C          OF THE CYLINDER.
      GO TO 39
   31 IF(PLABZP .GE. 0.) GO TO 33
      YMINR = -PLABYP*PLABZP*R/XPZP
      IF(ABS(YMINR) .GE. ABS(YPMHP)) GO TO 32
      RMIN2P = PLXP2*R2/XPZP
      RMAX2P = AMAX1(R2,RP2)
      GO TO 34
   32 RMIN2P = RP2
      RMAX2P = R2
      GO TO 34
   33 RMIN2P = R2
      RMAX2P = RP2
   34 TIPP = 0.
   39 IF(YT .LE. YMAX) GO TO 44
      IF(RT2 .LE. CAT2) GO TO 40
      YCUT = YTMHP*BETA
      IF(YCUT .LE. YWALL) GO TO 45
   40 R2WALT = ((R*PLABYT + PLABZT*YWALL)**2 + PLXT2*YWALL**2)/PLABYT**2
      IF(PLABZT .GE. 0.) GO TO 42
      YMINR = -PLABYT*PLABZT*R/XPZT
      IF(YMINR .GT. YWALL) GO TO 41
      RMIN2T = PLXT2*R2/XPZT
      RMAX2T = AMAX1(R2,R2WALT)
      GO TO 43
   41 RMIN2T = R2WALT
      RMAX2T = R2
      GO TO 43
   42 RMIN2T = R2
      RMAX2T = R2WALT
   43 TIPT = (1. - YWALL/YTMHP)*TLENG
      GO TO 55
   44 IF(RT2 .LE. CAT2) GO TO 51
   45 IF(PLABZT .GE. 0.) GO TO 47
      RMIN2T = PLXT2*R2/XPZT
      GO TO 48
   47 RMIN2T = R2
   48 RMAX2T = CAT2
      TIPT = (1. - BETA)*TLENG
      GO TO 55
   51 IF(PLABZT .GE. 0.) GO TO 53
      YMINR = -PLABYT*PLABZT*R/XPZT
      IF(ABS(YMINR) .GE. ABS(YTMHP)) GO TO 52
      RMIN2T = PLXT2*R2/XPZT
      RMAX2T = AMAX1(R2,RT2)
      GO TO 54
   52 RMIN2T = RT2
```

```
      RMAX2T = R2
      GO TO 54
   53 RMIN2T = R2
      RMAX2T = RT2
   54 TIPT = 0.
   55 RMIN2 = AMIN1(RMIN2P,RMIN2T)
      RMAX2 = AMAX1(RMAX2P,RMAX2T)
      IF(RMAX2 - RMIN2 .LT. DIFMIN) GO TO 130
      IF(TIPP .EQ. 0.) GO TO 56
      IL = INT(TIPP/ELSP(KASE+1))
      ETIPP = EEL(IL,KASE+1) + (TIPP - ELL(IL,KASE+1))*(EEL(IL+1,KASE+1)
     1        - EEL(IL,KASE+1))/ELSP(KASE+1)
      EDEPP = EP - ETIPP
      GO TO 57
   56 EDEPP = EP
   57 IF(TIPT .EQ. 0.) GO TO 58
      IL = INT(TIPT/ELSP(KASE+2))
      ETIPT = EEL(IL,KASE+2) + (TIPT - ELL(IL,KASE+2))*(EEL(IL+1,KASE+2)
     1        - EEL(IL,KASE+2))/ELSP(KASE+2)
      EDEPT = ET - ETIPT
      GO TO 59
   58 EDEPT = ET
   59 EDEPOS = EDEPP + EDEPT
C        EDEPOS IS THE TOTAL ENERGY DEPOSITED IN THE LIVE SPACE.
      GO TO 120
   60 IF(YP .LT. YMAX) GO TO 70
      IF(YT .GE. YMAX) GO TO 130
      IF(RT2 .LE. CAT2) GO TO 65
   61 IF(YTMHP*BETA  .GE. YWALL) GO TO 130
      IF(PLABZT .GE. 0.) GO TO 62
      YMINR = -PLABYT*PLABZT*R/XPZT
      IF(YMINR .GT. YWALL) GO TO 62
      RMIN2T = PLXT2*R2/XPZT
      GO TO 63
   62 RMIN2T = ((R*PLABYT + PLABZT*YWALL)**2 + PLXT2*YWALL**2)/PLABYT**2
   63 IF(CAT2 - RMIN2T .LT. DIFMIN) GO TO 130
      TIPT = TLENG*(1. - BETA)
      WTIPT = TLENG*(1. - YWALL/YTMHP)
C        WTIPT IS THE LENGTH OF TRITON TRACK THAT EXTENDS TO THE LEFT OF
C        THE LIVE SPACE-DEAD SPACE WALL. HERE, THE REACTION SITE IS IN
C        THE DEAD SPACE BECAUSE HP IS GREATER THAN YMAX.
      IL = INT(TIPT/ELSP(KASE+2))
      ETIPT = EEL(IL,KASE+2) + (TIPT - ELL(IL,KASE+2))*(EEL(IL+1,KASE+2)
     1        - EEL(IL,KASE+2))/ELSP(KASE+2)
      IL = INT(WTIPT/ELSP(KASE+2))
      EWTPT = EEL(IL,KASE+2) +(WTIPT - ELL(IL,KASE+2))*(EEL(IL+1,KASE+2)
     1        - EEL(IL,KASE+2))/ELSP(KASE+2)
      EDEPOS = EWTPT - ETIPT
      GO TO 120
   65 R2WALT = ((R*PLABYT + PLABZT*YWALL)**2 + PLXT2*YWALL**2)/PLABYT**2
      IF(PLABZT .GE. 0.) GO TO 66
      YMINR = -PLABYT*PLABZT*R/XPZT
      IF(YMINR .LE. YTMHP .OR. YMINR .GE. YWALL) GO TO 66
      RMIN2T = PLXT2*R2/XPZT
      IF(AMAX1(RT2,R2WALT) - RMIN2T .LT. DIFMIN) GO TO 130
      GO TO 67
   66 IF(ABS(RT2 - R2WALT) .LT. DIFMIN) GO TO 130
```

```
 67 WTIPT = TLENG*(1. - YWALL/YTMHP)
    IL = INT(WTIPT/ELSP(KASE+2))
    EDEPOS = EEL(IL,KASE+2) + (WTIPT-ELL(IL,KASE+2))*(EEL(IL+1,KASE+2)
   1           - EEL(IL,KASE+2))/ELSP(KASE+2)
    GO TO 120
 70 IF(YT .LT. YMAX) GO TO 80
    IF(RP2 .LE. CAT2) GO TO 75
    IF(YPMHP*ALPHA .GE. YWALL) GO TO 130
 71 IF(PLABZP .GE. 0.) GO TO 72
    YMINR = -PLABYP*PLABZP*R/XPZP
    IF(YMINR .GT. YWALL) GO TO 72
    RMIN2P = PLXP2*R2/XPZP
    GO TO 73
 72 RMIN2P = ((R*PLABYP + PLABZP*YWALL)**2 + PLXP2*YWALL**2)/PLABYP**2
 73 IF(CAT2 - RMIN2P .LT. DIFMIN) GO TO 130
    TIPP = PLENG*(1. - ALPHA)
    WTIPP = PLENG*(1. - YWALL/YPMHP)
    IL = INT(TIPP/ELSP(KASE+1))
    ETIPP = EEL(IL,KASE+1) + (TIPP - ELL(IL,KASE+1))*(EEL(IL+1,KASE+1)
   1           - EEL(IL,KASE+1))/ELSP(KASE+1)
    IL = INT(WTIPP/ELSP(KASE+1))
    EWTPP = EEL(IL,KASE+1) + (WTIPP -ELL(IL,KASE+1))*(EEL(IL+1,KASE+1)
   1          - EEL(IL,KASE+1))/ELSP(KASE+1)
    EDEPOS = EWTPP - ETIPP
    GO TO 120
 75 R2WALP = ((R*PLABYP + PLABZP*YWALL)**2 + PLXP2*YWALL**2)/PLABYP**2
    IF(PLABZP .GE. 0.) GO TO 76
    YMINR = -PLABYP*PLABZP*R/XPZP
    IF(YMINR .LE. YPMHP .OR. YMINR .GE. YWALL) GO TO 76
    RMIN2P = PLXP2*R2/XPZP
    IF(AMAX1(RP2,R2WALP) - RMIN2P .LT. DIFMIN) GO TO 130
    GO TO 77
 76 IF(ABS(RP2 - R2WALP) .LT. DIFMIN) GO TO 130
 77 WTIPP = PLENG*(1. - YWALL/YPMHP)
    IL = INT(WTIPP/ELSP(KASE+1))
    EDEPOS = EEL(IL,KASE+1) + (WTIPP-ELL(IL,KASE+1))*(EEL(IL+1,KASE+1)
   1           - EEL(IL,KASE+1))/ELSP(KASE+1)
    GO TO 120
 80 IF(RP2 .LE. CAT2) GO TO 100
    IF(RT2 .LE. CAT2) GO TO 90
    IF(YPMHP*ALPHA .GE. YWALL) GO TO 61
    IF(YTMHP*BETA  .GE. YWALL) GO TO 71
    IF(PLABZT .GE. 0. ) GO TO 81
    YMINR =-PLABYT*PLABZT*R/XPZT
    IF(YMINR .GT. YWALL) GO TO 81
    RMIN2T = PLXT2*R2/XPZT
    GO TO 82
 81 RMIN2T = ((R*PLABYT + PLABZT*YWALL)**2 + PLXT2*YWALL**2)/PLABYT**2
 82 IF(PLABZP .GE. 0.) GO TO 83
    YMINR = -PLABYP*PLABZP*R/XPZP
    IF(YMINR .GT. YWALL) GO TO 83
    RMIN2P = PLXP2*R2/XPZP
    GO TO 84
 83 RMIN2P = ((R*PLABYP + PLABZP*YWALL)**2 + PLXP2*YWALL**2)/PLABYP**2
 84 RMIN2 = AMIN1(RMIN2T,RMIN2P)
    IF(CAT2 - RMIN2 .LT. DIFMIN) GO TO 130
    TIPT = TLENG*(1. - BETA)
```

```
      TIPP = PLENG*(1. - ALPHA)
      WTIPT = TLENG*(1. - YWALL/YTMHP)
      WTIPP = PLENG*(1. - YWALL/YPMHP)
      IL = INT(TIPT/ELSP(KASE+2))
      ETIPT = EEL(IL,KASE+2) + (TIPT - ELL(IL,KASE+2))*(EEL(IL+1,KASE+2)
     1          - EEL(IL,KASE+2))/ELSP(KASE+2)
      IL = INT(TIPP/ELSP(KASE+1))
      ETIPP = EEL(IL,KASE+1) + (TIPP - ELL(IL,KASE+1))*(EEL(IL+1,KASE+1)
     1          - EEL(IL,KASE+1))/ELSP(KASE+1)
      IL = INT(WTIPT/ELSP(KASE+2))
      EWTPT = EEL(IL,KASE+2) + (WTIPT -ELL(IL,KASE+2))*(EEL(IL+1,KASE+2)
     1          - EEL(IL,KASE+2))/ELSP(KASE+2)
      IL = INT(WTIPP/ELSP(KASE+1))
      EWTPP = EEL(IL,KASE+1) + (WTIPP -ELL(IL,KASE+1))*(EEL(IL+1,KASE+1)
     1          - EEL(IL,KASE+1))/ELSP(KASE+1)
      EDEPOS = EWTPP + EWTPT - ETIPP - ETIPT
      GO TO 120
   90 IF(YPMHP*ALPHA .GE. YWALL) GO TO 65
      IF(PLABZP .GE. 0.) GO TO 91
      YMINR = -PLABYP*PLABZP*R/XPZP
      IF(YMINR .GT. YWALL) GO TO 91
      RMIN2P = PLXP2*R2/XPZP
      GO TO 92
   91 RMIN2P = ((R*PLABYP + PLABZP*YWALL)**2 + PLXP2*YWALL**2)/PLABYP**2
   92 R2WALT = ((R*PLABYT + PLABZT*YWALL)**2 + PLXT2*YWALL**2)/PLABYT**2
      IF(PLABZT .GE. 0.) GO TO 94
      YMINR = -PLABYT*PLABZT*R/XPZT
      IF(YMINR .LE. YTMHP) GO TO 93
      IF(YMINR .GE. YWALL) GO TO 94
      RMIN2T = PLXT2*R2/XPZT
      GO TO 95
   93 RMIN2T = RT2
      GO TO 95
   94 RMIN2T = R2WALT
   95 RMIN2 = AMIN1(RMIN2T,RMIN2P)
      IF(CAT2 - RMIN2 .LT. DIFMIN) GO TO 130
      WTIPT = TLENG*(1. - YWALL/YTMHP)
      WTIPP = PLENG*(1. - YWALL/YPMHP)
      TIPP = PLENG*(1. - ALPHA)
      IL = INT(WTIPT/ELSP(KASE+2))
      EWTPT = EEL(IL,KASE+2) + (WTIPT -ELL(IL,KASE+2))*(EEL(IL+1,KASE+2)
     1          - EEL(IL,KASE+2))/ELSP(KASE+2)
      IL = INT(WTIPP/ELSP(KASE+1))
      EWTPP = EEL(IL,KASE+1) + (WTIPP -ELL(IL,KASE+1))*(EEL(IL+1,KASE+1)
     1          - EEL(IL,KASE+1))/ELSP(KASE+1)
      IL = INT(TIPP/ELSP(KASE+1))
      ETIPP = EEL(IL,KASE+1) + (TIPP - ELL(IL,KASE+1))*(EEL(IL+1,KASE+1)
     1          - EEL(IL,KASE+1))/ELSP(KASE+1)
      EDEPOS = EWTPT + EWTPP - ETIPP
      GO TO 120
  100 IF(RT2 .LE. CAT2) GO TO 110
      IF(YTMHP*BETA .GE. YWALL) GO TO 75
      IF(PLABZT .GE. 0.) GO TO 101
      YMINR = -PLABYT*PLABZT*R/XPZT
      IF(YMINR .GT. YWALL) GO TO 101
      RMIN2T = PLXT2*R2/XPZT
      GO TO 102
```

```
101 RMIN2T = ((R*PLABYT + PLABZT*YWALL)**2 + PLXT2*YWALL**2)/PLABYT**2
102 R2WALP = ((R*PLABYP + PLABZP*YWALL)**2 + PLXP2*YWALL**2)/PLABYP**2
    IF(PLABZP .GE. 0.) GO TO 104
    YMINR = -PLABYP*PLABZP*R/XPZP
    IF(YMINR .LE. YPMHP) GO TO 103
    IF(YMINR .GE. YWALL) GO TO 104
    RMIN2P = PLXP2*R2/XPZP
    GO TO 105
103 RMIN2P = RP2
    GO TO 105
104 RMIN2P = R2WALP
105 RMIN2 = AMIN1(RMIN2T,RMIN2P)
    IF(CAT2 - RMIN2 .LT. DIFMIN) GO TO 130
    WTIPP = PLENG*(1. - YWALL/YPMHP)
    WTIPT = TLENG*(1. - BETA)
    IL = INT(WTIPP/ELSP(KASE+1))
    EWTPP = EEL(IL,KASE+1) + (WTIPP -ELL(IL,KASE+1))*(EEL(IL+1,KASE+1)
   1          - EEL(IL,KASE+1))/ELSP(KASE+1)
    IL = INT(WTIPT/ELSP(KASE+2))
    EWTPT = EEL(IL,KASE+2) + (WTIPT -ELL(IL,KASE+2))*(EEL(IL+1,KASE+2)
   1          - EEL(IL,KASE+2))/ELSP(KASE+2)
    IL = INT(TIPT/ELSP(KASE+2))
    ETIPT = EEL(IL,KASE+2) + (TIPT - ELL(IL,KASE+2))*(EEL(IL+1,KASE+2)
   1          - EEL(IL,KASE+2))/ELSP(KASE+2)
    EDEBOS = EWTPP + EWTPT - ETIPT
    GO TO 120
110 R2WALP = ((R*PLABYP + PLABZP*YWALL)**2 + PLXP2*YWALL**2)/PLABYP**2
    R2WALT = ((R*PLABYT + PLABZT*YWALL)**2 + PLXT2*YWALL**2)/PLABYT**2
    IF(PLABZP .GE. 0.) GO TO 112
    YMINR = -PLABYP*PLABZP*R/XPZP
    IF(YMINR .LE. YPMHP) GO TO 111
    IF(YMINR .GE. YWALL) GO TO 112
    RMIN2P = PLXP2*R2/XPZP
    RMAX2P = AMAX1(RP2,R2WALP)
    GO TO 113
111 RMIN2P = RP2
    RMAX2P = R2WALP
    GO TO 113
112 RMIN2P = R2WALP
    RMAX2P = RP2
113 IF(PLABZT .GE. 0.) GO TO 115
    YMINR = -PLABYT*PLABZT*R/XPZT
    IF(YMINR .LE. YTMHP) GO TO 114
    IF(YMINR .GE. YWALL) GO TO 115
    RMIN2T = PLXT2*R2/XPZT
    RMAX2T = AMAX1(RT2,R2WALT)
    GO TO 116
114 RMIN2T = RT2
    RMAX2T = R2WALT
    GO TO 116
115 RMIN2T = R2WALT
    RMAX2T = RT2
116 RMIN2 = AMIN1(RMIN2P,RMIN2T)
    RMAX2 = AMAX1(RMAX2P,RMAX2T)
    IF(RMAX2 - RMIN2 .LT. DIFMIN) GO TO 130
    WTIPP = PLENG*(1. - YWALL/YPMHP)
```

```
      WTIPT = TLENG*(1. - YWALL/YTMAP)
      IL = INT(WTIPP/ELSP(KASE+1))
      EWTPP = EEL(IL,KASE+1) + (WTIPP-EEL(IL,KASE+1))*(EEL(IL+1,KASE+1)
     1          - EEL(IL,KASE+1))/ELSP(KASE+1)
      IL = INT(WTIPT/ELSP(KASE+2))
      EWTPT = EEL(IL,KASE+2) + (WTIPT-EEL(IL,KASE+2))*(EEL(IL+1,KASE+2)
     1          - EEL(IL,KASE+2))/ELSP(KASE+2)
      EDEPOS = EWTPP + EWTPT
  120 I = INT(EDEPOS*RCHNWD)
      CHAN(I) = CHAN(I) + WT
      WTSP(NEUEN) = WTSP(NEUEN) + WT
      IF(IETEST .EQ. 0) GO TO 140
      GO TO 549
  130 LOST(NEUEN) = LOST(NEUEN) + 1
      WTLST(NEUEN) = WTLST(NEUEN) + WT
      IF(IETEST .EQ. 0) GO TO 140
      C = 1.E15
      XXB = XNB*C
      YYB = YNB*C
      ZZB = ZNB*C
      PLAPP = PLABP*C
      PLATT = PLABT*C
      C = 1.E-9
      VCSYXX = VCSYSX*C
      VCSYYY = VCSYSY*C
      VCSYZZ = VCSYSZ*C
      WRITE(3,548) XXB,YYB,ZZB,VCSYXX,VCSYYY,VCSYZZ,PLAPP,PLATT,YOUT
  548 FORMAT(27H    LOST  (XNB,YNB,ZNB) = (2(   F7.2,1H,),F7.2,11H) VCSY
     548LS = (2(F7.2,1H,),F7.2,9H) PLABP =,F7.2,8H PLABT =,F7.2,7H YOUT =,
     5482    F7.2)
  549 C = 1.E15
      XPCM = XPCM*C
      YPCM = YPCM*C
      ZPCM = ZPCM*C
      PLAXXP = PLABXP*C
      PLAYYP = PLABYP*C
      PLAZZP = PLABZP*C
      PLAXXT = PLABXT*C
      PLAYYT = PLABYT*C
      PLAZZT = PLABZT*C
      WRITE(3,550) HP,R,KASE,COSPHI,SIN2HI,CTH,CTH2,PHIP,PPCM,XPCM,YPCM,
     1ZPCM,PLAXXP,PLAYYP,PLAZZP,PLAXXT,PLAYYT,PLAZZT,EP,ET,PLENG,TLENG,
     2XP,YP,ZP,XT,YT,ZT,RP2,RT2,ALPHA,BETA,R2WALL,R2WALT,RMIN2P,RMIN2T,
     3RMIN2T,RMAX2T,YMINR,TIPP,TIPT,WTIPP,WTIPT,EDEPOS
  550 FORMAT(131H  HP    R KASE COSPHI SIN2HI CTH  CTH2 PHIP PPCM E15 XPCM    YPCM
     5501  ZPCM  PLABXP PLABYP PLABZP PLABXT PLABYT PLABZT EP(E6) ET(E6) PL
     5502ENG  TLENG/F6.2,F5.2,I2,4(1X,F8.2),F5.3,   10F7.3,6P2F7.3,0P2F7.4/
     5503132H  XP     YP     ZP     XT     YT     ZT     RP2   RT2  ALPHA  BETA R2
     550AWALP R2WALT RMIN2P RMAX2P RMIN2T RMAX2T YMINR  TIPP  TIPT WTIPP WTIPT ED
     5505EPOS/6F6.2,F7.2,F6.2,2F6.3,6F6.2,5F6.3,6F6.2)
  140 IF(NEUTRN .LT. NUTRNS) GO TO 17
C         LET NUTRNS BE THE NUMBER OF NEUTRONS THAT WILL CROSS A SURFACE
C         OF ONE SQUARE CENTIMETER FROM ANY DIRECTION (INCLUDING EITHER
C         FRONT OR BACK) IN ONE SECOND.  THEN CHAN(I) WILL BE THE NUMBER
C         OF COUNTS PER SECOND REGISTERED IN THE I-TH CHANNEL.
      ITOP = NCHANS + 1
```

```
  141 ITOP = ITOP - 1
      IF(CHAN(ITOP) .GT. 0.) GO TO 144
      IF(ITOP .EQ. 1) GO TO 142
      GO TO 141
  142 WRITE(3,143) NEUEN
  143 FORMAT(22H NO COUNTS FOR NEUEN =,I3)
      CHAN(1) = 1.
      WTSM(NEUEN) = 1.
  144 J = MOD(NEUEN-1,3) + 1
C         ITOP IS THE TOP CHANNEL THAT HAS ANY COUNTS.  J RANGES FROM 1
C         TO 3.  IT IS ONLY TO ALLOW THE RESULTS FROM 3 CYCLES ON NEUEN
C         TO BE STORED AND THEN PRINTED ALL AT ONCE TO CONSERVE PAPER.
      KJ(J) = NEUEN
      DO 145 I = 1,NCHANS
      COUNTS(I,J) = CHAN(I)
      CPITP(I,J) = CHAN(I)*1000./CHAN(ITOP)
      CNORM(I,J) = CHAN(I)*1000./WTSM(NEUEN)
  145 CONTINUE
C         CPITP IS PROPORTIONAL TO CHAN AND FIXED SO THAT THE TOP CHANNEL
C         HAS 1000.  CNORM IS NORMALIZED SO THAT THE SUM OF ALL CHANNELS
C         IS 1000.
      WRITE(3,560) NEUEN,INTERP,EN,PART,SIGP,SIGD,SIGTOT,CHOICE,WTFCTR,
     1 PNEUTL,VCMSYS,PNUTCM,ENCM,PHEBCM,EHCM,ETCM,ITOP,CHAN(ITOP),J
  560 FORMAT(///127H NEUEN INTERP   EN  PART SIGP SIGD SIGTOT CHOICE  WTF
     5601CTR    PNEUTL      VCMSYS      PNUTCM      ENCM      PHEBCM      EHCM
     5602     ETCM/  2I5,6E10.2,4E5.2,F8.5,6E10.2/7H ITOP =,I4,13H CHAN(ITOP)
     5603 =,E12.4,5H  J =,I3)
      IF(J .NE. 3 .AND. NEUEN .NE. NENS) GO TO 150
      WRITE(3,146)((KJ(K),L = 1,3),K = 1,J)
  146 FORMAT(12H1  I  E(MEV),3(11H  COUNTS(I,,I2,11H)  CPITP(I,,I2,
     1461     11H)  CNORM(I,,I2,1H)))
      ITOPP5 = ITOP + 5
      IF(ITOPP5 .GT. NCHANS) ITOPP5 = NCHANS
      DO 148 I = 1,ITOPP5
      ENERGY = ENLIN*FLOAT(I)/(1.E6*ELVOLT*FLOAT(NCHANS))
      WRITE(3,147) I,ENERGY,(COUNTS(I,K),CPITP(I,K),CNORM(I,K),K = 1,J)
  147 FORMAT(I4,F8.2,3(E15.5,2F11.3))
  148 CONTINUE
      KJ1 = KJ(1)
      KJJ = KJ(J)
      WRITE(3,149) (K,WTSM(K),K,LOST(K),K = KJ1,KJJ)
  149 FORMAT(///3(6H WTSM(,I2,3H) =,E14.6,7H  LOST(,I2,3H) =,I7))
      WRITE(3,570) (K,WTLST(K),K = KJ1,KJJ)
      WRITE(3,571) (K,TOTAL(K),K = KJ1,KJJ)
  570 FORMAT(3(19X,6HWTLST(,I2,3H) =,E14.6))
  571 FORMAT(3(19X,6HTOTAL(,I2,3H) =,E14.6))
  150 IF(IPPLOT .EQ. 0) GO TO 160
      DO 155 I = 1,NCHANS
      IF(CHAN(I) .GT. 0.) GO TO 152
      LCHN(I) = -9999
      GO TO 155
  152 CHN = ALOG10(CHAN(I))
      LCHN(I) = INT(SIGN(1000.*ABS(CHN) + .5,CHN))
      IF(LCHN(I) .LE. (-10000)) LCHN(I) = -9999
  155 CONTINUE
C         LCHN IS 1000 X (LOGARITHM(BASE 10) OF CHAN).
      WRITE(14,1) NCHANS,NTABS,NENS,IFTEST,IPPLOT,NUTRNS,VOLTS,TIME,
```

```
     1     ELOW,EHIGH,EN
           WRITE(14,157) (LCHN(I),I = 1,NCHANS)
 157 FORMAT(16I5)
 160 CONTINUE
     CALL CLOCKI(TIM3)
     WRITE(3,575) TIM1,TIM2,TIM3
 575 FORMAT(7H TIM1 =,F13.2,7H TIM2 =,F13.2,7H TIM3 =,F13.2)
     STOP
     END
```

```
$IBFTC LENGTH
      SUBROUTINE LENGTH(NTABS,ENLIM,ENER,ERG,RPAIR,EL,ELMAX,ELSP,ELL,EEL
     1     )
      DIMENSION ENER(600),ERG(600),RPAIR(600),EL(600,4)
      DIMENSION ELMAX(4),ELSP(4),ELL(600,4),EEL(600,4)
      FNTABS = FLOAT(NTABS)
      ELVOLT = 1.60207E-12
      RHOHE = .116629
      RHOKR = 3.455
      PHE = 2.
      PKR = 10.
      DENOM = PHE*RHOHE + PKR*RHOKR
      WHE = PHE*RHOHE/DENOM
      WKR = 1. - WHE
      DO 3 I = 1,NTABS
C        THIS LOOP COMPUTES TRACK LENGTH VS. PARTICLE ENERGY AND STORES
C        THE LENGTH IN THE ARRAY EL.  THE FORMULAS ARE FROM WANG, P.73-
C        75 (UCRL-10770). WITH SLIGHT CORRECTIONS.  J = 1,2,3,4 IMPLIES
C        PROTON,TRITON,DEUTERON,DEUTERON, RESPECTIVELY.
      E = ENLIM*FLOAT(I)/(1.E6*ELVOLT*FNTABS)
      ENER(I) = E
      ERG(I) = ENLIM*FLOAT(I)/FNTABS
      RPKR = RPAIR(I)*(1.89 -.25*ALOG10(E)) - .36
      RPHE = RPAIR(I)*(1.82 + .043*ALOG10(E))
      J3 = INT(FLOAT(I)/3. + .001)
      J2 = INT(FLOAT(I)/2. + .001)
      PAR3 = FLOAT(MOD(I,3))/3.
      PAR2 = FLOAT(MOD(I,2))/2.
      RPAIR3 = RPAIR(J3) + PAR3*(RPAIR(J3+1) - RPAIR(J3))
      RPAIR2 = RPAIR(J2) + PAR2*(RPAIR(J2+1) - RPAIR(J2))
      RTKR = 3.*(RPAIR3*(1.89 - .25*ALOG10(E/3.)) - .36)
      RTHE = 3.*RPAIR3*(1.82 + .043*ALOG10(E/3.))
      RDKR = 2.*(RPAIR2*(1.89 -.25*ALOG10(E/2.)) - .36)
      RDHE = 2.*RPAIR2*(1.82 + .043*ALOG10(E/2.))
      RTP = 1./(WHE/RPHE + WKR/RPKR)
      RTT = 1./(WHE/RTHE + WKR/RTKR)
      RTD = 1./(WHE/RDHE + WKR/RDKR)
      EL(I,1) = RTP/DENOM
      EL(I,2) = RTT/DENOM
      EL(I,3) = RTD/DENOM
      EL(I,4) = EL(I,3)
    3 CONTINUE
      DO 7 J = 1,4
      ELMAX(J) = EL(NTABS,J)
      ELSP(J) = ELMAX(J)/FNTABS
      I = 0
      EL(I,J) = 0.
      ELL(I,J) = 0.
      EEL(I,J) = 0.
      DO 6 I = 1,9
      EL(I,J) = EL(10,J)*FLOAT(I)/10.
C        EL(I,J) FOR I = 1,9 ARE INTERPOLATED FROM EL(10,J) BECAUSE THE
C        FORMULA GIVES NEGATIVE VALUES IN THIS VERY LOW ENERGY REGION.
    6 CONTINUE
    7 CONTINUE
      WRITE(3,8)
```

```
    8 FORMAT(49H1  I  E(MEV) E*E6(ERGS) L-P(CM)  L-T(CM)  L-D(CM),10X,
   *17HL-P(CM) E(I-P)*E6(ERGS) L-T(CM) E(I-T)*E6(ERGS) L-D(CM) E(I-D)*
   *2E6(ERGS))
C        ELL(I,J) IS TRACK LENGTH OF PARTICLE J.ELL(NTABS,J)=EL(NTABS,J)
C        THE DIFFERNECE BETWEEN EL AND ELL IS THAT ELL VALUES VARY
C        LINEARLY FROM 1 TO NTABS, WHILE EL(I,J) IS THE TRACK LENGTH OF
C        THE J-TH PARTICLE OF ENERGY ERG(I), WHERE ERG VARIES LINEARLY
C        FROM 1 TO NTABS.  EEL IS THE ENERGY THAT CORRESPONDS TO ELL.
C        THE ELL-EEL RELATION IS THE INVERSE OF THE ERG-EL RELATION. THE
C        LOOP TO STATEMENT 15 COMPUTES AND PRINTS THESE ARRAYS.
      DO 15 I = 1,NTABS
      DO 13 J = 1,3
      ELL(I,J) = ELSP(J)*FLOAT(I)
      ITRY = 1
    9 IF(EL(ITRY,J) .GT. ELL(I,J)) GO TO 10
      IF(ITRY .GE. NTABS) GO TO 12
      IF(EL(ITRY+1,J) .GE. ELL(I,J)) GO TO 11
      ITRY = ITRY + 1
      GO TO 9
   10 IF(ITRY .LE. 1) GO TO 11
      ITRY = ITRY - 1
      GO TO 9
   11 PART = (ELL(I,J) - EL(ITRY,J))/(EL(ITRY+1,J) - EL(ITRY,J))
      EEL(I,J) = ENLIM*(FLOAT(ITRY) + PART)/FNTABS
      GO TO 13
   12 PART = (ELL(I,J) - EL(ITRY-1,J))/(EL(ITRY,J) - EL(ITRY-1,J))
      EEL(I,J) = ENLIM*(FLOAT(ITRY-1) + PART)/FNTABS
   13 CONTINUE
      EEL(I,4) = EEL(I,3)
      ELL(I,4) = ELL(I,3)
      WRITE(3,14) I,ENER(I),ERG(I),(EL(I,J),J = 1,3),(ELL(I,J),EEL(I,J),
     1    J = 1,3)
   14 FORMAT(I4,F9.2,6PF9.3,0PF9.4,8X,3(0PF12.4,6PF13.4))
   15 CONTINUE
      RETURN
      END
```